Flow-Accelerated Corrosion in Steam Generating Plants

Barry Dooley and Derek Lister

ABSTRACT

Flow-accelerated corrosion (FAC) has been researched for over 50 years at many locations around the world, and scientifically all the major influences are well recognized. However, the application of this science and understanding to fossil, combined-cycle/HRSG and nuclear plants has not been entirely satisfactory. Major failures are still occurring and the locations involved are basically the same as they were in the 1980s and 1990s. This paper reviews the latest theory of the major mechanistic aspects and also provides details on the major locations of FAC in plants, the key identifying surface features of single- and two-phase FAC, the cycle chemistries used in the plants and the key monitoring tools to identify the presence of FAC. The management aspects as well as the inspection, predictive and chemistry approaches to arrest FAC are described, and the different approaches that are needed within fossil, HRSG and nuclear plants are delineated.

1 Introduction

However you account for them, the costs of metallic corrosion and its ramifications in general are huge. After a two-year study, one estimate that included the cost of preventive strategies put the total for all industries in the United States in 2002 at 276 x 10^9 USD [1]. For the US power industry alone, a report published in 2001 reckoned the cost for the 1998 year was 17 x 10^9 USD – about 7.9 % of the total cost of electricity to consumers [2]. About 22 % of this was considered to be avoidable using "practical, cost-effective measures". Of the various types of metallic corrosion occurring in power plants, flow-accelerated corrosion (FAC) of carbon steel has been characterized as a "major issue for nuclear plants" [3] and a "major problem in nuclear, fossil and industrial plants" [4]. In 1987, the costs of monitoring and preventive measures for FAC in a nuclear plant in the US were estimated to average 100 000 USD per outage [5]. As recently as 2014, it was the "leading cause of damage and failure in heat recovery steam generators (HRSGs)", as found in combined-cycle plants [6].

As will be described later, much research into corrosion related to boiler systems has been undertaken since the early 1900s. Flow-accelerated corrosion, usually called erosion-corrosion (E-C) in the early days, was identified in the 1940s as the cause of several failures in power plant and industrial piping made of carbon steel, but these were not well documented and were generally addressed as maintenance issues; pipes were simply replaced, and operation resumed. By the 1960s, FAC had been the subject of several studies [7–9] and by the 1980s it was believed that it was adequately understood. Confidence was growing that the parallel research conducted in Germany, France, Russia and the United Kingdom throughout the 1970s for different facets of the nuclear and steam turbine industries had addressed the major concerns. No serious damage was reported during the 1970s, and the importance of the first major case of FAC in single-phase water flows at the Navajo fossil plant in Arizona in 1982 [10] was apparently not identified or recognized. A similar incident at the Trojan pressurized water reactor (PWR) in1985 raised no serious discussion, either [11].

This level of confidence was removed in 1986 when four workers were killed at the Surry nuclear plant [12]. A guillotine break occurred in a 90 ° elbow in the 457 mm (18 inch) suction line leading to the feedwater pump. The wall of the elbow had been severely thinned by FAC. Shortly afterwards, a bulletin issued by the US Nuclear Regulatory Commission (USNRC) [13] identified 34 US nuclear plants (comprising one high temperature gas-cooled reactor (HTGR), six boiling water reactors (BWRs) and 27 PWRs) that had experienced FAC between 1967 and 1986. There were six types of single-phase water systems and six types of two-phase steam-water systems typically involved. The Surry accident led to an international effort to ensure that FAC was understood at the power plant level. Many research programmes were undertaken and systems of inspection and non-destructive evaluation (NDE) were developed, leading eventually to the development of a number of computer codes and models for data management and inspection protocols.

Unfortunately, this increased research effort did not lessen the incidences of FAC in the nuclear and fossil power industries. Once again, the seriousness and complexity of FAC in high energy systems had not been fully appreciated. Since 1986, there have been three more accidents where plant workers have been killed as a result of FAC in single-phase water: at Pleasant Prairie (1995) [14,15], at Mihama (2004) [16] and at Iatan (2007) [17]. Numerous non-injurious incidents of FAC in two-phase steam-water flows have also taken place. Table 1 shows a list of these major incidents of FAC, which were all single-phase. Although there were no fatalities, the initial major failures at the Navajo fossil plant and the Trojan nuclear plant are included here for comparison, as they involved the rupture of large diameter pipes. Discussion of the major points in relation to the FAC mechanism and to these and other FAC occurrences in operating plants is included in Section 4.

During the mid-1900s, a new electricity generating source, the combined-cycle gas turbine (CCGT) with a boiler or HRSG, emerged. Since the first commercial unit was introduced at the Belle Isle plant in Oklahoma, USA, in 1949, more and more have been installed around the world and they now exist in enormous numbers. Very quickly, FAC became the prime availability problem in HRSGs with many single- and two-phase FAC failures occurring. This is still the case today [19]. Lately, in a water-constrained world, an increasing number of these combined-cycle plants and fossil plants in general have been built with air-cooled condensers (ACC). These are carbon-steel exchangers with huge surface areas which have experienced FAC and the associated generation of large amounts of corrosion products that foul the circuits [20].

The awareness of FAC appears to be undergoing a revival as plant operators worldwide continue the search for cost reductions and increased efficiency and strive to improve safety. Since 2007, more research, plant assessments and laboratory studies have been undertaken and new prediction codes and inspection techniques have been developed. An international benchmarking of prominent calculation methods was coordinated by the International Atomic Energy Agency in 2012 [21]. There have been four international conferences concentrating on FAC in nuclear plants and two for fossil/combined-cycle plants. It would seem an opportune time for a comprehensive review.

The primary purposes of this review are to update the previous reviews of the authors, one describing the situation in fossil and combined-cycle plants [18] and the other critiquing the state-of-the-art of the accepted FAC

	Navajo 2 (fossil) [10]	Trojan (PWR) [11]	Surry 2 (PWR) [12]	Pleasant Prairie 1 (fossil) [14,15]	Mihama 3 (PWR) [16]	Iatan 1 (fossil) [17]
Date (fatalities)	11/1982 (0)	3/1985 (0)	12/1986 (4)	2/1995 (2)	8/2004 (5)	5/2007 (2)
Location	90° bend between booster pump and HP boiler feed pump	14-inch (356 mm) heater drain pipe	90° bend following a tee off main feedwater suction header	Feedwater pipe between isolation valve and economizer inlet	22-inch (560 mm) feedwater pipe between low-pressure heaters and deaerator	Superheater attemperation line from discharge of boiler feed pump
Temperature [°C (°F)]	195 (382)	176 (349)	190 (374)	232 (450)	142 (287)	171 (340)
Pressure [MPa (psig)]	4.14 (600)	3.11 (450)	2.55 (370)	13.8 (2 000)	0.93 (134)	20 (2 900)
Max fluid velocity [$m \cdot s^{-1}$ (ft/sec)]	7.3 (24)	7.3 (24)	5.3 (17.6)	6.1 (20)	2.2 (7.2)	
Range of pH (typical)	8.8–9.6 (9.0)	(9.0)	8.9–9.0	Average 8.75	8.6–9.3	8.9–9.1
Oxygen [$\mu g \cdot kg^{-1}$ (ppb)]	< 1	4	4	< 1	< 5	< 5
Reducing agent	Hydrazine	Hydrazine	Hydrazine	Hydrazine	Hydrazine	Carbohydrazide
Steel type	A105	A106 Gr B	A106 Gr B	A106 Gr C	JIS G3103 SB42	A106 Gr C
Feedwater heaters	Stainless steel	Copper-containing alloy		Stainless steel	Copper-containing alloy (HP and LP)	Stainless steel

Table 1:
Major FAC incidents in fossil and nuclear plants – all in single-phase water (after original table in [18]).

mechanisms [22], and to summarize the recent work into a concise understanding of the mechanisms of FAC and the ramifications for controlling FAC in operating plants. The science of FAC is now much better understood (Section 2) and not a random situation or a mystery, and this science can and should be easily applicable to all steam/electric generating plants. The paper deals primarily with FAC in conventional fossil plant feedwater systems, combined-cycle/HRSG feedwater, economizer and evaporator systems, and in air-cooled condensers. For the first time, causes of damage and remedies for vulnerable systems are collected in one document. Nuclear plants, in which FAC is documented systematically by the various industry regulatory and utility organizations around the world, are covered in rather less detail. Plant assessments have also been made worldwide with this same understanding for steam generating plants associated with various industries such as oil refineries, chemical plants, pulp and paper plants, dairies, liquified natural gas (LNG) facilities, desalination plants, etc.

From all these assessments, it is now clear that FAC is heavily controlled and influenced by the cycle chemistry. For the fossil and combined-cycle plants the latest documents of the International Association for the Properties of Water and Steam (IAPWS) [23–26] provide advice and guidance on how to optimize the chemistry to significantly reduce or eliminate FAC. Many of the principles apply also to nuclear plants. Tools have been introduced which allow the plant operators to determine the key chemistry deficiencies, called repeat cycle chemistry situations (RCCS), which unless corrected will lead to FAC (Section 7.6).

2 Theory

This section is intended to give the reader an overview of the important factors underlying FAC in power plants, including new information on mechanisms, to relate to the descriptions of plant observations discussed in later sections. More comprehensive reviews have been published elsewhere (for example, see [27,28]).

It is generally understood that FAC is controlled by the oxide film that forms on the carbon steel and affords a barrier to diffusion. Dissolved iron species are transported from the surface to the flowing bulk water, so the mass transport characteristics of the flow regime are important and are usually postulated to be controlling (this is discussed later in Section 2.5). As the oxide dissolves into the water and is replenished by the metal oxidation, the film attains a steady-state thickness. The thicker and more compact the film – the greater the barrier to diffusion – the more protective it is. The following sections consider the influence of oxide properties and fluid flow on FAC. They point out that explanations of FAC based solely on mass transfer and fluid flow are incomplete; the properties and dissolution kinetics of the oxide film must be considered.

2.1 General Corrosion of Carbon Steel and Oxide Formation

The general corrosion of carbon steel in static or low velocity, high temperature water in the context of boiler systems was evaluated in the 1930s [29], resulting in the classic curve of relative rate of attack at 310 °C versus $pH_{25°C}$ (generated with a strong base or strong acid) that showed a minimum at $pH_{25°C}$ of about 11 [30]; this verified the basis for high pH treatment of coolant systems. In autoclave tests, the steel was shown to develop a double-layered film of the corrosion product oxide magnetite. The film comprises a fine-grained inner layer of crystallites of size 30–50 nm [31] next to the metal, affording a barrier to diffusion, overlaid with an outer layer of crystallites of size 1–10 µm. This is the so-called Potter-Mann double layer [32]. The inner layer develops at the metal-oxide interface (M-O), occupying the volume of metal corroded, and the outer layer by precipitation at the oxide-solution interface (O-S), so that the interface between the layers corresponds to the original surface of the metal.

The pores-solution model of Castle and Masterson [33] postulates that, in high temperature water (~ 300 °C) under reducing and slightly alkaline conditions, porosity in the oxide allows access of water oxidant to the metal. In the constrained environment of the M-O, approximately 50 % of the corroded iron forms the fine-grained inner layer magnetite (the volume ratio of oxide to metal, the Pilling-Bedworth ratio, is 2.1); the rest diffuses outwards through the pores to the O-S and precipitates freely as the outer layer of solution-grown magnetite crystallites, often of octahedral shape. The model predicts the parabolic kinetics of steel corrosion quite well. Several objections to the pores-solution model were raised by Robertson [34], however, most notably that the activation energy for the corrosion (120 $kJ \cdot mol^{-1}$) is much higher than common values for aqueous diffusion (~ 15 $kJ \cdot mol^{-1}$). He proposed instead that water as the oxidant penetrates to the M-O along micropores in the oxide but that the controlling process is the outward, solid-state diffusion of iron ions along the oxide grain boundaries.

Under the neutral or slightly alkaline (pH25°C up to about 11) environments encountered in aqueous power systems with reducing or low oxygen conditions, the chemical reactions at the metal-oxide interface can be written as:

$$Fe = Fe^{2+} + 2e^{-} \quad (1)$$

$$2H_2O + 2e^{-} = 2H\cdot + 2OH^{-} \quad (2)$$

Under alkaline conditions at high temperature, as in reactor primary coolants, the hydrogen atoms generated by

Eq. (2) diffuse into the metal, and if the steel is the containment system for the fluid, they combine at the outer surface and are released to the atmosphere as hydrogen molecules:

$$2H^{\cdot} = H_2 \quad (3)$$

The gas generation is quantitative and in fact its measurement has been used as a measure of the corrosion rate [31] of steel in high temperature, lithiated water; it is used as the basis of a non-intrusive instrument for monitoring corrosion rates of piping in aqueous systems [35]. The effusion of the hydrogen into the metal at the lower temperatures and conditions encountered in feedwater systems is unlikely to be the same.

The arrangement of the anodic areas (Eq. (1)) and cathodic areas (Eq. (2)) and the resulting hydrogen production on the corroding surface determine the morphology of the initially formed oxide [36]. In contrast to the situation where the hydrogen from Eq. (2) effuses through the metal and a tightly knit oxide forms [37], if the steel is a component completely immersed in the fluid, the hydrogen atoms congregate in interstitial positions in the metal matrix and reach an equilibrium level; at this stage the hydrogen diffuses outwards and is released to the fluid, while a more porous oxide develops. In highly alkaline environments (for example, at concentrations of NaOH of 15 %), the high corrosion rates produce very porous oxides and most of the hydrogen is released to the fluid [37].

Magnetite is formed at the M-O from half of the ferrous ions generated by Eq. (1) and the hydroxide ions generated by Eq. (2) via:

$$Fe^{2+} + 2OH^{-} = Fe(OH)_2 \quad (4)$$

and the subsequent Schikorr reaction [38]:

$$3Fe(OH)_2 = Fe_3O_4 + 2H_2O + H_2 \quad (5)$$

The reaction in Eq. (5) is an oxidative process at both the M-O and the O-S, generating hydrogen which diffuses to the bulk water.

2.2 FAC and Oxide Properties

In contrast to the above mechanisms that occur in relatively static conditions in solutions that are saturated in dissolved iron, flow-accelerated corrosion (FAC) occurs in systems in which the oxide on the steel tends to dissolve (the solution is under-saturated in dissolved iron so the reaction in Eq. (5) does not occur at the O-S) and where the solution is turbulent (hence acceleration of the corrosion by flow). Under-saturation typically occurs because the fluid flows through a temperature gradient, which increases the iron solubility. Thin magnetite layers with little or no outer precipitation develop; the thinner the magnetite, the less

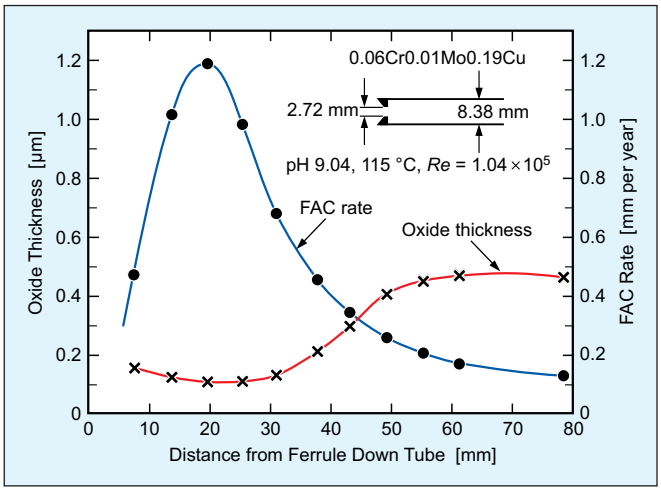

Figure 1:
Oxide film thickness and FAC rate [39].

the protection afforded and the greater the rate of FAC. Observations from operating plant and laboratory experiments confirm that high FAC rates are associated with thin oxides (for example, see Figure 1, which presents measurements of the thickness of the oxide film on a 0.06Cr0.01Mo0.19Cu steel downstream of a nozzle or ferrule under laboratory feedwater conditions; the inverse relation is nicely illustrated) [39]. A steady-state develops when the rate of magnetite formation at the M-O equals the rate of dissolution at the O-S, leading to a constant FAC rate. The dissolution reaction is the reverse of Eq. (5):

$$Fe_3O_4 + 2H_2O + H_2 = 3Fe(OH)_2 \quad (6)$$

and hence is a reductive process. It is noted that the quantity of hydrogen diffusing through the oxide from Eq. (5) at the M-O is exactly what is required at steady-state to dissolve reductively the magnetite via Eq. (6) at the O-S. The fundamental processes occurring within the oxide film during FAC are schematically summarized in Figure 2. The scheme is generally accepted as describing the underlying basic principles of FAC. It will be noted that it is equivalent to the pores-solution model, described

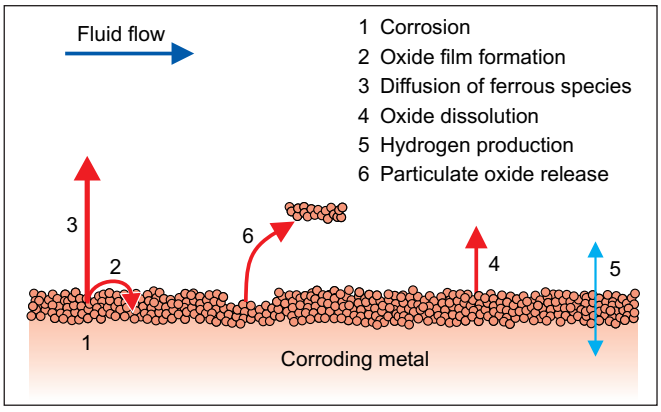

Figure 2:
Schematic of processes occurring during FAC.

above for steel corrosion in aqueous systems saturated in dissolved iron [33], but with dissolution of the oxide at the O-S rather than precipitation.

As will be mentioned later, the processes in Eqs. (1), (2), (4) and (5) are electrochemical, depending on the electrochemical corrosion potential of the system, and Eq. (6) depends on Eq. (4). At steady-state, the oxide film has a constant thickness and mass balances indicate that Eq. (1) = (2) + (3) and Eq. (2) = (4) + (6). The cross-section scanning-electron microscope (SEM) image in Figure 3 of the oxide film on an experimental specimen that has undergone FAC under nuclear reactor primary coolant conditions at ~ 300 °C is compatible with the schematic diagram of Figure 2.

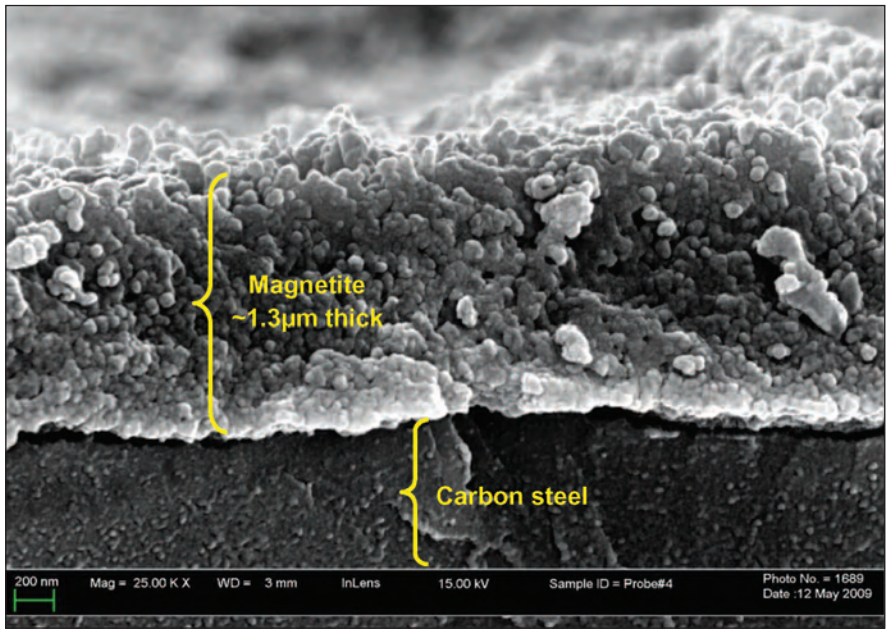

Figure 3:
Scanning-electron image of oxide film on carbon steel exposed under CANDU primary coolant conditions; specimen fractured under liquid nitrogen [40] (courtesy of Canadian Nuclear Laboratories).

Chemistry of the fluid, temperature and, of course, flow greatly affect FAC. At 130–150 °C attack is rapid and as flow rate increases the effect of temperature becomes more pronounced (Figure 4). The solubility of magnetite is affected in concert (Figure 5), reflecting the dependence of the mechanism on the dissolution of the magnetite film. As might be expected from Figure 5, which shows how the solubility at typical feedwater temperatures decreases with pH as controlled with ammonia, FAC rates decrease with increasing alkalinity. Accordingly, practical feedwater systems are operated with $pH_{25°C}$ in the range of ~ 8.8 to ~ 9.8 (depending upon the presence or absence of copper alloys in the circuit).

In contrast to FAC under these general feedwater conditions, FAC rates under nuclear reactor primary coolant conditions of ~ 300 °C increase with increasing $pH_{25°C}$ greater than ~ 10 (with a strong base such as LiOH). This supports the oxide dissolution mechanism, since the solubility of magnetite, while comparatively low, increases in that range [43] (see Figure 6). Accordingly, in CANDU primary coolant systems (which operate typically between 265 and 310 °C), reactor operators are now recommended to adjust the concentration of Li to give a $pH_{25°C}$ at the lower end of the specified range of alkalinity (which has dissolved Li from 0.5 x 10^{-4} to 2.0 x 10^{-4} mol · kg^{-1}) [44]. This reduces the FAC rate of the carbon steel outlet feeder pipes which lead the primary coolant from the reactor to the steam generators.

A water treatment process that is steadily gaining acceptance for controlling corrosion and oxide transport in power plants is the application of film-forming substances, which are additives that contain surface-active

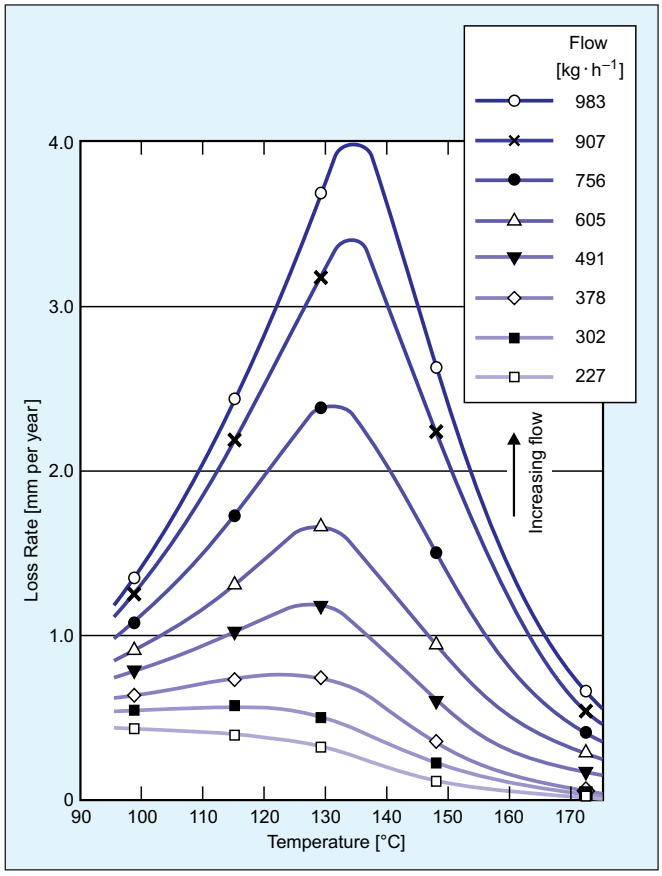

Figure 4:
Effect of temperature and flow on FAC at $pH_{25°C}$ 9.0 (with ammonia) [41].

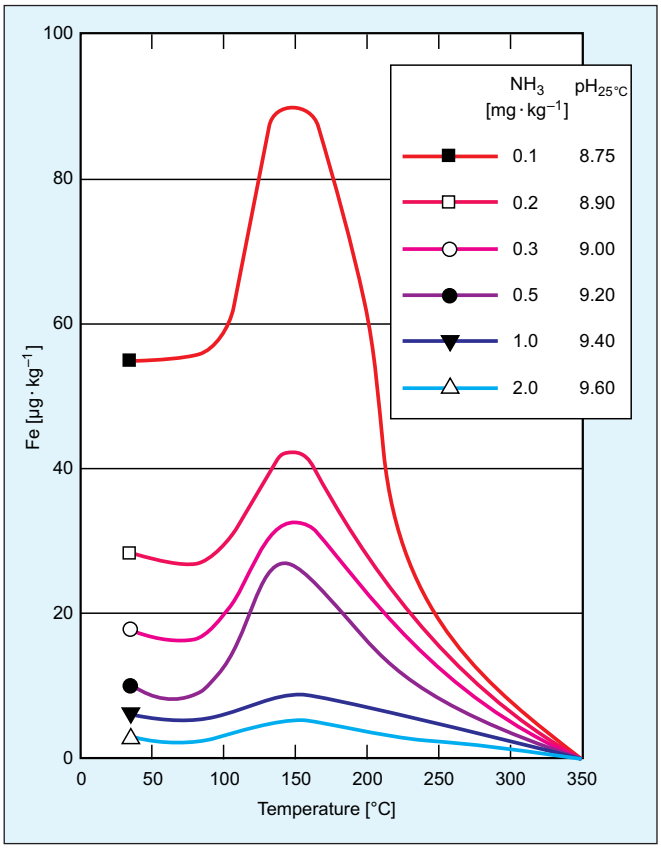

Figure 5:
Effect of temperature and $pH_{25°C}$ (with ammonia) on solubility of magnetite [42].

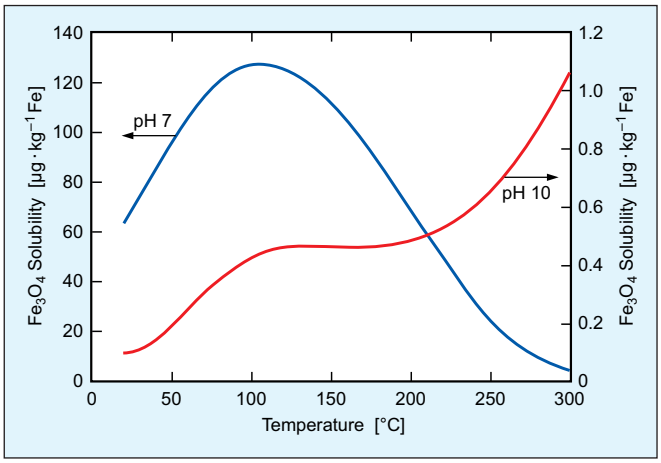

Figure 6:
Effect of temperature and $pH_{25°C}$ (with strong base) on solubility of magnetite [43].

substances that adsorb on metals and oxides to form protective films (see also Section 3.2). While their beneficial properties have been known for decades, the adverse effects of haphazard treatments and overdosing led to their being largely ignored until the last few years. Recently, IAPWS has issued a technical guidance document (TGD) [45] describing them and their use in fossil plants, and their possible use in nuclear plants has been discussed [46]. A review of their properties and use has been published [47] and two IAPWS international conferences on the subject have been held recently, in Lucerne, Switzerland, in 2017 and in Prague, Czech Republic, in 2018. Practical aspects of their application in power plants are discussed in a later section below.

For convenience, film-forming substances are divided into two groups – film-forming amine products (FFAP) and other film-forming products (FFP). The former contain film-forming amines (FFA) and are the more common, the latter contain no amines but have other surface-active substances. For proprietary reasons the ingredients of FFPs are generally secret but the FFAs are known to be long-chain organic molecules with one or more amine groups. Common examples are octadecylamine (ODA), oleylamine (OLA) and oleylpropane diamine (OLDA). The lone-pair electrons on the nitrogen atoms of the amine groups bond strongly to surfaces and leave the aliphatic groups to protrude into the fluid (Figure 7). Opened components that have been treated with FFAs have hydrophobic surfaces, indicating that the organic film is left exposed even after

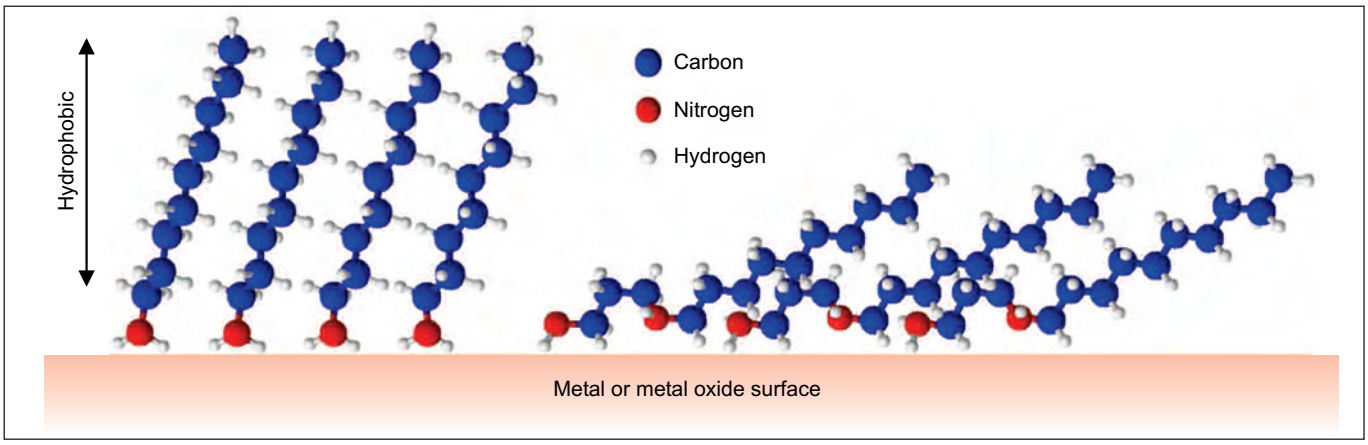

Figure 7:
Schematic representation of adsorbed FFA films (left, monoamine; right, diamine).

the surface has been dried. Proprietary FFAPs often contain other ingredients, especially alkalizing agents such as ammonia or cyclohexylamine (CHA), to provide extra protection to feedwater systems by raising the pH.

Laboratory experiments have demonstrated directly the reduction of FAC when an FFAP is introduced to the corroding surface. For example, in a high temperature water loop operating at 140 °C with essentially zero dissolved oxygen, a carbon steel on-line probe monitored FAC as the chemistry conditions were changed [48]. Starting at neutral $pH_{25°C}$, a high rate of wall thinning of 6.0 mm per year was monitored until the commercial product Cetamine® V219, which contains the FFA OLDA and the alkalizing agent CHA, was added to an FFA concentration of ~ 0.8 mg · kg^{-1}.

As illustrated in Figure 8, the $pH_{25°C}$ jumped immediately to 9.2 and the FAC rate (the slope of the wall thickness curve) fell to 0.35 mm per year. Over the next eleven days, the FFA concentration declined to an apparent equilibrium value of 0.4 mg · kg^{-1} as it adsorbed on loop surfaces, but the $pH_{25°C}$ and FAC rate remained constant. On day 17, ion exchange (IX) was valved in to reduce the $pH_{25°C}$ back to neutral, which removed the FFA from the bulk water and increased the FAC rate to 2.0 mm per year – evidently, the FFA still provided some protection to the probe surface.

After five days, however, that protection disappeared and the FAC rate spontaneously doubled. Adding CHA alone to give the previous $pH_{25°C}$ value of 9.2 decreased the FAC rate to 0.82 mm per year – considerably higher than that monitored during the exposure to the FFAP earlier in the experiment. The experiment demonstrated that the FFAP was more effective than the alkalizing agent CHA at the same $pH_{25°C}$, that some surface protection survived for several days after the FFA was removed from the bulk water, and suggested that the adsorbed FFA consisted of more than a single layer. A simple first-order adsorption-desorption model applied to the measured FFA concentrations after addition to and removal from the loop provided [49] kinetic constants in agreement with other determinations noted in the literature [50]. Later studies indicated that the FFAP Cetamine® G851, consisting basically of the same FFA (OLDA) as in Cetamine® V219 but without the alkalizing agent CHA, was also effective under the same feedwater conditions [51,52]. Probe surfaces examined after exposure to FFA chemistry were generally hydrophobic and showed very broad absorption spectra in a laser-Raman microscope, indicating coverage by FFA. The hydrophobicity, as tested by applying water drops and observing the shape, was stable on the dried specimen surfaces for at least many weeks and months. When many drops were applied in quick succession, however, the surface was wetted and the hydrophobicity was lost

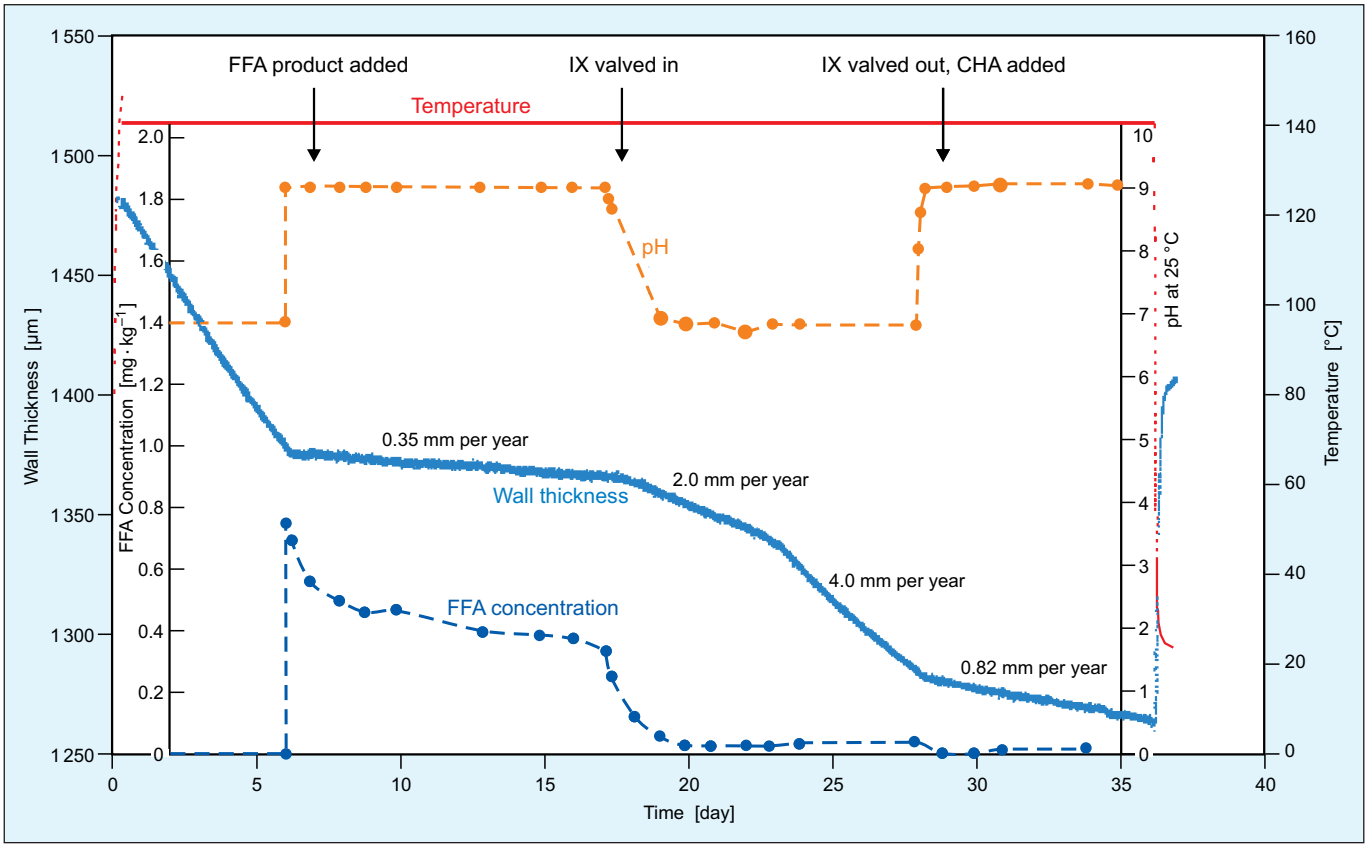

Figure 8:
Evolution of wall thickness of carbon steel FAC probe with changes in chemistry [48].

but returned once more after drying [53]. This argues against the idea that the adsorbed FFA film inhibits FAC by totally excluding water from the surface.

By contrast, laboratory studies under two-phase steam-water flows have shown no mitigation of FAC by film-forming substances – other than that afforded by any accompanying alkalizing agent. In an experimental loop operating at 200 °C with steam voidages up to 97 %, the addition of Cetamine® V219 reduced FAC rates as monitored by on-line probes by only the same amount as the constituent CHA [48]. Furthermore, probe surfaces after exposure in the loop showed no evidence of an FFA film, such as hydrophobicity or broad Raman absorption, although loop surfaces in contact with fully condensed single-phase water downstream of the probes were hydrophobic. Suggestions as to the ineffectiveness under the loop two-phase conditions centred on the velocity of the two-phase fluid, which imposed high shear stresses on the surface of the FAC probe, and on the relative volatility of the FFA in the commercial product [48] (we note here that the experiments involved two-phase systems generated by throttling single-phase water flows, which nevertheless apparently produced equilibrium conditions at the test specimens [54]). It is pertinent to note that observations of the distribution of an FFA around the circuit of an operating power plant similarly found no deposition on evaporator or high-pressure turbine surfaces [55], but hydrophobic surfaces are seen in downstream locations such as the low-pressure (LP) turbine and condenser, and clear benefits have been observed in the two-phase flow locations of air-cooled condensers as discussed later in Section 4.7.

The presence of metals such as chromium, copper and molybdenum in the carbon steel has long been known to affect the rate of FAC [56]. Chromium in particular reduces FAC rates substantially [18,57], and the carbon steel outlet feeders in CANDU reactor primary coolant systems are now stipulated to contain a minimum amount. Substitutions of SA 106 Grade B carbon steel containing 0.019 % Cr with SA 106 Grade C containing 0.33 % Cr have reduced FAC rates of CANDU feeders by about 50 % [44]. In 1998, a model for the effect of chromium on FAC rate for different exposures was proposed. It was based on the premise that below a level of 0.04 % Cr in the steel there was no effect of further decreases in chromium content and that the mitigating effect increased with exposure time (Figure 9); however, later laboratory tests have shown a definite effect between 0.019 and 0.001 % Cr (Figure 10), indicating that if there is a lower limit it must be below 0.019 % Cr.

The mechanisms by which chromium mitigates FAC are not completely understood. Since the advent of probes that can accurately monitor FAC continuously on-line, experiments such as those leading to Figure 10 have

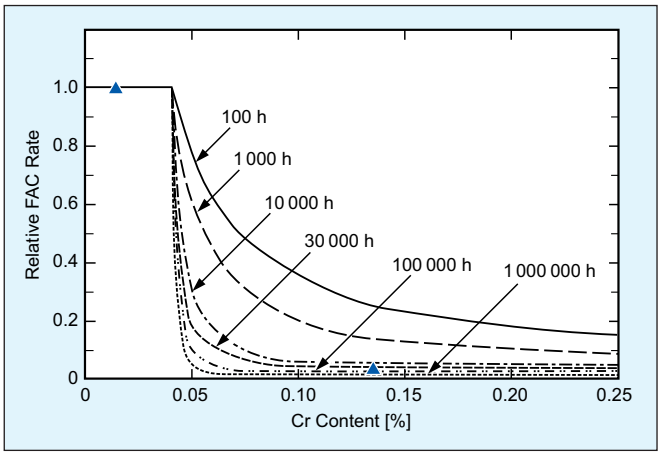

Figure 9:
Bouchacourt model of effect of chromium on FAC rate [3].

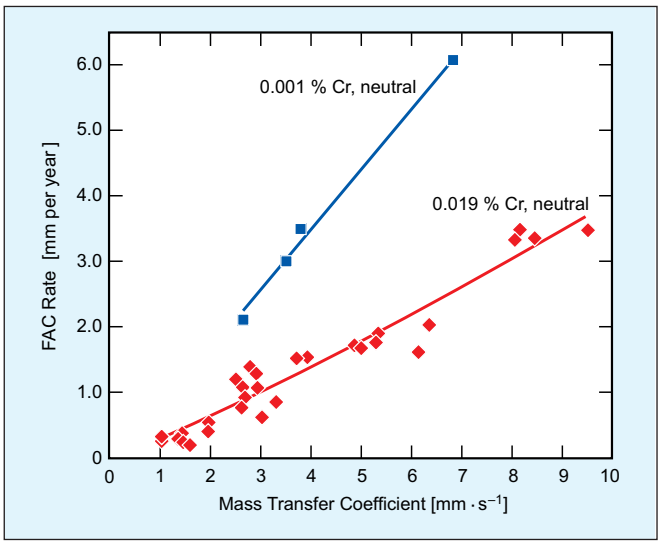

Figure 10:
Effect of chromium content of carbon steel on FAC rate (neutral water, 140 °C) [22].

shown [22] that a constant FAC rate reflecting the chromium effect is established rapidly on exposure of the steel to the water environment, that for constant experimental conditions the rate remains constant during exposure (typical experiments have lasted for many days and several weeks), and that steels of 0.001 % Cr and 0.019 % Cr after experiments of similar duration had similar levels of chromium in their oxide films. These observations cannot all be explained simply by invoking different dissolution rates of the oxides on the steels (chromium-based oxides are relatively insoluble under reducing conditions, so chromium is retained in the magnetite film as the iron is dissolved away). On the other hand, the FAC rates of steels of different chromium contents have been predicted quite well [58] with a model that assumes the formation of a chromium-based diffusion barrier immediately on exposure of the metal to the water, rather like a

less protective version of the barrier formed when stainless steel is first exposed and immediately begins to corrode at a low rate; the other processes of oxide dissolution and chromium buildup in the bulk oxide continue as before. Until such a barrier can be proven by detailed experiment or direct analysis of oxidized metal, it remains a useful hypothesis.

2.3 Effect of Dissolved Oxygen

While FAC proceeds efficiently under chemically reducing conditions, the addition of oxygen to the process water raises the surface potential and disrupts the electrochemical reactions. As described in Section 3, the recommended water treatment for fossil and combined-cycle/HRSG plants that have compatible materials in the feedwater and evaporator systems involves operation under oxidizing conditions to minimize FAC [18,24]. The presence of steam generators in nuclear plants such as CANDUs and PWRs prohibits the use of oxidizing conditions because of the susceptibility of steam generator tubing alloys to localized corrosion.

It is customary to attribute the inhibiting effect of oxygen to the formation of the higher oxide of iron, haematite, α-Fe_2O_3, rather than the magnetite that is normally formed during FAC as described in Section 2.2. Haematite, the relatively insoluble ferric oxide, is distinguished by its characteristic red colour and is usually seen on surfaces of opened components where single-phase FAC has been arrested. Maghaemite, γ-Fe_2O_3 – often seen as an intermediate compound in the oxidation of magnetite to haematite – may also be present. Another ferric oxide, lepidocrocite, γ-FeOOH, may occur but as a common component of rust it is often formed by exposure of unprotected surfaces to air and water when components are opened.

The formation of ferric oxides, however, is not necessary for arresting or "stifling" FAC; the primary effect of adding oxygen to a reducing system sustaining FAC would be to replace water as the oxidant as magnetite continues to be formed. The Schikorr reaction, Eq. (5), is then replaced with:

$$6Fe(OH)_2 + O_2 = 2Fe_3O_4 + 6H_2O \quad (7)$$

The other possible oxidation is the cathodic corrosion reaction at the M-O, Eq. (2), which would be replaced with:

$$2H_2O + O_2 + 4e^- = 4OH^- \quad (8)$$

This would also stop the production of hydrogen atoms and any effusion into the metal. The surface potential is raised when these reactions occur and the FAC stops.

Addition of more oxygen than required for these basic reactions would produce higher ferric oxides; also, after stifling with minimum amounts of oxygen, prolonged exposure would gradually convert the magnetite to ferric oxides such as haematite and turn surfaces red:

$$2Fe_3O_4 + \tfrac{1}{2}O_2 = 3Fe_2O_3 \quad (9)$$

If new surfaces were continuously exposed to oxidizing conditions, ferric-based oxides would be formed from the outset and there would be no FAC.

The mechanism of stifling by oxygen has been explored with experiments in a laboratory loop in which the conditions at the corroding surface could be controlled precisely. The FAC of a low chromium (0.001 % Cr) steel was monitored continuously as oxygen was added to single-phase water in steps of increasing concentration lasting for several days [59]. Under feedwater conditions (140 °C, ammonia at $pH_{25°C}$ 9.2 and no reducing agent) with two fluid velocities in tubular on-line probes of different diameter (Figure 11), the FAC rate was approximately constant until a concentration of oxygen between 1.12 and 1.22 $\mu g \cdot kg^{-1}$ was attained, when the FAC was "stifled" (in similar experiments when hydrazine was present at 100 $\mu g \cdot kg^{-1}$, oxygen concentrations of between 1.8 and 2.9 $\mu g \cdot kg^{-1}$ were necessary for stifling [59]). It should be borne in mind here that in operating plants with large surface areas considerably higher concentrations of oxygen would be necessary at the injection point in order to achieve sufficiently oxidizing conditions on all components.

At the end of the experiment the probes with the stifled FAC were removed and their inner surfaces examined and compared with those from probes that had been exposed under similar conditions and continued to corrode. Scanning electron microscopy revealed no difference

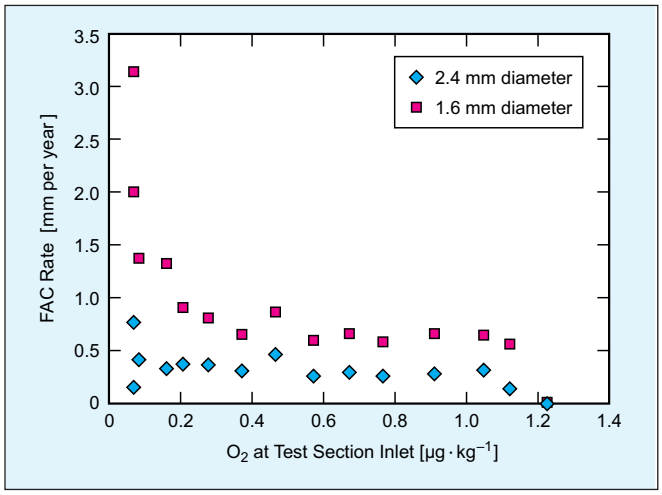

Figure 11:
The effect of gradual oxygen additions on FAC of carbon steel (experimental probes exposed to water at $pH_{25°C}$ 9.2 and 140 °C) [59].

between the oxide film morphologies on the active and stifled probes, and confocal laser-Raman microscopy similarly indicated that both sets of oxides were magnetite with only occasional traces of haematite and lepidocrocite; in fact, the oxides were typical of those found on corroding probe surfaces after many FAC experiments, including those under conditions with zero oxygen.

The controlling mechanism for oxygen stifling is considered to be mass transfer of the oxygen from the bulk water to the surface; the higher the FAC rate, the greater the required flux of oxygen. Woolsey [60] demonstrated this with several observations of FAC, plotting measured values of oxygen concentration against FAC rate divided by the product of the density of water and the oxygen mass transfer coefficient; he obtained a distinct dividing line between data for arrested (stifled) FAC and data for non-arrested FAC. The slope of the line should correspond to the stoichiometry of the oxidation reaction; however, the slopes of lines obtained at two temperatures – 115 and 150 °C – were low compared with the value of 0.285 expected from the stoichiometry of the reaction:

$$Fe + ½O_2 + H_2O = Fe(OH)_2 \quad (10)$$

equivalent to Eq. (8) for all the corroded iron converted to ferrous hydroxide.

Applying the mass transfer theory to the data in Figure 11, we note that the oxygen mass transfer coefficients in the 1.6 mm and 2.4 mm probes were 7.8 $mm \cdot s^{-1}$ and 3.7 $mm \cdot s^{-1}$, respectively (obtained from the diffusivity data of Ferrell and Himmelblau [61] and the correlation of Berger and Hau [62]). With the measured stifling concentrations between 1.22 and 1.12 $\mu g \cdot kg^{-1}$, the only pertinent oxidation reaction requiring oxygen fluxes with such concentration driving forces is half of the corroded iron as ferrous species forming magnetite. For these laboratory FAC rates of 0.6 mm per year and 0.3 mm per year, the corresponding stifling concentrations consistent with the stoichiometry of Eq. (7) are calculated to be 0.99 $\mu g \cdot kg^{-1}$ and 1.06 $\mu g \cdot kg^{-1}$, respectively, in good agreement with the measurements.

It is unlikely that the stifling reaction occurs at the M-O, since the oxides were of the order of 1 µm thick and had low porosity (suggested by Sanchez-Caldera et al. to be about 5.0 x 10^{-4} [63] or in later work to be about 0.1 [64]). The driving force at the measured concentration is insufficient for oxygen to diffuse to the M-O with either porosity. The remaining possibilities are that the $Fe(OH)_2$ diffusing through the oxide is converted to magnetite at the O-S and precipitates there, enhancing the diffusion barrier, or that the dissolution reaction (Eq. (6)) is arrested.

A different picture emerges from similar laboratory experiments under neutral conditions at 140 °C, which indicated that the higher FAC rates were stifled at higher oxygen concentrations (between 38 and 28 $\mu g \cdot kg^{-1}$ – see Figure 12).

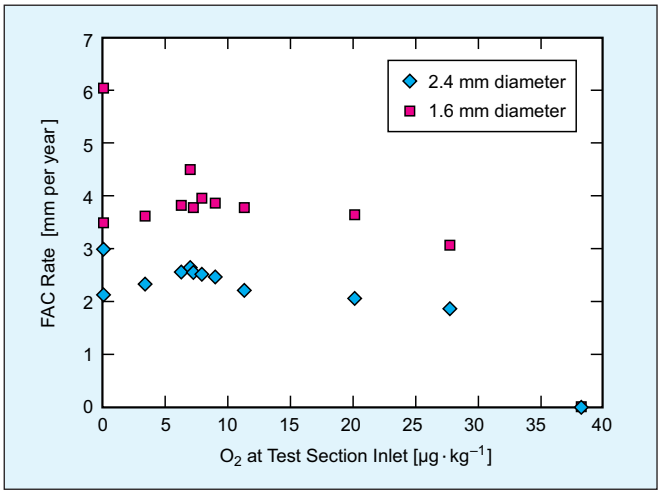

Figure 12:
The effect of gradual oxygen additions on FAC of carbon steel (experimental probes exposed to water at $pH_{25°C}$ 7 and 140 °C) [59].

An interpretation of the data of Figure 12 involving no diffusion barrier in the oxide and employing oxygen mass transfer coefficients of 4.6 $mm \cdot s^{-1}$ and 3.2 $mm \cdot s^{-1}$ for the 1.6 mm and 2.4 mm probes, respectively, is provided by the stoichiometry of the reaction:

$$4Fe(OH)_2 + O_2 = 2Fe_2O_3 + 4H_2O \quad (11)$$

In other words, all of the corroded iron (as ferrous species) at the O-S from that diffused through the oxide and that dissolved is converted immediately to ferric species (e.g., haematite), leading to predicted stifling concentrations of oxygen of 29.6 $\mu g \cdot kg^{-1}$ and 25.5 $\mu g \cdot kg^{-1}$, respectively, for the 1.6 mm and 2.4 mm probes – in good agreement with the measurements of between 38 $\mu g \cdot kg^{-1}$ and 28 $\mu g \cdot kg^{-1}$. Analyses of probe surfaces exposed to oxygen under neutral conditions indicated higher concentrations of ferric oxides than seen on probes exposed at high pH [65]. Such a difference in mechanism between the $pH_{25°C}$ 9.2 and the neutral laboratory experiments may be ascribed to the effect of pH on the oxidation of ferrous species; at low $pH_{25°C}$, fully oxidized lepidocrocite and goethite tend to be formed while magnetite is formed under alkaline conditions [66].

It is of interest that oxidizing conditions in an FAC laboratory experiment involving multiple tubular specimens exposed to $pH_{25°C}$ 9.2 water at 140 °C deposited thick layers of haematite on top of magnetite on one corroding specimen. As illustrated by the electron micrograph in Figure 13, the deposit appeared to have formed from

upstream to downstream and ended abruptly in the middle of the probe, presumably by precipitation from a high concentration of iron in solution [54]. This is another mechanism for haematite formation on component surfaces and reflects observations of haematite seen in the low- and intermediate-pressure drums of heat recovery steam generators in combined-cycle power plants.

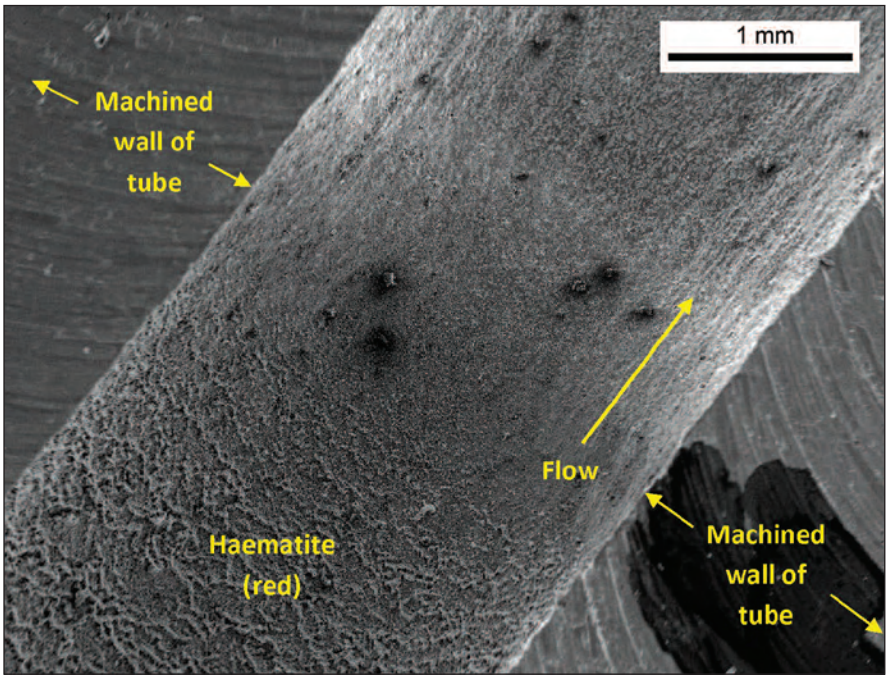

Figure 13:
Inner surface of tubular carbon steel probe showing haematite deposited on top of FAC-formed magnetite [67].

2.4 FAC and Flow

The effect of flow of water on FAC is crucial (Figure 4); however, it cannot be a simple dependence on bulk flow rate, since different sections of the same pipe containing the same fluid experience different FAC rates. Turbulence is clearly involved, because flow disturbances such as bends, constrictions, expansions, etc., which increase turbulence, are areas of increased attack. Figure 1 illustrates the increased attack downstream of a constriction (ferrule) at the place where the effects of turbulence are expected to be at a maximum (the streamlines of the flow issuing from the orifice (ferrule) reattach to the pipe surface about two pipe diameters downstream, creating a backward-circulating eddy). In fact, computational fluid dynamic (CFD) modelling of flows downstream of an orifice routinely show the position of maximum FAC to be close to the position of reattachment of the separated flow, where fluid shear stress and mass transfer are high. Poulson [68] has suggested that mass transfer profiles downstream of a sudden expansion are more likely to reflect FAC attack than shear stress profiles. Figure 14 presents the normalized measured profiles of the walls of initially identical carbon steel tubes immediately downstream of a sudden expansion after exposures of 14 days to neutral water at 140 °C at different Reynolds numbers. Figure 15 presents the corresponding values of the Sherwood number for mass transfer for the same tubes as computed with the ANSYS-CFX CFD code [69] (the Sherwood number $Sh = k_m \cdot d \cdot D_{AB}^{-1}$, where k_m is the mass transfer coefficient, d is the initial diameter of the tube and D_{AB} is the mass diffusion coefficient; Sh was computed via the corresponding

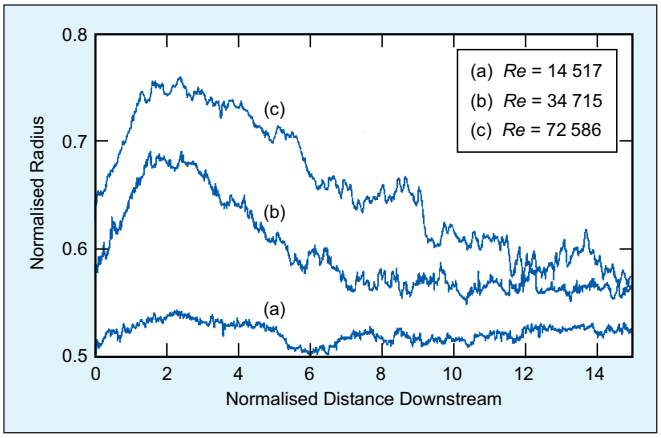

Figure 14:
Averaged experimental profiles of carbon steel tubes downstream of a sudden 100 % expansion that were exposed to laboratory neutral conditions at 140 °C for 14 days at three different pipe Reynolds numbers [69].

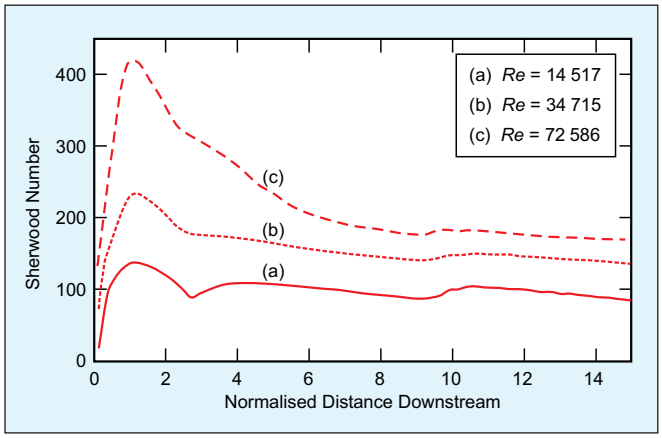

Figure 15:
Sherwood number downstream of a sudden 100 % expansion; computed for tubes in Figure 13 [69].

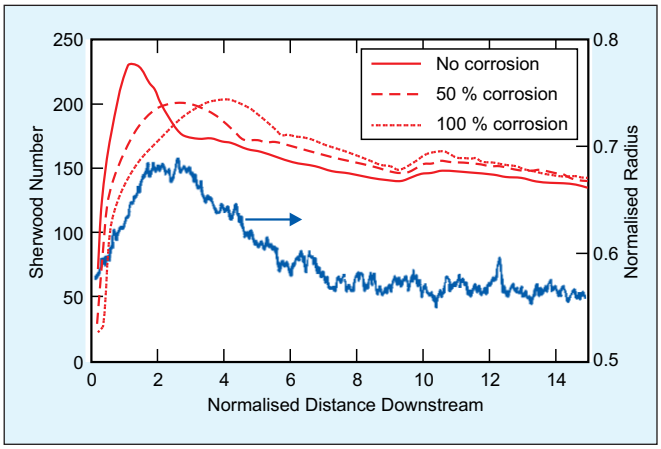

Figure 16:
Developing Sherwood number at the wall along with final corrosion profile of tube at *Re* = 34 715 in Figure 14. Diagrams from [69] superimposed.

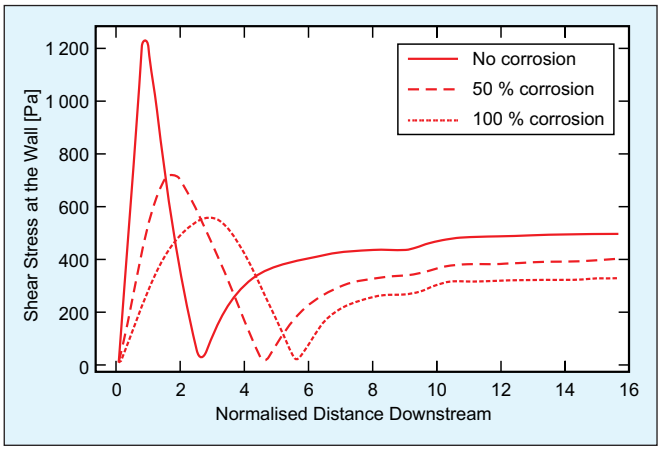

Figure 17:
Computed shear stress at the wall downstream of an expansion in a carbon steel tube (as in Figure 14); development of the profile as corrosion proceeds at *Re* = 46 770 [69].

heat transfer parameters in ANSYS, which cannot compute mass transfer directly). In such modelling, however, it is important to remember that as the FAC proceeds, the profile of the metal evolves, shifting the values and the profiles of the flow parameters. Accounting for the developing profile shifts and broadens the computed Sherwood number profile shown in Figure 15 to that shown in Figure 16, which also shows the correspondence with the measured damage profile from Figure 14.

Profiles of fluid shear stress and other flow parameters also change as the damage profile develops. Figure 17 shows how the computed profile of fluid shear stress at the wall downstream of a sudden expansion in a tube corroding with the characteristics of those illustrated in Figure 14 shifts as the corrosion damage proceeds. Like the mass transfer peak in Figure 16, the shear stress peak shifts downstream; also, the overall profile tends to flatten and it is clear that the effect of the theoretical minimum at the fluid reattachment point is distributed along the length by the damage. Reasonable correlations of FAC rate with computed static shear stress downstream of an orifice have been obtained [70].

2.5 FAC Mechanisms and Mass Transfer

Modelling of mass transfer has been done for pipe bends under CANDU reactor primary coolant conditions, although the effects of evolving damage were not considered [71]. The computed patterns were shown to correspond spatially quite well to measurements of FAC damage. It was concluded that the FAC was mass transfer controlled and could be quantified by the product of the local mass transfer coefficient and the concentration difference for ferrous ions between the O-S and the bulk water. This echoes the vast majority of papers describing FAC mechanisms and is the basis of complex codes for FAC prediction.

Theoretically, however, the mass transfer model is untenable – as has been argued before (for example, see [22]). The difficulty arises because mass transfer is only the second step in the overall mechanism. The first step is the regulation of the thickness of the oxide film by dissolution, creating half the ferrous ions at the O-S that are transported across the fluid flow boundary layer to the bulk solution; the other half arrive at the O-S by diffusion through the oxide from the M-O – Eqs. (1), (4) and (5). In a much-quoted paper, Berge [72] formulated these two steps in series as:

$$\text{FAC rate} = k_d k_m (C_{eq} - C_b)/(0.5k_m + k_d) \quad (11)$$

where k_d is the dissolution rate constant, km is the mass transfer coefficient, C_{eq} is the solubility of iron at the conditions of the FAC exposure and C_b is the concentration of iron in the bulk liquid. Because flow is clearly important in FAC, the dissolution term in Eq. (11) was ignored (implying $k_d >> k_m$) so that Eq. (11) becomes:

$$\text{FAC rate} = k_m (C_{eq} - C_b) \quad (12)$$

This is a commonly used expression; it is equivalent to the Pietralik formulation [71], since with mass transfer control the effective concentration at the O-S approaches C_{eq}. It forms the basis of computer codes for predicting FAC, such as Electricité de France's BRT-CICERO™ [73]. It is emphasized that the approach is untenable, because the dissolution step cannot be ignored. This was recognized in 2002 [64], when early data [74] on the dissolution kinetics of magnetite under reactor primary coolant conditions had indicated that for CANDU feeders $k_d << k_m$. An alternative model was developed, wherein dissolution weak-

ens the forces binding the oxide crystallites at the O-S so that fluid forces can remove them more easily and provide an additional process for thinning the oxide [75]. Microscope images of the cross-section of an oxide film on a steel that has undergone FAC under reactor primary coolant conditions reveal the aggregate crystallite structure and suggest that the mechanism is plausible (Figure 3). The mechanism of particle removal – spalling or erosion – was postulated for the model to be driven by fluid shear stress at the wall. While it has been pointed out [76] that fluid shear stresses are too weak to cause direct mechanical removal of oxide, the loosening of the crystallites by dissolution may make them amenable to removal by the weak shear forces involved. It is also possible, however, that the removal is facilitated by "freak" turbulence events propagating through the boundary layer and imposing stronger forces on the surface [75,77]. The apparent non-correspondence of shear-stress profiles with FAC damage, particularly downstream of flow disturbances where the reattachment of separated flows gives rise to a theoretical stagnation point [68], also suggests that other forces predominate, although such comments usually ignore the shifting of the profiles as FAC proceeds – as illustrated in Figure 17.

Since oxide film dissolution is a prime mechanism in FAC, it is relevant that some computed shear stress profiles across magnetite disks dissolving under the impact of a submerged jet in laboratory experiments under power plant conditions have been shown to correspond nicely to the dissolution craters. As shown in Figure 18, for a 10 mm-diameter disk impacted centrally with a jet of water at 140 °C and neutral $pH_{25°C}$ issuing from a 0.5 mm orifice, dissolution was less in the region of the central stagnation point [78]. The corresponding condition in Table 2 indicates that the dissolution was overall under dissolution control with some influence of mass transfer (the dissolution rate constant averaged over the whole crater was 2.2 $mm \cdot s^{-1}$ and the average mass transfer coefficient was 13.9 $mm \cdot s^{-1}$). Unlike the reattachment point in pipe flow after a constriction, because of the

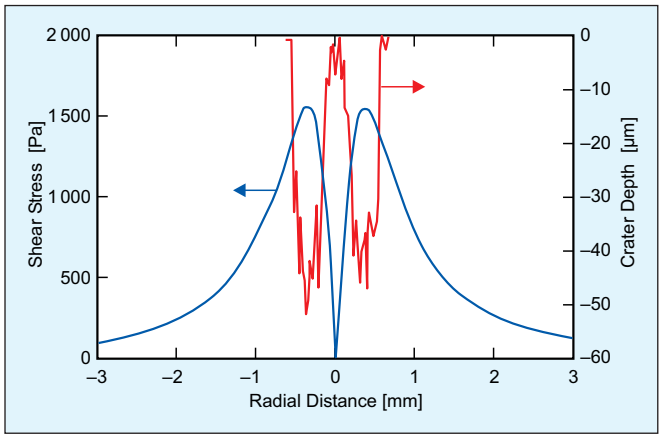

Figure 18:
Shear stress and crater profiles across a magnetite disk dissolving under the impact of a submerged jet (neutral chemistry, 140 °C) [78].

centro-symmetric geometry the stagnation point in the jet experiments evidently did not move as the surface profile developed.

Dissolution rate constants of magnetite have now been measured over a range of conditions. Table 2 summarizes the results of jet impingement experiments on sintered magnetite disks under several conditions, including those pertinent to power plants.

Mass transfer coefficients in power plant circulation systems typically range from about 2 to 20 $mm \cdot s^{-1}$, although estimates are usually from correlations formulated from results of experiments under less rigorous conditions and are clouded by uncertainty (e.g., the value for the pipe at the Mihama-3 PWR downstream of the orifice where the rupture occurred was estimated separately to be 3 $mm \cdot s^{-1}$ [80] or 30 $mm \cdot s^{-1}$ [81]). A straightforward application of k_d values from Table 2 in models such as that of Berge et al. [72] indicates that, under the alkaline conditions typical of power plant feedwater and nuclear primary coolant, FAC is controlled by dissolution kinetics

Temperature [°C]	$pH_{25°C}$	k_m in Dissolution Experiment [$mm \cdot s^{-1}$]	k_d [$mm \cdot s^{-1}$]
310	10.5 (LiOH)	47.5	0.33 ± 0.2
140	9.2 (NH3)	13.9	0.03
140	neutral	13.9	*2.13 ± 0.08
**55	neutral	5.3	0.85
**25	neutral	2.8	0.25 ± 0.05

Table 2:
Dissolution rate constant, k_d, of magnetite [79].
* One of these two runs was with single crystal magnetite.
** FAC not experienced in power plants under these conditions.

and there is minimal effect of flow – clearly an untenable conclusion. On the other hand, mass transfer is important under neutral chemistry conditions, as indicated by the experiments illustrated by Figure 10.

It is noted that the dissolution of magnetite during FAC is an electrochemical reaction; it is reductive (Eq. (6)), involving electron transfer, and therefore depends upon the surface potential attained during corrosion. Modelling [64,82] has indicated that the potential may increase these k_d values by up to an order of magnitude, depending upon the corrosion conditions, but still leave dissolution apparently controlling under the tenets of the Berge model [72]. Table 2 suggests that, under neutral conditions, some influence of mass transfer is expected at low values of Sherwood number. This is borne out by the almost linear dependence of FAC on k_m obtained in experiments under neutral conditions illustrated in Figure 10. In contrast, the very high dependence on flow measured in similar FAC experiments under alkaline conditions probably resulted from the influence of crystallite erosion [22].

A further point to consider about the application of the simple Berge-type model is that the effective saturation concentration of iron under plant conditions (C_{eq} in Eq. (12)) also depends upon the electrochemical potential of the corroding surface. For FAC under CANDU reactor primary coolant conditions, the electrochemical corrosion potential of the corroding steel has been reported [83,84] as between –0.75 and –1.0 V relative to the saturated hydrogen electrode (SHE). In early modelling of FAC [64], including the electrochemical effect in the evaluation of equilibrium solubility changed the value of C_{eq} by a factor of between 5 and 11 depending on the location in a CANDU circuit. A fully comprehensive description of FAC should incorporate the electrochemistry of corrosion, oxide growth and dissolution and couple the effects with the pertinent fluid dynamics and redox reactions of the coolant (see, for example, the extensive Japanese-led studies, in particular as they relate to FAC in nuclear systems) [85].

2.6 Two-Phase Flows

In power plants in general, wet steam systems such as in feedwater heater drains, heat recovery steam generators, deaerators, air-cooled condensers and low-pressure turbines are prone to two-phase FAC (Section 4, below). Only wetted surfaces can be affected and damage is often severe. It is to be borne in mind that the effectiveness of additives to control FAC, such as the amines, is affected by the presence of the vapour phase. Ammonia, for example, partitions to the steam phase in power plant systems and cyclohexylamine acts in similar fashion, while ethanolamine (ETA) tends to prefer the liquid phase [54]. Oxygen has little beneficial effect in two-phase systems. The volatility is to be considered along with the basicity as key properties when choosing an additive for controlling FAC. This is discussed in more detail in a later section.

At low steam qualities, the FAC resembles single-phase attack, so that the mechanisms described above are predominant. We note that the outlet feeders in the pressurized heavy-water reactor plants of the CANDU reactor type that experienced primary-coolant FAC categorized as single-phase attack in many cases had steam voidages up to 20 %. The single-phase characteristics are to be expected from regimes that have liquid as the major phase with steam as bubbles progressing to "slugs" and then to annular flows with entrained droplets and liquid films as the quality increases. High steam qualities promote thin liquid films with cores of high velocity vapour and entrained droplets and in some cases the liquid film can develop patches or rivulets. The FAC then becomes influenced by mechanical effects such as liquid droplet impingement and mechanical erosion.

If the fluid characteristics in low quality flows can be determined, the FAC can be modelled on the basis of single-phase mechanisms as described in Section 2.5. Thus, the mass transfer and fluid shear stress at the wall for steam-water flow in a tube can be determined from standard correlations and estimates of the friction coefficients of the separate phases, based on the fluid properties and the phase Reynolds numbers. If the chemistry conditions of the liquid vis à vis the vapour and the susceptibility of the steel (e.g., from the chromium content) are known, these parameters may be put into a single-phase model and the FAC estimated. Figure 19 presents the predictions and measurements of FAC in experimental tubes exposed in a laboratory loop at 200 °C to chemistries with different amines at $pH_{25°C}$ 9.2 and over a range of steam voidages [86].

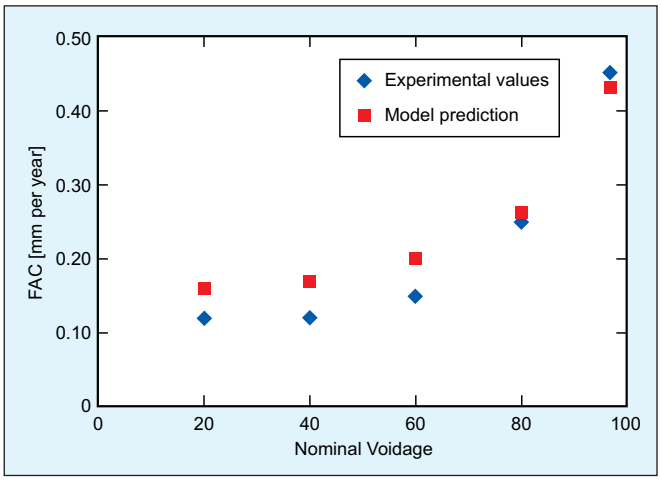

Figure 19:
Predictions and measurements of two-phase FAC in an experimental water loop: 200 °C, on-line probes of 0.019 % Cr steel, $pH_{25°C}$ 9.2 with different amines [86].

The more severe physical conditions at high steam qualities promote higher FAC rates. Irregular patterns of damage occur, such as "tiger striping", when the corroding film flows in rivulets, or "shot-gun", when entrained liquid droplets impact the surface at high velocity (see examples in later sections). The latter, termed "liquid droplet impingement" or LDI, often has the characteristics of cavitation erosion/corrosion. As described below, the latter is seen in air vent lines and feedwater heaters in steam raising plant. It is often subcategorized into LDI corrosion and LDI erosion [87]. LDI corrosion is like aggravated single-phase FAC controlled by chemistry, metal properties, droplet size and collision velocity determined by the overall flow pattern. LDI erosion has been described empirically with a relation linking R, the ratio of volumetric metal loss to volume of liquid impinged, with v_r, the droplet collision velocity, and d_p, the droplet diameter:

$$\log(R) = 4.8\log(v_r) - \log(N_e) - 16.65 + 0.67\log(d_p) - 0.22K \quad (13)$$

where N_e is an "erosion resistance number" [88] that depends on the mechanical properties of the metal and allows direct comparisons of the metal with other metals, and K is a geometry factor ranging from 0 for a plane surface to 1 for a curved surface. According to Okada et al. [87], LDI erosion causes significant wall thinning at steam velocities greater than 200 $m \cdot s^{-1}$ for steam qualities between 95 % and 99.8 % and droplet diameters between 5 and 100 µm.

2.7 Scalloping

FAC is usually accompanied by a sculpting or characteristic dimpling of the corroding surface called scalloping that produces a cuspate texture. Many examples found in industrial equipment are shown in Section 4.7. Figure 20 is a scanning electron image of an example of the scalloping found in the outlet feeder pipes of CANDU reactors that used a low chromium (0.019 % Cr) steel; the contacting coolant was heavy water (note that the $pH_{apparent}$, in the example adjusted with lithium oxide, is the apparent $pH_{25°C}$ of the solution in D_2O measured at room temperature with an electrode calibrated in H_2O solution). Unlike at feedwater temperatures, at primary coolant temperatures the solubility of magnetite increases with $pH_{25°C}$ (Figure 6) so that increasing alkalinity increases FAC rates. The scallops in the figure are roughly 0.5–0.75 mm across and 0.2 mm deep and are covered with a magnetite film of average thickness 0.8 µm; the corrosion rate averaged over the 14 years of exposure was 110 µm per year [64].

There are natural analogues of corrosion-induced scalloping. The sculpting of river beds and caves by fast flowing streams often produces scalloped formations of much larger scale than the FAC-formed scallops in pipes, ascribed to the uneven dissolution of the rock by the adjacent turbulent fluid [90]. The hollows and grooves on melting ice surfaces have been ascribed to the cellular properties of vortices in the adjacent air [91], and snow fields can develop scalloped surfaces by turbulent air flows. At a different scale, the scalloping of the snow field in Antarctica (Figure 21) bears a remarkable resemblance to that of the feeder pipe in Figure 20.

Many of the ideas of scallop development, including attempts to determine whether they originate from defects in the surface or are solely dependent on the fluid dynamics, have derived from experiments on water flowing over plaster of Paris. Allen [90] incised defects on plane plaster surfaces in a rectangular channel and watched how they grew into "flutes" (like heel impressions) and "grooves" (narrow flutes) with exposure time. With no artificial initiation, they formed naturally from inherent defects in the plaster and as many developed with time they merged into scallop patterns. The concept of a scallop Reynolds number of 23 000, in which the characteristic dimension is the average scallop size, emerged from hydrodynamic studies at about this time [93]. Later work [94] compared the behaviour of tubular surfaces of pure plaster with that of surfaces of plaster seeded with sand grains under the same dissolution conditions and concluded that defects were necessary for scallops to form. Attempts to model the effects of scallops on FAC have largely concentrated on the increased mass transfer [95,96], typically calculated from the classic analogy with pressure drop as the scallops present a relative roughness at the pipe wall. This approach is a simplification, however, since the natural profiles of scallops make the pressure drop in the contrary direction of flow greater than that in the direction of flow that created them, while the latter situation has promoted pressure drops that cannot be modelled realistically with the classic relative roughness concepts [97].

Early observations of the scallops formed by the FAC of reactor outlet piping (as in Figure 20) led to the opinion [98] that the fluid dynamics were responsible for the patterns formed during corrosion, and that the properties of the metal had little or no influence. It is instructive to compare the patterns from such industrial pipes with those generated in small tubes in laboratory experiments. Figure 22 shows the inner surface of a low chromium (0.001 % Cr) carbon steel tube that underwent FAC for 184 days under feedwater conditions ($pH_{25°C}$ 9.2 with ammonia, temperature 140 °C). The bore was 2.4 mm initially and has increased to 3.2 mm, indicating an average FAC rate of 0.8 mm per year. We can compare these scallop characteristics, generated at an average pipe Reynolds number of 6.0×10^4, with those of the reactor pipe in Figure 20 at a Reynolds number of 8.0×10^6. The scallop size in the small bore sample averages ~ 0.7 mm, indicating a scallop Reynolds number of 19 000, while in the reactor pipe the scallop Reynolds number is 63 000. The concept of a universal scallop Reynolds number clearly does not apply to such examples of FAC.

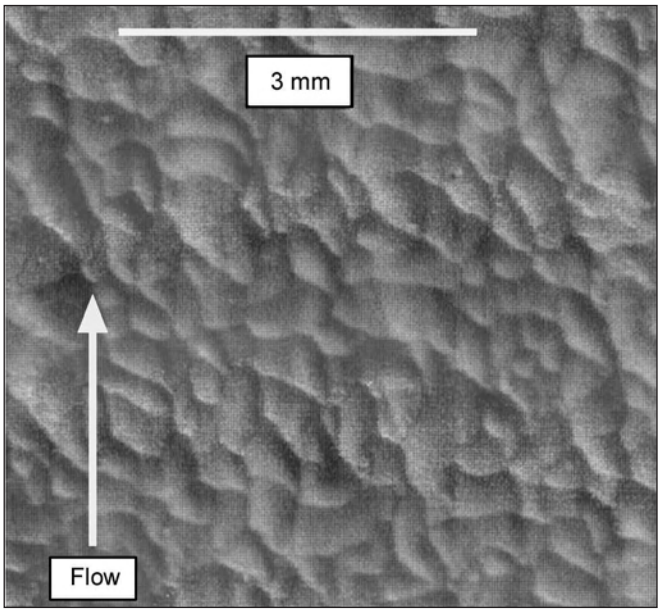

Figure 20:

The inside surface of an outlet feeder from the Point Lepreau CANDU reactor removed after ~ 14 years of operation [89]: pipe nominal inner diameter 6.4 cm, 0.019 % Cr steel, coolant heavy water at 310 °C, $pH_{apparent}$ ~ 10.6, velocity 16.2 $m \cdot s^{-1}$.

Figure 21:

Scalloped surface of Antarctic snow field produced by effects of sun and katabatic winds [92].

It is likely that the scale of turbulence combines with inhomogeneities in the metal surface to determine the final scallop pattern. The latter influence the oxide structures, which grow differently on the different metal grains and over pearlite can protrude up to a micrometre or so above the oxide on surrounding ferrite – as in the higher magnification views in Figure 22. Similarly, Figure 23 shows the irregular profile at high magnification of the magnetite film formed on an experimental specimen exposed for 28 days to neutral water at 140 °C with < 10 $\mu g \cdot kg^{-1}$ dissolved oxygen; the average FAC rate was 4.8 mm per year. The protruding, coral-like morphology of the magnetite oxide on the pearlite grains in the metal can be seen.

As the surface corrodes and recedes, new scallops are initiated as the oxide structures disturb the flow; some develop and some are wiped away. This suggests that for a given turbulence regime, the finer the grain structure of the metal, the more numerous will be the scallops. The cross-section micrographs in Figure 24 show the pearlite structures of the steels in Figures 20 and 22; the finer structure in the former is clear.

Moreover, it is noted from the turbulence theory of Kolmogorov [99] that the smallest turbulent eddies in the large pipe at the high Reynolds number are about half the size of those in the small tube at the lower Reynolds number (in both the pipe and the tube the ratio of the smallest to the largest is approximately equal to $Re^{-0.75}$). Accordingly, the tube, which has the smaller Reynolds number and the larger pearlite grains in its metal microstructure, would tend to generate larger scallops than the industrial pipe – as is observed. Also, regions of higher turbulence in a single piece of equipment, such as downstream of an orifice or in the extrados of an elbow in a pipe, have higher FAC rates than elsewhere; they have smaller scallops [100,101], again corresponding to smaller local eddies.

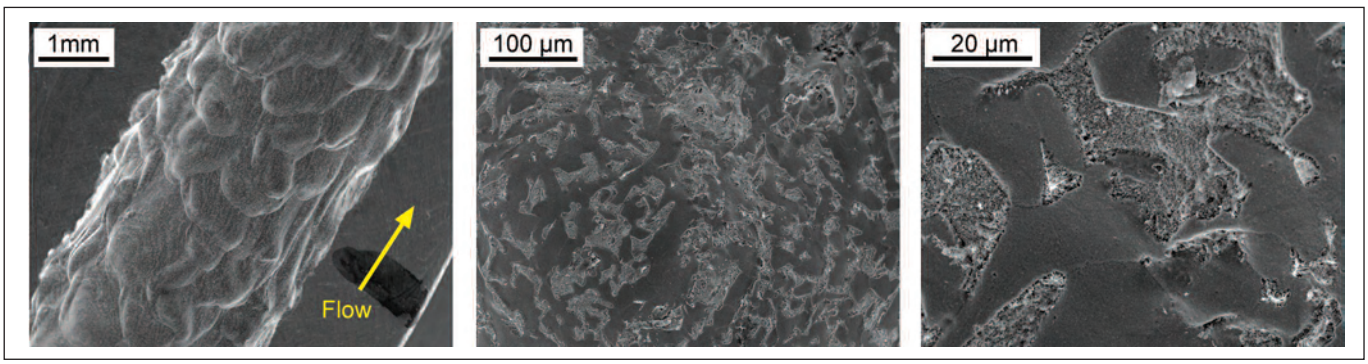

Figure 22:

SEM pictures of inner surface of small bore tube of carbon steel after 184 days exposure to water at 1.6 $L \cdot min^{-1}$, 140 °C, $pH_{25°C}$ 9.2 (ammonia).

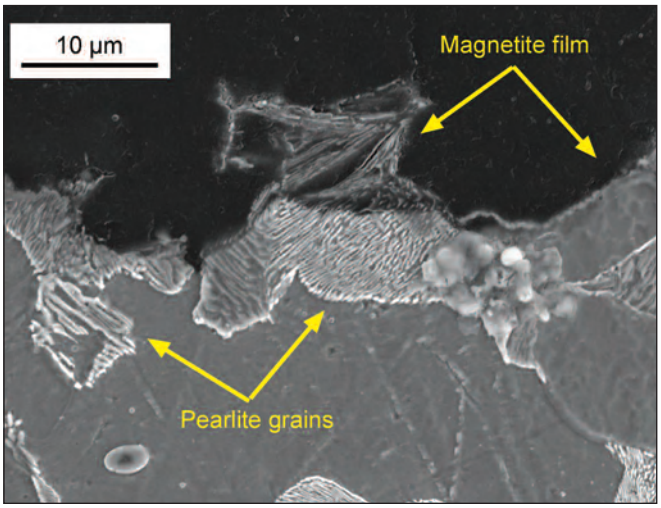

Figure 23:
Section through specimen of STPT carbon steel and oxide film developed during 28 days of exposure to neutral water at 140 °C.

In two-phase steam-water flows as in wet steam lines, feedwater heater drains, deaerator-separator equipment, etc., the local characteristics of scallops are similar to those in single-phase equipment. Scalloping in fossil and combined-cycle/HRSG plants is discussed in Section 4.7. However, because FAC only occurs on water-touched surfaces and because the water-steam distribution depends upon local geometry, steam quality and bulk flow, the overall patterns of FAC vary from place to place. Within the liquid film, however, the mechanisms of FAC as described above for single-phase systems still apply. Thus, besides the fluid dynamics, the local chemistry is important; as detailed earlier, all-volatile treatment (AVT), for example, may have the $pH_{25°C}$ component distributed to the steam phase leaving the liquid relatively corrosive, while oxidizing environments and oxygenated treatment are ineffective in the two-phase regions for the same reason. Corroded equipment opened after exposure often shows regions where liquid has created FAC adjacent to non-corroded regions. Presumably, once a region of FAC has been established, the liquid will tend to channel there and exacerbate attack. The so-called "tiger-striping" is a severe example of this. Examples are presented in later sections below.

2.8 Commercial Codes

Several computer codes have been produced to manage FAC in power plants, most of them for application to nuclear systems. Their objective is to provide information that allows operators to minimize the potential for damage to piping and components. Basically, they are data management tools, taking measurements of wall thickness from the prescribed monitoring of pipework and components and pointing out areas of vulnerability. As will be seen, any predictive capability is ultimately empirical, using derived functions to incorporate the effects of material, fluid flow and chemistry and making adjustments as plant information becomes available. Interpolation and extrapolation of measurements from ultrasonic testing, for example, indicate the situation in remote areas and the potential for excessive damage. If a mechanistic model is employed, as mentioned in Section 2.5, it too will have parameters that are adjusted to conform to measurements. The major codes have been described in some detail elsewhere (see, for example, [28]); here, only brief descriptions are provided with comments.

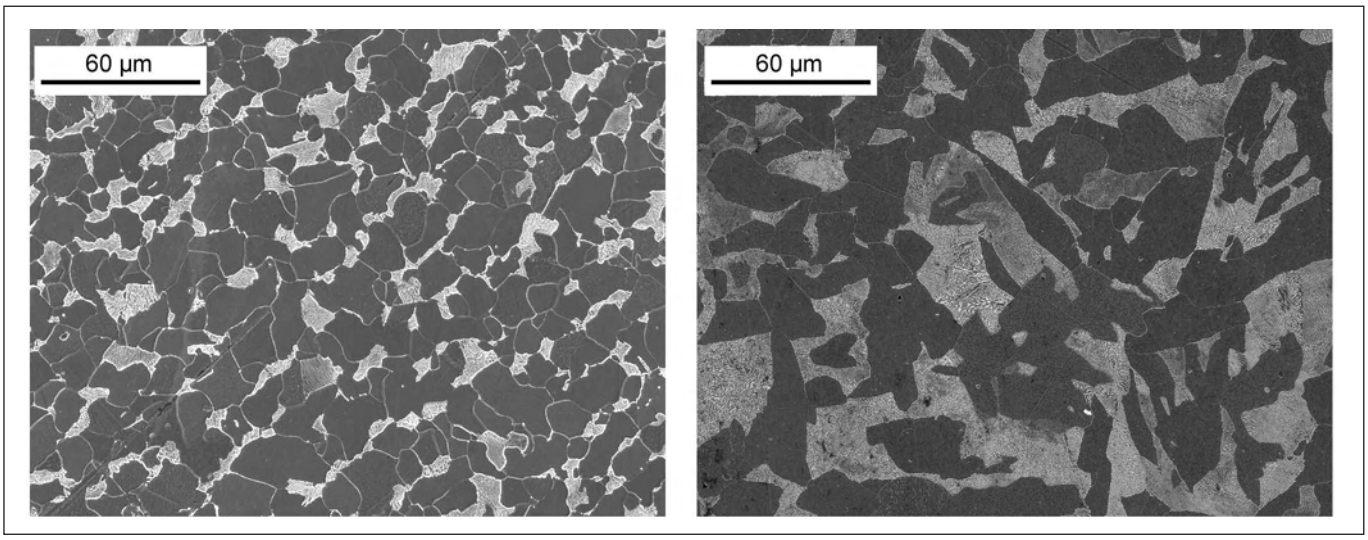

Figure 24:
Micrographs of polished and etched cross-sections: left – SA 106 Grade B steel (from archived feeder pipe at Point Lepreau nuclear plant); right – STPT 480 steel (from experimental FAC probe).

The most widely used software internationally is Checworks®, along with the Chec suite of derivative codes such as Checmate®. It was developed by the Electric Power Research Institute in the US. The basic principles are incorporated into a version produced for fossil plants – the Fossil FAC Advisor®. The computer algorithm calculates the FAC rate as the product of factors that describe the effects of temperature, mass transfer, geometry, pH, oxygen level, alloy composition and steam quality. Interestingly, it purports to be based upon the Berge model [72] but ignores the dissolution kinetics of the corrosion product oxide (magnetite); as discussed in Section 2.5 above, this creates an anomaly, which is presumably overcome by adjustment of the factors as the algorithm is validated against the database of plant and laboratory measurements. A Checworks® user typically sets up a model of the plant with design parameters, heat balances, etc., and inputs up-to-date operating conditions, material and geometry of components (size and wall thickness), information on any component replacements, and inspection data. The program predicts FAC rates and wall thicknesses for susceptible lines and compares predictions with inspection data. The time to reach critical thickness is provided. The Checworks Owners Group (CHUG) have alerted plant operators to the possibility of increased attack immediately downstream of a component of more resistive material, since the fluid boundary layer there is relatively low in dissolved iron and therefore more corrosive (the so-called entrance effect [102] – not to be confused with the entrance effect from the development of the hydraulic boundary layer, although the two must interact).

Electricité de France (EDF) developed the BRT-CICERO® code from mechanistic principles. The basis is the Berge model [72] for FAC, ignoring the oxide dissolution kinetics and thereby introducing the anomaly discussed in Section 2.5. Mass transfer then becomes the controlling factor, and is calculated with a standard correlation for straight pipe modified for other geometries with an empirical factor. Many loop experiments verified the mass transfer relations. For piping elements, the correlation accounts for scalloping by introducing a constant value for roughness height of 40 μm (see Section 2.7 above for comments on the effects of scalloping). Material effects are taken into account with factors for the concentrations of chromium, molybdenum and copper raised to powers less than one. Chromium has the biggest effect, but is assumed to have a threshold value as in Figure 9 (the inapplicability of this assumption is discussed in Section 2.2). Oxygen influences single-phase FAC depending upon its access to surfaces by the mass transfer coefficient. The mechanism is assumed to be the formation of haematite rather than magnetite (see Section 2.3 for a discussion of oxygen effects); a threshold concentration of between 7 and 15 $\mu g \cdot kg^{-1}$ is assumed from loop experiments at high temperature. As experience with BRT-CICERO® in all the French plants has grown and a huge database has accumulated, a probabilistic treatment of the measurements has evolved in order to improve the reliability of predictions and optimize the frequency of inspections and maintenance operations. Input measurements include pipe thicknesses (taken on prescribed grid patterns), material chromium content, thermalhydraulic conditions and geometry for each component, and operating chemistry during the cycle. The program indicates high risk areas for component thinning and has been successful at indicating severe damage. It appears to be highly conservative for some components [103].

After the accident from severe FAC at the Surry PWR in 1986, KWU/Siemens-AG in Germany developed the WATHEC code to analyse inspection data and help plant operators prevent further damage to piping systems [104]. It is applicable to two-phase steam-water systems as well as single-phase water flows. The empirical relationships between pipe wall loss and operating parameters such as flow rate, temperature, material composition and pH were established early on in a comprehensive laboratory programme at the AREVA test facilities. Geometry factors were included to account for bends, tees, constrictions, etc. Two-phase flows were included by applying the relationships in the context of the liquid film, taking into account the distribution of alkalizing agents and oxygen between the liquid and vapour. As plant data became available, the relationships were continually refined. The code selects lengths of piping that are susceptible and then identifies specific locations for potentially high FAC on the basis of flow and geometry. The predictive model estimates the wall thinning and assesses it in the light of the information in the plant database. Since 1998, the code has been expanded and absorbed into the COMSY software system as a comprehensive tool for component aging and plant life management in general. A COMSY user supplies a model of the plant system and its thermalhydraulic parameters along with material compositions, chemistry conditions, etc. In-depth analyses require component details such as manufacturing tolerances and yield stress and are typically presented as charts of lifetime evolution.

The RAMEK code was developed in Russia towards the end of the 1980s to predict FAC in single-phase water and two-phase steam-water systems. The mechanisms are purported to be substantially different between the two [105]; however, the basic processes of attack on the magnetite layer occurring within the liquid film in wet steam or low quality flows seem to be the same as those within single-phase water flows when the flow characteristics and the partitioning of additives and dissolved gases between liquid and vapour are taken into account. The flow regime in steam-water mixtures is taken to be the more aggressive, with high shear stresses and droplet impingement leading to mechanical erosion of the contacted surfaces.

The regime of FAC arising from the removal of dissolved iron is described by a combination of the conventional convective mass transfer coefficient and a coefficient accounting for the increased turbulence that occurs in local "freak" events such as the turbulent bursts mentioned in Section 2.5. The coefficients are additive in a rate equation equivalent to Eq. (12). The second FAC regime, from the removal of particulate oxide, is assumed to be proportional to a combination of the average fluid shear stress at the wall and an extreme value of shear stress. The expressions for the two FAC regimes are additive and their contained constants, dependent on the material properties and the thermalhydraulic and chemistry parameters of the system, were developed and refined from an extensive programme of laboratory experiments. RAMEK is used routinely to estimate the FAC of piping of components and to predict the places of maximum attack. It contains a database of plant systems, listing the susceptible areas and their measured FAC, and is often utilized as a tool for organizing inspection programmes and maintenance schedules. Betova et al. [28] mention a later series of codes, the ECI series and the ECI-DS code, that have been qualified for application in the water-water energetic reactor (VVER) reactors. Although no details are available, the codes appear to be based on the same mechanistic principles as RAMEK. The ECI-01 version is shown to be generally conservative in predicting pipe wall loss.

In summary, in the light of recent information and analyses, it is clear that the fundamental mechanisms upon which several of the commercial codes are based are flawed. That may account for differences in predictive capability that became evident during the recent international benchmarking study organized by the International Atomic Energy Agency (IAEA) [2I]; the no more than "fair" agreement among the codes was attributed to variations in the theory and the models employed [106]. Nevertheless, the empiricisms that are introduced to fit the codes to measurements and the continual adjustments that are made as databases expand appear to be sufficient to lead to acceptable predictions of component degradation by FAC within individual plants. At the very least, the pin-pointing of high risk areas and the data management capabilities of codes make them useful tools for plant operators.

2.9 Summary of FAC Mechanisms

Section 2 has discussed in detail the latest thoughts on the theory and mechanisms of FAC. Figure 25 shows a simple schematic of the mechanisms in terms of the chemical reactions and processes occurring within the oxide film under reducing conditions. As mentioned earlier, it is equivalent to the pores-solution model for the general corrosion of carbon steel in solutions saturated or near-saturated in dissolved iron, only with dissolution occurring at the oxide-solution surface instead of the precipitation of an outer layer.

Control is afforded by the protectiveness of the oxide film, which regulates the various diffusion processes. In the simplest explanation, water is assumed to percolate easily to the metal, where the anodic reaction produces ferrous ions and the balanced cathodic reaction generates hydrogen atoms ("nascent hydrogen") and hydroxyl ions. At high temperature (~ 300 °C), all the hydrogen atoms effuse through the metal (in Figure 25, x = 12) but at lower temperatures some will combine to form molecules that make their way through the oxide towards the bulk fluid. The ferrous ions at the metal-oxide interface combine with the hydroxyl ions to form dissolved ferrous hydroxide, half of which decomposes oxidatively to magnetite to fill the volume of metal that has reacted and releases hydrogen molecules that diffuse towards the fluid. The other half diffuses through the oxide and is itself released to the bulk fluid (in normal corrosion it would precipitate as the magnetite outer layer). At the outer surface of the oxide (the O-S) the magnetite dissolves reductively to ferrous hydroxide, at steady-state consuming exactly the amount of hydrogen produced by its formation at the metal surface (the M-O). Conditions that increase the dissolution rate, through chemistry by increasing the magnetite solubility and dissolution kinetics and through fluid dynamics by increasing the mass transfer and removal of dissolved iron from the surface, tend to thin the oxide and increase the transport processes, leading to increased corrosion and magnetite production at the M-O until steady-state is resumed. The thinner the oxide, the faster is the FAC. Typical oxide films in single-phase feedwater systems are up to a micrometre or so thick, but under two-phase conditions below ~ 150 °C they can be a fraction of that, actually appearing as interference films if they are coherent enough (see below). The steady-state situation in Figure 25 shows how six atoms of iron oxidized/corroded at the M-O are balanced by six molecules of ferrous hydroxide released in solution at the O-S to be carried across the fluid flow boundary layer by mass transfer. Increased turbulence thins that boundary layer and increases the mass transfer, in turn increasing the oxide dissolution and the FAC rate. The dissolution can promote the erosion or removal of oxide particles by fluid forces.

The chemistry of the fluid influences FAC by affecting the oxide dissolution; under feedwater conditions the dissolution rate and solubility of magnetite are at a maximum at ~ 140 °C and decrease with increasing pH (Figure 5), so an alkalizing agent is added to minimize FAC. Under nuclear reactor primary coolant conditions, the solubility increases with $pH_{25°C}$ above ~ 10 and increases with temperature above ~ 300 °C, so alkalinity is kept at the bottom of the allowable range to minimize FAC. Under both sets of conditions, however, the dissolution rate constant of magnetite is lower than the mass transfer coefficient and in the

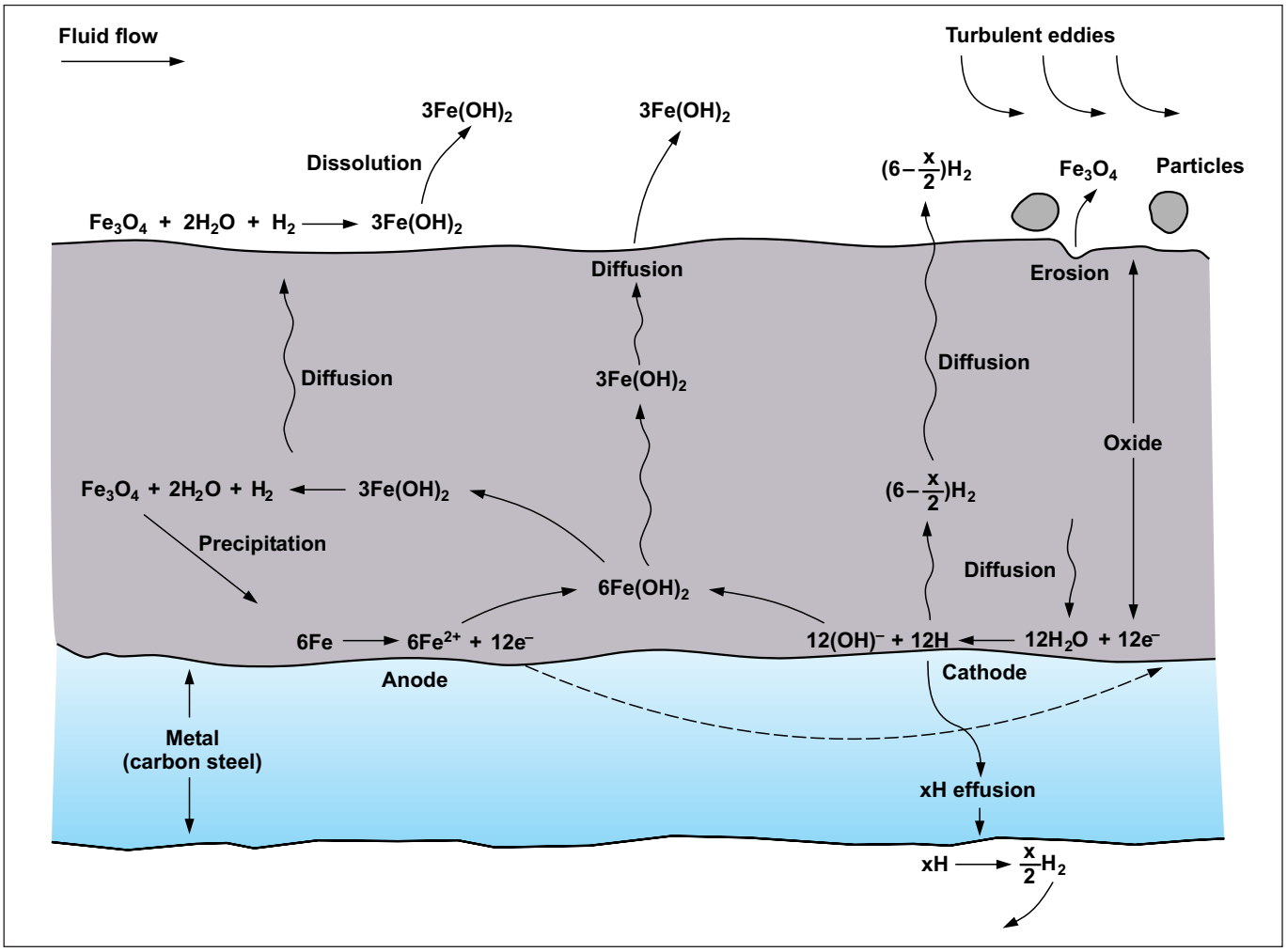

Figure 25:
Schematic of the mechanism of FAC at steady-state, showing the associated stoichiometrically balanced chemical reactions and transport processes.

basic pores-solution model would control, leading to no effect of fluid flow. To overcome this anomaly, modelling has quantified the particulate erosion induced by fluid-dynamic forces and facilitated by dissolution; this complementary process for thinning the oxide has led to good predictions of observed FAC rates.

If the conditions of the scheme in Figure 25 are made sufficiently oxidizing by introducing dissolved oxygen to the system, magnetite is produced with no accompanying hydrogen and the dissolution at the O-S stops, stifling the FAC. Prolonged exposure to oxygen tends to convert magnetite and to produce ferric oxides such as the virtually insoluble haematite and lepidocrocite.

3 Cycle Chemistry Aspects of Controlling FAC

Section 2 has provided an extensive discussion on the theory behind the FAC mechanism, and illustrated that in all generating systems FAC is controlled by the cycle chemistry used on the plant. As will be discussed later, operating with non-optimum chemistry controls and procedures most often leads to FAC in fossil and combined-cycle/HRSG plants. In nuclear plants, feedwater systems are operated primarily to minimize risks to the reactor in direct-cycle plants and to the steam generator (SG) in dual-cycle plants. This entails in large part controlling corrosion product transport. The boiling water reactors (BWRs) control ingress to the reactor mostly with high-efficiency filtration and condensate polishing. The dual-cycle reactors rely on chemistry adjustment to protect the SGs; high pH decreases FAC and corrosion product ingress while reducing conditions minimize the risk of stress corrosion cracking (SCC). Since the latter conditions are likely to promote FAC of carbon steel, plants with vulnerable materials must optimize the chemistry. At the same time, regular inspections to keep track of pipe wall thinning are a crucial requirement; the incidents in Table 1 above were in poorly monitored areas.

The purpose of this sub-section is not to provide a treatise on cycle chemistry for power plants but to discuss documented principles of chemistry control to mitigate FAC. For nuclear plants, chemistry is most often specified by the reactor vendor and complemented with recommendations from research and development efforts by industry organizations such as the Electric Power Research Institute (EPRI) in the US, VGB PowerTech in Germany and Electricité de France (EDF) for light water reactors, and the CANDU Owners Group (COG) for the Canadian pressurized heavy water reactors (PHWRs). Details of the control schemes are not generally available to outsiders [107,108] but the overall principles are similar and are often disclosed in publications and conference proceedings [109]. Their applications to FAC control are discussed briefly below. Likewise, for fossil and combined-cycle/HRSG plants, brief outlines of the most recent chemistries advocated by IAPWS for the control of FAC are included in the next section [23–26,45,110].

3.1 Cycle Chemistry Treatments for Fossil and Combined-Cycle Plants

Most often a volatile alkalizing agent, usually ammonia, is added to the condensate/feedwater to increase the pH. Alternatively, an alkalizing amine can be added in place of ammonia. Recently there are examples of film-forming substances (FFS) being added instead of the ammonia or alkalizing amine to help address FAC [45]. FFSs include film-forming amines (FFA), film-forming amine products (FFAP) and film-forming products (FFP) which do not contain an amine. These FFSs are usually proprietary compounds where the exact composition is not known by the user and most often they are supplied as blends with an alkalizing amine and then referred to as a film-forming amine product. Much work is currently being conducted internationally to provide guidance on these FFSs to confirm their ability to reduce FAC (see also Section 2.2).

Following are descriptions of the three commonly used volatile treatments that can be applied to the condensate and feedwater in fossil plants and to condensate, feed - water and evaporator water in combined-cycle/HRGS plants. As these treatments are controlled and defined by the oxidation-reduction potential (ORP), a few words are first provided on this important parameter [111].

ORP is identical to the redox potential that is used extensively in electrochemistry and corrosion science. ORP should not be confused with corrosion potential, although its value does provide a useful indicator of the corrosivity of the environment. The ORP reflects the oxidizing/reducing power of the environment, and the corrosion potential reflects the corrosion reaction occurring on the metal surface. The corrosion potential generally reflects the ORP, but they do not have the same value. ORP can be an excellent tool to control fossil plant feedwater chemistry, corrosion and FAC. However, care has to be taken in interpreting the values measured as ORP changes with $pH_{25°C}$, partial pressure of oxygen in the solution, mass transport properties, flow rates and the materials in the cycle. Thus, ORP cannot be directly compared from unit to unit, and similar units containing similar amounts of oxygen and/or reducing agent will not necessarily read the same ORP, because of differences in measuring parameters. Also, the voltage at which conditions change from "reducing" to "oxidizing" (redox neutral potential) will not always be the same. But ORP can be used to control the oxidizing power of the feedwater in all-ferrous systems, or the reducing power of the feedwater for mixed-metallurgy feedwater systems. The former is rarely used in practice, but the latter is the vital control for mixed-metallurgy feedwater systems [24].

AVT(R) – All-Volatile Treatment (Reducing) [24]
This treatment involves the addition of ammonia or an amine, an FFS, a blend of amines of lower volatility than ammonia and a reducing agent (usually hydrazine or one of the acceptable substitutes such as carbohydrazide) to the condensate or feedwater of the plant. In combination with a relatively low oxygen level (from air in-leakage) of about 10 $\mu g \cdot kg^{-1}$ or less in the condensate (usually measured at the condensate pump discharge, CPD), the resulting feedwater will have a reducing ORP. Higher levels of oxygen (> 20 $\mu g \cdot kg^{-1}$) (due to high air in-leakage) will usually preclude generation of the reducing environment, but are often incorrectly accompanied by excessive dosing of the reducing agent. AVT(R) provides protection to copper-based alloys in mixed-metallurgy feedwater systems in fossil plants. AVT(R) should not be used in multi-pressure HRSG systems due to concerns for single-phase FAC as discussed in Section 2. Thus, a key basic international rule is that reducing agents should not be used in fossil plants with all-ferrous feedwater systems and in combined-cycle/HRSG plants to prevent single-phase FAC [24].

AVT(O) – All-Volatile Treatment (Oxidizing) [24]
This all-volatile treatment has emerged as the much preferred treatment over the last 25 years for fossil plant feedwater systems which only contain all-ferrous materials (copper alloys can be present in the condenser) [112] and for combined-cycle/HRSG plants. In these cases, a reducing agent should not be used during any operating or shutdown/layup period. Ammonia or an amine, an FFS, or a blend of amines of lower volatility than ammonia is added at the CPD or condensate polisher outlet (if a polisher is included within the cycle). This is the treatment of choice for multi-pressure combined-cycle/HRSG plants which have no copper alloys in the feedwater. In combined-cycle/HRSG plants with relatively good control of air in-leakage (oxygen levels in the range 10–20 $\mu g \cdot kg^{-1}$), the resulting feedwater will yield a mildly oxidizing ORP.

OT – Oxygenated Treatment [24]
For conventional fossil plants, optimized OT involves one oxygen injection location at the condensate polisher outlet (CPO), operating with the vents on the feedwater heaters and deaerator closed. Ammonia is added at the condensate polisher outlet. There is often a minimum level of oxygen which is required to provide full passivation of the single-phase flow locations in the main feedwater line and the drain lines, and to maintain this protection. For drum units, this is usually between 30 and 50 $\mu g \cdot kg^{-1}$ at the economizer inlet (with the actual level being set in accord with the boiler recirculation ratio), and for once-through/supercritical units this is usually 30–150 $\mu g \cdot kg^{-1}$ at the economizer inlet. Application of OT in combined-cycle/HRSG plants is much rarer, but often it is found that the use of AVT(O) with low levels of oxygen ($< 10 \mu g \cdot kg^{-1}$) on these plants does not provide sufficient oxidizing power to passivate the very large internal surface areas associated with preheaters, LP, intermediate-pressure (IP) and high-pressure (HP) economizers, and LP evaporators, especially if a deaerator is included in the LP circuit. In these cases, oxygen can be added at the same level as for conventional recirculating cycles. This is the feedwater of choice for fossil units with all-ferrous feedwater heaters and a condensate polisher and with an ability to maintain a conductivity after cation exchange (CACE) of $< 0.15 \mu S \cdot cm^{-1}$ under all operating conditions.

Boiler water treatment is commonly applied to avoid FAC in the LP and IP evaporators and economizer circuits of the HRSGs of combined-cycle plants. Two non-volatile alkalizing agents which can be used for this are tri-sodium phosphate (phosphate treatment (PT)) or sodium hydroxide (caustic treatment (CT)) [25]:

PT – Phosphate Treatment [25]
Phosphates of various types have been the bases of the most common boiler/HRSG evaporator treatments worldwide. However, historically there has been a multitude of phosphate compounds and mixtures blended with other treatment philosophies, which have resulted in a wide range of control limits for the key parameters (pH, phosphate level, and sodium-to-phosphate molar ratio) and a number of reliability issues. Most recently, for more than 25 years, consolidated good operating experiences worldwide have led to the recognition that tri-sodium phosphate (TSP) should be the only phosphate chemical added to a boiler/HRSG, and that the operating range should be bounded by a sodium-to-phosphate molar ratio of 3:1, a TSP level of 1 $mg \cdot kg^{-1}$ with a minimum of 0.3 $mg \cdot kg^{-1}$, and NaOH to give a $pH_{25°C}$ above 9.0. This precludes addition of mono- and/or di-sodium phosphate and thus eliminates the possibility of acid phosphate corrosion. It should also be emphasized that the 0.3 $mg \cdot kg^{-1}$ level is regarded as a minimum and that better protection will be afforded by operating at as high a level of phosphate as possible without exceeding the steam sodium limits.

CT – Caustic Treatment [25]
Caustic treatment (CT) can be used in HRSG drum-type boilers to reduce the risk of FAC where all-volatile treatment has proved ineffective, or where PT has been unsatisfactory due to hideout or has experienced difficulties of monitoring and control. The addition of sodium hydroxide to the boiler/evaporator water has to be carefully controlled to reduce the risk of caustic carryover into the steam, which could lead to damage of steam circuits and turbines due to stress corrosion cracking.

The application and use of film-forming substances (FFS) in fossil and combined-cycle/HRSG plants has been increasing worldwide and has shown a reduction in FAC rates in fossil and combined-cycle/HRSG plants, and in air-cooled condensers as discussed later in this paper.

FFSs – Film-Forming Substances [45]
As described earlier (Theory, Section 2.2), FFSs work in a different way from the conventional treatments by being adsorbed onto metal and metal oxide/deposit surfaces, thus providing a physical barrier at the molecular or multimolecular level between the water/water-steam and the surface. Evidence of adsorbed films is provided by the hydrophobic properties of the surfaces of drained components after treatment. There are three main active chemical substances which have been used historically: octadecylamine (ODA), oleylamine (OLA) and oleylpropane diamine (OLDA). As well as these compounds, other substances such as alkalizing amines, emulsifiers, reducing agents, and dispersants (e.g., polycarboxylates) are often contained in commercial FFSs. There is currently much confusion about their application for normal operation and for shutdown/layup, and there has not been any international guidance until a document issued recently by IAPWS [45] on deciding whether to use an FFS and whether it will provide a benefit to the plant. An FFS must be customized to each plant, which requires an extensive cycle chemistry review prior to application of the FFS. The FFS is added at the CPD or polisher outlet (if a polisher is included within the cycle). There are an increasing number of experience reports that FFSs provide single- and, in some areas of the plant, two-phase FAC protection (see Section 2.2).

3.2 Cycle Chemistry Treatments for Nuclear Plants

Minimizing the generation and transport of corrosion products in the feedwater system is a priority of nuclear plant chemistry control. In boiling water reactors (BWRs), corrosion products enter the reactor directly and can affect the performance of the fuel; their transport is controlled by condensate polishing and high performance filtration. In the dual-cycle reactors, the steam generators can undergo efficiency losses from tube fouling by corrosion products, which at the same time can harbour and

concentrate aggressive impurities; their ingress is controlled largely by chemistry. As of 2017, there were reportedly [113] 1281 steam generators operating in water-cooled nuclear reactors around the world and 193 under construction. The PWRs have tubing alloys of Incoloy (Alloy 800) and Inconel (Alloy 600 and Alloy 690), the VVERs of austenitic stainless steel (with later models using nickel alloy), and the PHWRs of Alloy 800, Alloy 600 and Monel (Alloy 400). Much of the early research into FAC was done in the United Kingdom [41] with regard to their advanced gas-cooled reactor (AGR), of which 14 reactors had up to 12 boilers (steam generators), each tubed with a progression of alloys because of the high primary side gas temperature: carbon steel in the economizer, ferritic Fe9Cr1Mo steel in the evaporator and austenitic AISI type 316 stainless steel in the secondary superheater. To protect SG alloys from localized corrosion, particularly SCC, cycle chemistry is controlled to ensure reducing conditions (low electrochemical corrosion potential (ECP)), while FAC and corrosion product generation are controlled by high pH with some limited applications of oxygen injection. It is noted that reducible corrosion product oxides such as haematite, goethite, lepidocrocite and copper oxides can raise the ECP, so their ingress and formation at shutdown and layup, for example, are to be avoided. It has been pointed out [66] that maintaining high pH during maintenance outages will favour magnetite formation rather than the ferric species.

The preferred secondary cycle chemistry treatment for nuclear plants is now AVT – the all-volatile treatment similar to that just described for fossil plants and exemplified by the application in PWRs [109]. Although the wide range of materials and local conditions in nuclear plants ensure that no one optimum chemistry programme fits all plants, even those of nominally the same design [107], general principles have applied across the industry. Commercial software packages such as ChemWorks™ are available for directing chemistry control in specific plants. Since phosphate treatment was replaced mainly with ammonia in the 1970s and 1980s, the use of advanced amines has been introduced to provide better distribution around the steam cycle and reduction of corrosion and iron transport. Morpholine and ethanolamine, for example, are now in common use in PWRs and PHWRs, with some plants often employing mixtures of amines dictated by the requirements of the condensate polishing unit. As reported by EPRI [109], 25 PWRs use ETA, six use methoxypropylamine (MPA), four use mixtures of ETA and MPA, four use mixtures of ETA and dimethylamine (DMA), two use mixtures of MPA and DMA, one uses DMA alone and one uses morpholine alone. Plants that use these advanced amines must be aware of their thermal breakdown products like acetic acid and formic acid, which can upset normal chemistry control and under certain conditions can affect FAC under two-phase conditions [114]. For particularly vulnerable SGs, such as those that are tubed with mill-annealed Alloy 600 and therefore subject to SCC, plants may inject supplementary additives; boric acid, zinc, titanium and silica have proved beneficial in some instances [107]. Dispersants will increase blowdown efficiency by keeping particulate corrosion products in suspension, a prime example being polyacrylic acid, which has been applied in some SGs since the 1990s.

The requirement to maintain fully reducing conditions in the SG and restrictions on the use of hydrazine because of its toxicity have led to the search for alternative reducing agents [115]. Several candidates such as hydroquinone have been considered, but carbohydrazide and diethylhydroxylamine (DEHA) are the most common [107]. The latter has been tested at the Doel 2 plant in Belgium [115], where its efficiency was found to be somewhat lower than that of hydrazine. As with all complex molecules introduced into the secondary system, the effects of thermal breakdown products on SG integrity need to be evaluated. While it is important to exclude oxygen and oxidizing species from the SG, it may be possible to control feedwater chemistry in fine enough detail to allow relatively high values of ECP in selected areas. Thus, oxygen injection has been practised at the Philippsburg PWR in Germany to control FAC in the steam drain lines [107] and at the Tsuruga-2 PWR in Japan at the deaerator outlet [108]. The AGR steam generators (boilers) with helical tubing geometry inject both oxygen and hydrazine into the feedwater to ensure that the materials leading up to the upper part of the boiler have a relatively high ECP to suppress FAC, while the temperature rise throughout the boiler is enough to promote the reaction between hydrazine and oxygen so that the alloy in the upper tubing is under reducing conditions [116].

Film-forming substances have been used to provide secondary-side protection during layup of PWRs [109], where on-power application of FFAs imparts hydrophobic properties to the LP turbine and the condenser, reduces iron transport into the SG and generally mobilizes particulate corrosion products so that blowdown efficiency is improved [117]. The effectiveness of ODA (octadecylamine) in mitigating FAC and improving steam generator performance in the Kola VVER has been reported by Yurmanov [118]. Apparently, corrosion product particles entering the SG are smaller when FFAs are applied [119]. EPRI have recently reviewed [120] the general application of FFAs in nuclear plants (and included film-forming products other than amines, such as the commercial chemical Anodamine©). It was concluded that ODA is a promising additive in PWRs and PHWRs because it has been studied the most and its behaviour in the materials and environments of nuclear plants is the best understood. The perils of overdosing FFAs, which produces gelatinous spheroids around the system, are emphasized.

4 Plant Experiences of FAC

4.1 General Remarks on Plant Historical Experiences

No official FAC statistics have been kept worldwide for fossil, combined-cycle or nuclear plants. A number of unofficial and incomplete surveys have been made over the last 30 years at fossil cycle chemistry and boiler tube failure conferences as well as at HRSG users group meetings and forums that the authors run. For the nuclear industry, papers on FAC have appeared at about two-year intervals at international conferences on nuclear plant chemistry since the second Bournemouth conference in 1980, at which a paper mentioned the incidences of FAC in gas-cooled reactors that had occurred since those documented at the Tokai Murai plant in 1968 [121]. It was also pointed out that erosion-corrosion damage had occurred in the steam-generating components of sodium-cooled fast breeder reactors. Since the Surry accident in 1986, the US Nuclear Regulatory Commission (NRC) has made a point of compiling the reports of FAC occurrences in American plants (for example, see [13]). These, together with over 200 plant FAC assessments conducted by one of the authors, have led to an understanding of the key locations of FAC in power plants as well as in air-cooled condensers (ACC). These locations have not changed in the last 20 years and no new system locations of FAC under feedwater conditions in general have been identified worldwide.

In 1997, FAC was discovered in the primary-side feeders in CANDU reactors. These carbon steel pipes carry the heavy water primary coolant from the reactor core to the steam generators, and wall thinning rates were high enough to threaten reactor life spans, increasing the interest in FAC in Canada. Since reactor outlet coolant temperature is 310 °C or so and much information was available on the general corrosion of steel at those conditions and the mechanism was thought to be understood, FAC had been considered unlikely [122]; its occurrence spurred a rethink of the accepted mechanisms (discussed in Section 2).

4.2 Major FAC Incidents in Generating Plants

Table 1 shows a listing of the major incidents of FAC, which were all in single-phase water. It is worth studying this table in detail because there are some very important commonalities across the fossil and nuclear plants which should help in the initial screening of conventional fossil and nuclear plants in the future, and when designing/specifying new plant. First, it should be recognized that all incidences of aggravated FAC are associated with high fluid turbulence. The failures in fossil plants occurred with the AVT(R) feedwater chemistry (Section 3.1) and in feedwater systems where all the feedwater heaters (LP and HP) are fabricated in stainless steel (usually 304) and where the oxygen levels were extremely low (typically less than 1 $\mu g \cdot kg^{-1}$) either because the air in-leakage into the condensate was under very good control or because the location of failure was downstream of a deaerator. In each case a reducing agent (most often hydrazine) was injected at the start of the feedwater system. The low oxygen and the reducing agent ensured that the location of failure was under severe reducing potential conditions. It is also most significant that the $pH_{25°C}$ control range for the feedwater was in the range from 8.75 to 9.3, with the actual most often operated value being 9.1 or less. The temperature range at the failure location has varied widely from 142 to 232 °C (287 to 450 °F), as has the pressure from 0.93 to 20 MPa (134 to 2 900 psi). It is also interesting that most of the single-phase FAC failures such as at the economizer inlet header tubes, HP feedwater heater outlets and boiler feedpump outlets (Table 3) were also in systems where the feedwater heaters were all stainless and the feedwater was operating under AVT(R) with severe reducing conditions as described above for the major incidents [4,123,124].

As described earlier, the secondary systems in nuclear plants are mostly under reducing conditions with additions of a reducing agent to minimize risks to the steam generator and with AVT to minimize FAC – conditions similar to those in the fossil plants discussed above. Thus, the FAC failures at the Trojan, Surry and Mihama plants as listed in Table 1 happened at temperatures between 142 and 190 °C (287 and 374 °F), $pH_{25°C}$ between 8.6 and 9.3 and oxygen concentrations generally below the level of detection. All these failures occurred under extreme turbulence conditions: at Trojan, flow was directed from a fully open globe valve against the pipe wall that ruptured [11]; at Surry, flow from a 600 mm (24 inch) header entered a 450 mm (18 inch) pump suction line just ahead of the elbow that failed [12]; and at Mihama, the 558 mm (22 inch) feedwater pipe ruptured between one and two pipe diameters downstream of an orifice plate [16]. The importance of regular pipe inspections is emphasized.

4.3 FAC in Fossil Plants

The typical systems susceptible to FAC in fossil plants are shown in Tables 3 and 4 for single- and two-phase FAC respectively. Some of these locations of course can have both. Individual organizations have also reported similar compilations for many years. These overall compilations such as in Tables 3 and 4 are important to help determine the priorities for comprehensive inspection programmes, discussed later.

4.4 Combined-Cycle/HRSG Plants FAC Experience

In combined-cycle plants, FAC has been the leading cause of HRSG tube failures (HTF) over the last 20 years and represents about 35–40 % of all HTFs. Both single-

Locations
Low-Pressure Feedwater System Piping (Normally before Deaerator)
1. Expander in piping between feedwater heater and deaerator
2. Discharge of low-pressure drains pump
3. Low-pressure piping, 90° elbows
4. Discharge piping from low-pressure feedwater heaters
Feedwater Piping around Deaerator and Boiler Feed Pumps
1. Deaerator outlet piping to condensate booster pumps: elbows, tees
2. Condensate booster pump discharge piping: elbows
3. Boiler feed pump suction piping: tees and 90° bends in supply piping from deaerator
4. Boiler feed pump discharge: elbows, reducers, welds
5. Boiler feed pump discharge: superheater/reheater attemperation supply piping and fittings
6. Boiler feed pump discharge recirculation piping: after control valves
7. Boiler feed pump leak-off lines
8. Boiler feed pump balancing lines
9. Feedwater control systems: orifices, thermowells and regulating valves
10. Startup boiler feed pump warmup lines: bends following orifices
Attemperation Piping
1. Near main feedwater line: tees to superheater and reheater attemperation systems
2. Main steam attemperation piping: control valves, elbows

Table 3:
Locations of single-phase FAC damage in conventional fossil plants [3,18,125].

Locations
Low-Pressure Heater Drains
1. Low-pressure drains piping: control valves (before/after), valve bodies, expanders, tees
High-Pressure Heater Drains
1. High-pressure drains piping: control valves (before/after), reducers, expanders, elbows, valve bodies, gate valves (after)
Alternate Heater Drains (sometimes called emergency or high level drains)
1. From high-pressure heater to lower pressure heater: after control valves
2. From high-pressure heater to deaerator: after control valves
3. Tee joining normal and alternate high-pressure drain lines
4. HP and LP heater drains to condensers: after control valves, after gate valves, elbows (including elbows in condensers)
5. Drains bypass piping
Shells
1. Low-pressure heater shells (near to cascading drain entries)
2. Heater vent lines to condenser: elbows
3. High-pressure feedwater heater shells (near to cascading drain entries)
4. Deaerators (near to fluid entries especially HP cascading drains)
Reheater and Superheater Attemperation Stations
1. Piping upstream/downstream of temperature control valves

Table 4:
Locations of two-phase FAC damage in conventional fossil plants [3,18,125].

and two-phase FAC can occur in LP and IP evaporators and LP, IP and HP economizer tubing, but there are no reliable statistics which separate the circuits. Two-phase FAC has also been a problem in LP and IP evaporator drum steam separation equipment [126] and in the riser piping. The typical systems susceptible to FAC in combined-cycle plants are shown in Table 5 for single- and two-phase FAC [6].

4.5 Air-Cooled Condensers (ACC) FAC Experience

An increasing number of fossil and combined-cycle/HRSG plants worldwide are equipped with ACCs. Operating units with ACCs at the lower regimes of $pH_{25°C}$ provided in IAPWS guidance documents [24] will result in serious corrosion and FAC in the ACC tubes, most predominantly at the entries to the cooling tubes in the upper ducting (streets) [20].

The cycle chemistry influenced FAC damage in ACCs can be best described through an index for quantitatively defining the internal FAC status of an ACC. This is known by the acronym DHACI (Dooley Howell ACC Corrosion Index) [20]. This methodology was recently published as a Guideline of the ACC Users Group (ACCUG) [127]. The index separately describes the lower and upper sections of the ACC, according to the following:

The index provides a number (from 1 to 5) and a letter (from A to C) to describe/rank an ACC following an inspection. For example, an index of 3C would indicate mild corrosion at the tube entries, but extensive corrosion in the lower ducts. An example for the upper ACC section (upper duct/header, ACC A-frame tube entries) is shown in Figure 26. An example for the lower ACC section (turbine exhaust, lower distribution duct, risers) is shown in Figure 27.

Typical Tube and Header Materials, and Range of Operating Temperatures

- LP economizer/preheater (feedwater) tubes at inlet headers (SA 178A, SA 192 and SA 210C tubing; SA 106B headers; 40–150 °C, 105–300 °F)
- Economizer/preheater tube bends in regions where steaming takes place with particular emphasis being given to the bends closest to the outlet header (SA 178A, SA 192 and SA 210C tubing; SA 106B headers, 40–150 °C, 105–300 °F) (Note: Steaming can easily be identified in these areas by installation of thermocouples on the appropriate location)
- IP/LP economizer outlet tubes (SA 178A, SA 192, SA 210C tubing; SA 106B headers; 130–150 °C, 260–300 °F)
- HP economizer tube bends in regions where steaming takes place with particular emphasis being given to the bends closest to the outlet (SA 210 A1 and C tubing; ~ 160 °C, 320 °F)
- IP and HP economizer inlet headers (SA 106B; 60–100 °C, 140–210 °F)
- LP evaporator inlet headers with a tortuous fluid entry path or with any orifices installed (SA 106B; 130–170 °C, 260–340 °F)
- LP outlet evaporator tubes (SA 192, SA 178A and SA 210C; 150–165 °C, 300–330 °F)
- LP evaporator link pipes and risers (SA 106B; 150–165 °C, 300–330 °F)
- Horizontal LP evaporator tubes on vertical gas path (VGP) units especially at tight hairpin bends (SA 192; 150–160 °C, 300–300 °F)
- LP drum internals (belly plates in line with riser entries)
- IP economizer outlet tubes with bends (SA 178A, SA 192, SA 210A1 and C) and headers (SA 106B and C) (210–230 °C, 410–445 °F) if there is evidence of steaming
- IP evaporator inlet headers (SA 106B) with a tortuous fluid entry path or with any orifices installed (210–250 °C, 410–482 °F)
- IP outlet evaporator tubes (SA 178A, SA 192 and SA 210C; 230–240 °C, 445–465 °F) on triple-pressure units especially if frequently operated at reduced pressure
- IP outlet link pipes and evaporator risers (SA 106B) to the IP drum (230–240 °C, 445–465 °F)
- Piping around the boiler feed pump. Includes superheater and reheater desuperheating supply piping
- Reducers on either side of control valves
- Turbine exhaust diffuser
- Air-cooled condenser (see sub-section 4.5)

Table 5:
Locations of FAC in combined cycle/HRSGs [18,19].

The DHACI should be used to describe the status of a particular ACC during each ACC inspection in terms of its FAC history and is a very useful means of tracking changes that occur as a result of making changes in the cycle chemistry. A plant that has a relatively poor rating for FAC at a condensate cycle $pH_{25°C}$ of 8.5–8.8 (e.g., 4C) may increase the $pH_{25°C}$ to 9.4–9.6, and determine whether this change improves its rating (e.g., 3B). A poor rating (e.g., 4B) indicates the need to consider options to reduce the FAC rate especially at the tube entry areas. The DHACI can also provide a qualitative indication of total iron corrosion products flowing from the ACC into the plant condensate.

Additionally, the index provides a convenient tool for comparison between different units and when alternative chemistries are used. A number of plants worldwide have changed to the use of an amine or an FFS rather than ammonia, and by using the DHACI the improvements can be documented.

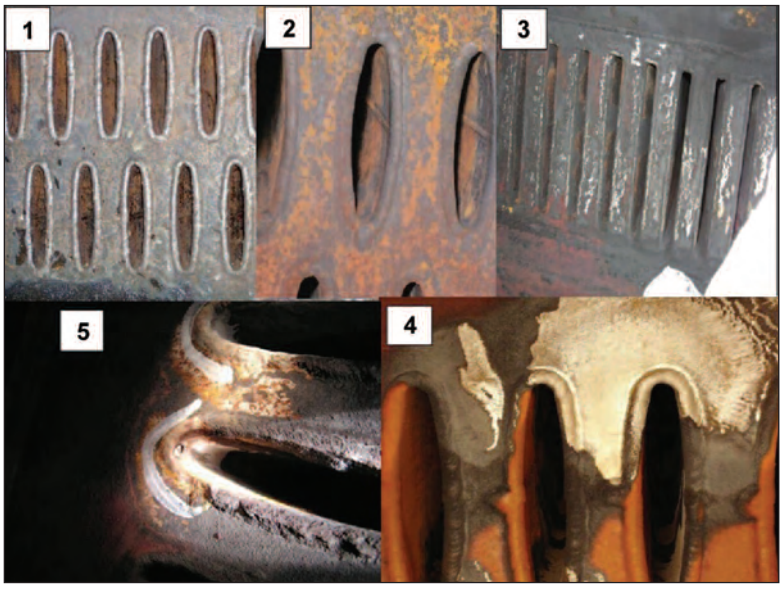

Figure 26:
Montage illustrating DHACI indices 1–5 for the upper ducts and tube entries of ACCs. The FAC damage increases with number [20].

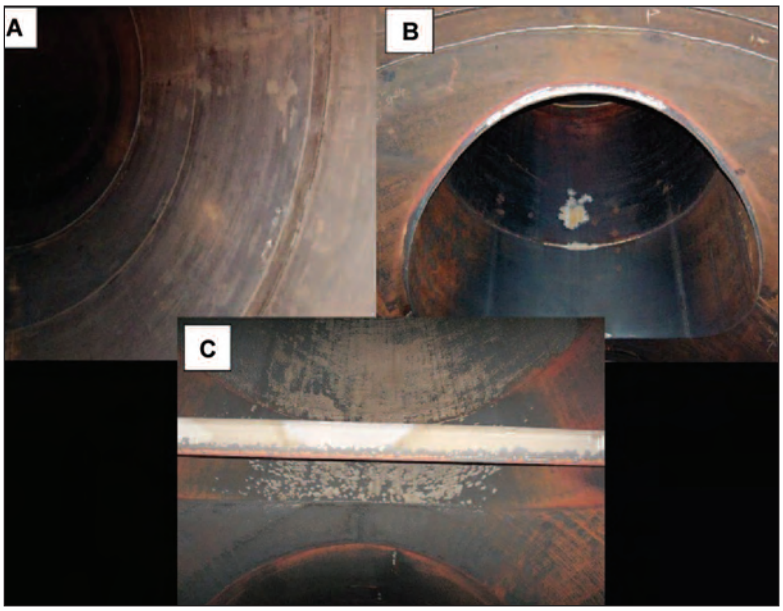

Figure 27:
Montage illustrating DHACI indices A–C for the lower ducts of ACCs from the steam turbine to the vertical risers to the upper duct. Increasing letters indicate more severe and extensive damage [20].

4.6 Nuclear Plants FAC Experiences

As mentioned earlier, nuclear plant issues for public scrutiny are generally reported by industry organizations. For example, the responses of US nuclear plants to the bulletin issued by the USNRC [13] after the Surry pipe rupture indicated that all had programmes in place to inspect for pipe wall thinning in two-phase systems and that most had inspected single-phase systems and instituted monitoring programmes as a result of the Trojan and Surry incidents. Two-phase FAC occurred in a variety of systems throughout the plants and single-phase FAC was widespread in feedwater-condensate systems – particularly the recirculation-to-condenser line ("minimum-flow" line). The reported incidences were:

Single-phase lines

- Main feedwater lines, straight runs, fittings
- Main feedwater recirculation line to condenser, straight runs, fittings
- Feedwater pump suction lines, straight runs, fittings
- Feedwater pump discharge lines, straight runs, fittings
- Condensate booster pump recirculation line fittings
- Steam generator letdown lines, straight runs, fittings

Two-phase lines

- Main steam lines
- Turbine cross-over piping
- Turbine cross-under piping
- Extraction steam lines
- Moisture separator reheater
- Feedwater heater drain piping

Six BWRs reported [13] pipe wall thinning in feedwater-condensate systems, specifying: elbows, reducers, straight runs and recirculation lines. Similarly, twenty-six PWRs reported [13] thinning in: elbows, drain pump discharge lines, reducers, straight runs, Y-connections, recirculation lines, heater drain piping, fittings, and straight runs downstream of the main feedwater loop isolation valve and downstream of main feed pump mini-flow valves. Although this USNRC document was first issued in 1988, we note that the systems and components listed are still vulnerable today (the document as obtained via the NRC website was reviewed and updated in 2015, apparently with no changes).

In the main feedwater line to the SGs in three Korean PWRs, FAC of the check valve nozzle outlet and the pipe just downstream reduced the wall thickness by up to 40 %. Temporary repairs at one plant were made by weld overlays and at the others by pipe replacements [128].

A recent seminar [129] under the auspices of the World Association of Nuclear Operators (WANO) cited the incidents at the Navajo (fossil) and Surry Unit 2 plants as focusing the industry's attention early on and then Mihama 3 later (Table 1). The seminar went on to list a few other fossil plant failures and these other failures in nuclear plants:

- Arkansas Nuclear One (US) PWR in 1989: two-phase FAC in pipe downstream of high-pressure extraction nozzle
- Santa Maria de Garona (Spain) BWR in 1989: blow-out of feedwater line downstream of flow meter; chemistry neutral, low-oxygen
- Loviisa Units 1 and 2 (Finland) VVERs in 1990 and 1993: similar through-failures in feedwater orifice flange, downstream of orifice plate; chemistry neutral, low oxygen and chromium content in flange steel much lower than in pipe steel
- Millstone 3 (US) PWR in 1990: simultaneous failures of two parallel lines just downstream of control valves after moisture-separator drain tank
- Millstone 2 (US) PWR in 1991: pipe downstream of level control valve in reheater drain line
- Sequoyah 2 (US) PWR in 1993: fish mouth rupture of 275 mm outside diameter pipe downstream of tee in high-pressure steam extraction line
- Millstone 2 (US) PWR in 1995: FAC downstream of gate valve in heater drain line thinned the pipe wall enough to rupture during water hammer – even though the wall was thicker than the minimum
- Fort Calhoun (US) PWR in 1997: catastrophic failure in 5-D sweep in high-pressure extraction line; elbow downstream also excessively thinned
- Point Beach 1 (US) PWR in 1999: fish mouth failure in 13 mm wall of feedwater heater, where entering steam deflected off impingement plate to the shell
- Callaway (US) PWR in 1999: 170 mm reheater drain line downstream of long run, with flow disturbed by backing ring; void fraction 55 %
- Susquehanna 1 (US) BWR in 2000: feedwater heater shells, tube supports and tie rods damaged; 142 °C, 91 % steam quality
- South Ukraine 2 (Ukraine) VVER in 2005: 45 ° elbow in 219 mm line from moisture separator tank to deaerator; 211 °C; also, drain line from HP heater to deaerator
- Kakrapar 2 (India) PHWR in 2006: 80 mm feedwater line downstream of orifice.

As in the fossil plants, the effects of chemistry, materials and flow regime are evident. For the nuclear plants with restricted options for applying oxidizing conditions, the importance of comprehensive and regular monitoring is emphasized.

4.7 Surface Appearances of FAC in Generating Plants and Air-Cooled Condensers (ACCs)

The previous sub-sections have provided information on the locations of FAC in generating plants and in ACCs. This section provides descriptions of the surface appearances of FAC in these systems. The identification of whether the FAC in a plant is of the single- or two-phase variety is tremendously important so that the owner/operator can make the correct decisions in moving forward to reduce the FAC rate. As has been clearly discussed in Section 2 different chemistry and hydrodynamic aspects control the two types of FAC; for similar aspects in different systems, the appearances will be similar. Thus, for similar materials and chemistries, the damage from FAC in feedwater components in nuclear plants will resemble that in equivalent components in fossil plants. Examples of the latter are provided below, including the unique appearance of FAC in ACCs, which have no equivalent in nuclear plants.

Figure 28 provides two examples of single-phase FAC in fossil and combined-cycle/HRSG plants. In locations where single-phase FAC is starting, such as towards the bottom of photograph A in Figure 28, individual horseshoes or chevrons can be clearly seen and always point in the direction of flow (bottom to top in photograph). As the turbulence becomes greater downstream of the bend and the FAC rate increases, such as towards the middle/top of photograph A in Figure 28, the chevrons overlap and produce the typical orange peel appearance of single-phase FAC. The chevrons are also clear in photograph B in Figure 28.

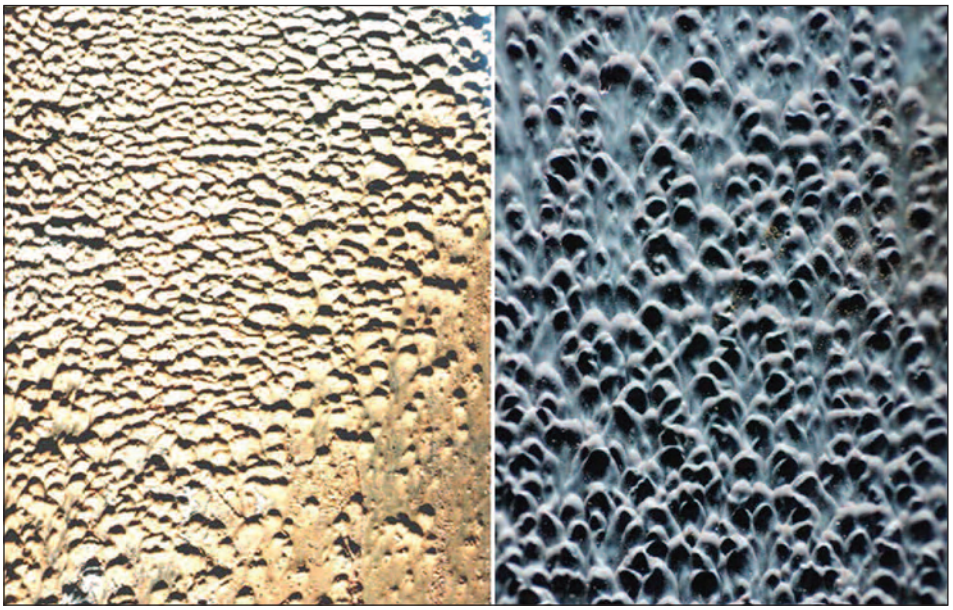

Figure 28:
Two views of the visual surface appearance of single-phase FAC. A is a typical detail from an economizer inlet header tube. Example B is a similar view from the FAC surface near to the inlet of an HRSG LP evaporator tube. In both cases the horseshoes or chevrons point in the direction of flow (bottom to top) [18].

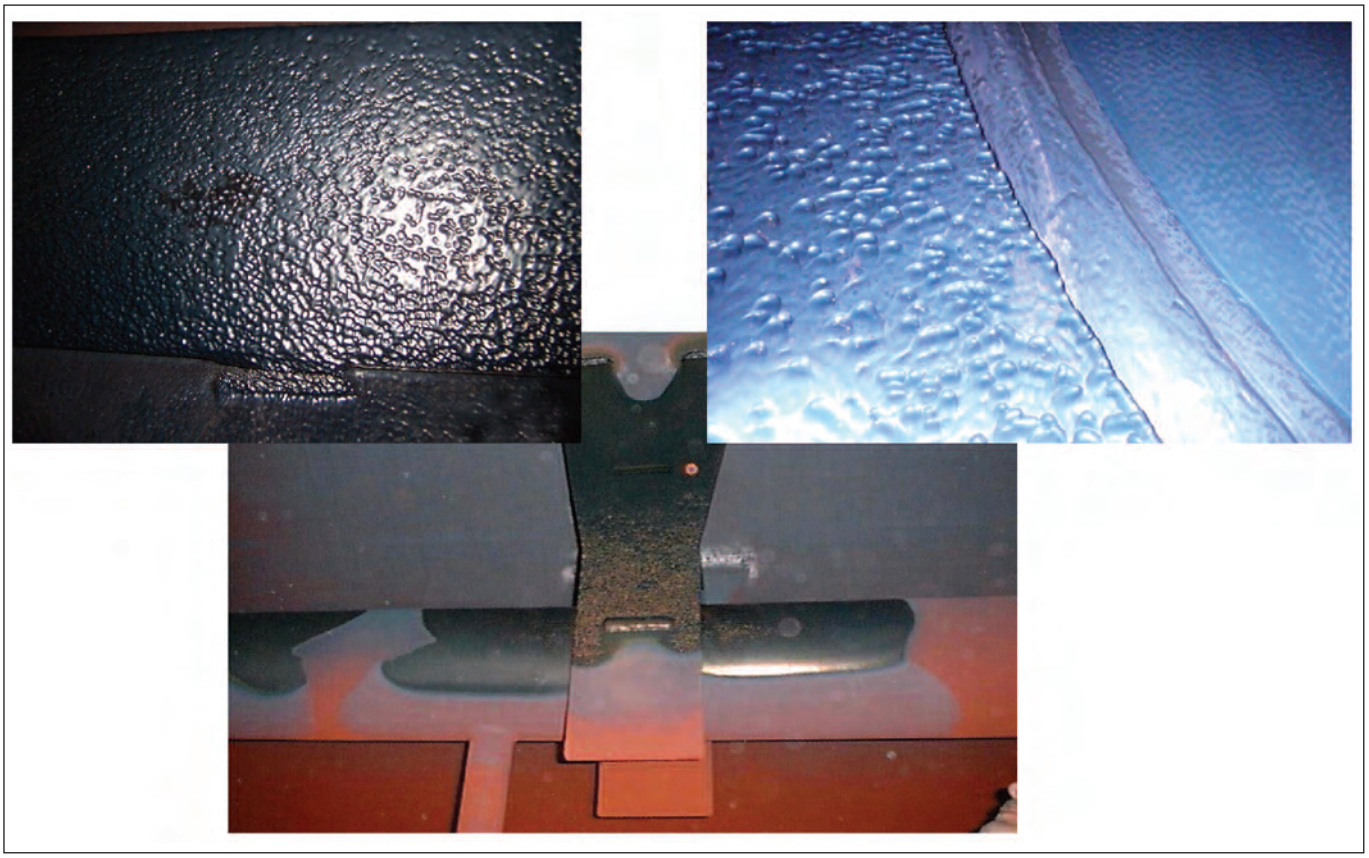

Figure 29:
Three examples of two-phase FAC in fossil plants. The lower photograph illustrates the black/shiny appearance of two-phase FAC, which can immediately be identified visually on inspection. The upper two photographs show the typical distinct two-phase FAC dimples in the black/shiny surfaces with no obvious directionality in respect to the flow.

Figure 29 provides three examples of two-phase FAC in fossil plants. The lower photograph shows the general black/shiny surface appearance which is most often clearly visible on inspection. When viewed in closer detail the upper two photographs again show the black/shiny appearance but now dimples are also visible on the surface.

Figure 30 provides three examples of two-phase FAC in HRSG LP evaporators where the different surface appearance of two-phase damage can be easily seen. This two-phase FAC damage is probably the most misidentified FAC in combined-cycle/HRSG plants. This is most important because increasing the oxidizing power of the fluid will have no effect on the damage as has been explained in Section 2. Established two-phase FAC always has a black shiny appearance (left photograph) and in areas where it is just starting or at the extreme of the damage there are often "dimples" which are often misidentified as damage from pitting corrosion on the surface (top right photograph). They most often do not show any directionality like the chevrons of single-phase FAC. As the turbulence becomes established and the FAC wear rate increases, the dimples overlap and sometimes the surface appearance then resembles single-phase FAC (as seen in Figure 28) but is black and shiny.

Figure 31 provides two examples of two-phase FAC in fossil deaerators. Both examples are close to where cascading drains fluid from HP feedwater heaters enters the deaerator and flashes against the deaerator surface. The surface appearance of two-phase FAC is mostly black and shiny and often has a dimpled appearance which is seen for other examples of two-phase damage such as in HRSGs (see Figures 29 and 30). This can be seen clearly in the middle of the black shiny area on Figure 31B and on the surface just below the drain entry on photograph A. Also, on plants operating under oxidizing conditions there is most often a very clear and sharp boundary between the single-phase flow areas (shown with red colouration under oxidizing conditions) and the areas where two-phase FAC is active. Figures 31B and 32 (left) show good examples.

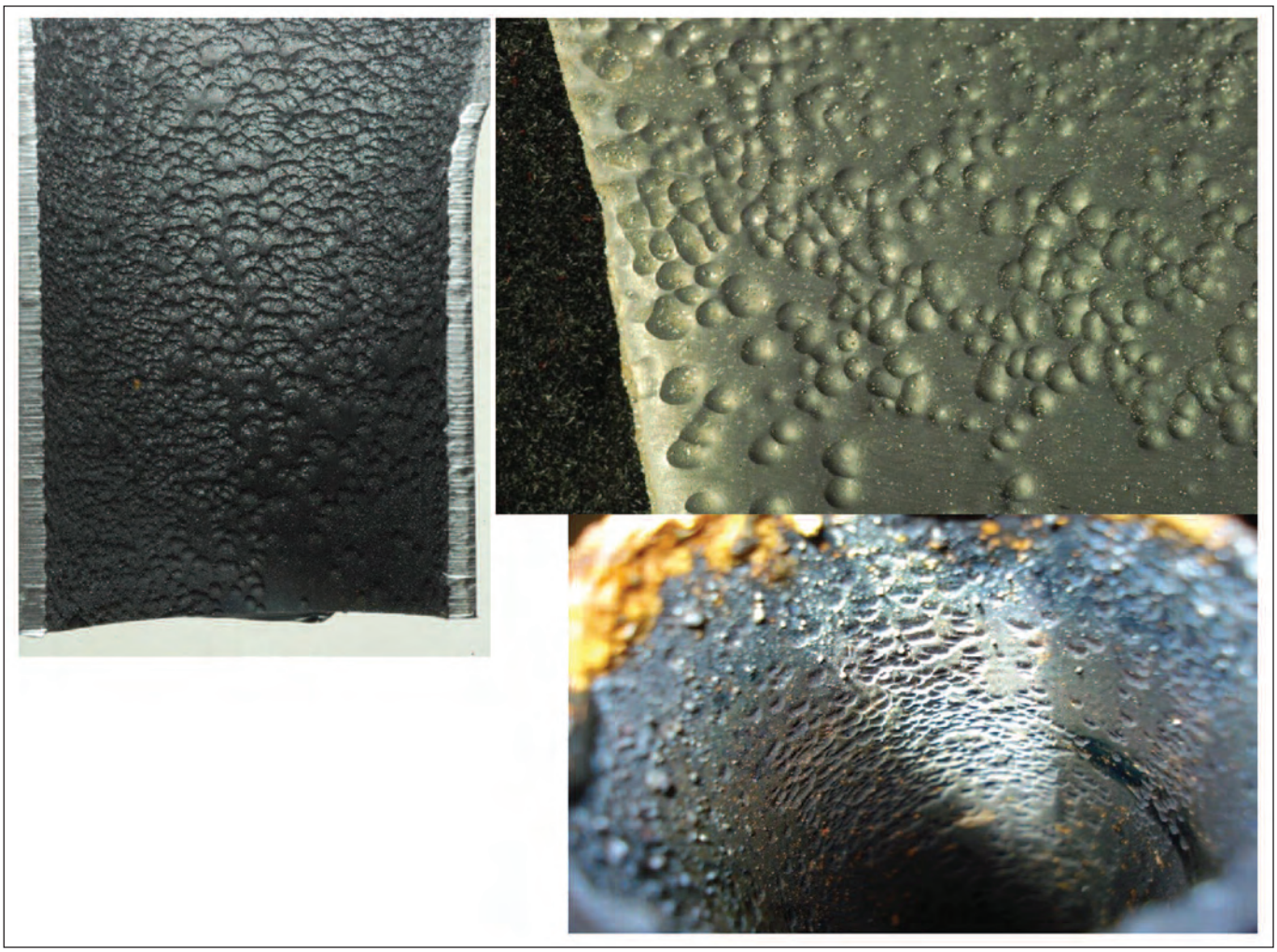

Figure 30:

Three examples of two-phase FAC in HRSG LP evaporator tubing. The left hand photograph shows the typical black/shiny appearance of established FAC. The top right photograph shows the distinct dimples of initiating FAC without any obvious directionality in respect to the flow. The lower right shows a view looking into an LP evaporator tubing from the outlet header with severe FAC (failure) on the left side of the photograph and initiating damage on the right.

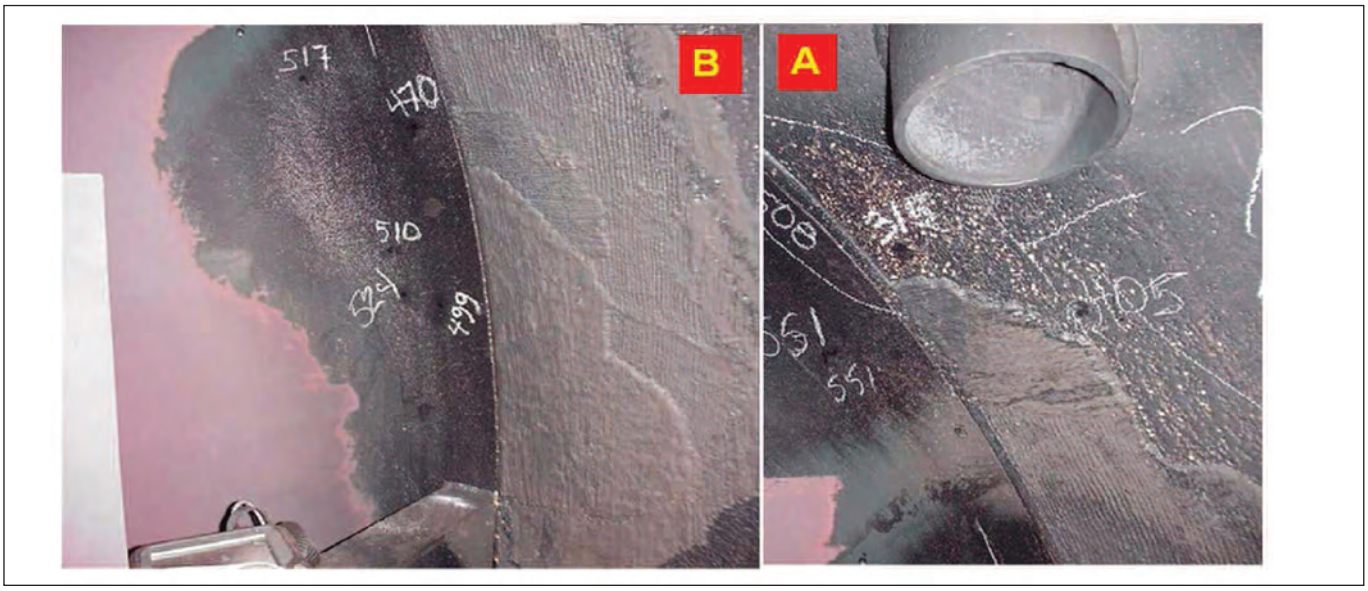

Figure 31:
Examples of severe two-phase FAC in deaerators. Example A is located adjacent to an HP cascading drain entry (shown) into a deaerator. Example B is directly in the path of the flashing steam/water mixture from another drain entry. In both cases the two-phase FAC areas are easily seen due to a black/shiny (enamel-like) appearance. In some very severe areas there are the typical two-phase FAC dimples. Some of the areas had previously been weld-overlaid with carbon steel material. The red colouration indicates where there is single-phase fluid because this is protected by the haematite covering [18].

Figure 32:
Two examples of two-phase FAC on the shell side of feedwater heaters. The left hand photograph is from a unit operating on OT, where the red colouration delineates single-phase water flow and where the surface is protected by the red haematite. The shiny black area is where two-phase FAC is taking place as a result of flashing of a cascaded drain entering the heater (source: R. Brooker and D. Swainsbury 2002). The right hand photograph shows the inside surface of a heater on a unit operating under reducing conditions (AVT(R)) where the two-phase FAC damage is darker (grey/black) than the areas with protective magnetite (light grey). Developed from [18].

Another important two-phase location of FAC is on the shells of fossil plant high- and low-pressure feedwater heaters at locations near to where the cascading drains from the higher pressure heater enter the shell of the lower pressure heater. Two examples are shown in Figure 32: the left photograph is from a unit operating under oxidizing (OT) conditions and the right photograph is from a unit operating under reducing conditions (AVT(R)). The former shows the black shiny appearance of two-phase FAC on a heater shell. The red areas (haematite) define the single-phase flow locations and indicate that the surface is protected from FAC. The black shiny areas define where the two-phase mixture of water/steam is striking the surface as a result of flashing of the cascading higher heater drain

entry into the vessel. No protection can be afforded in these black areas because there is no oxidizing power of the liquid in the two-phase mixture, despite the unit operating with about 150 $\mu g \cdot kg^{-1}$ of oxygen on OT. The grey magnetite can also be seen beneath the red haematite. There is a very sharp boundary between the protected (single-phase) and the unprotected (two-phase) areas in this region. This is highlighted because of the red/black boundary, but can also be seen in units operating with reducing treatments where the two-phase media can be equally as severe for FAC. The right photograph shows the boundary areas in a unit operating on AVT(R), where the darker (grey/black) areas are where the two-phase FAC has taken place, with the severest damage being the locations that have flash rusted during shutdown. The lighter grey areas are where the protective magnetite remains in place.

Figures 28–32 have shown the similarity of examples of single- and two-phase FAC in fossil and combined-cycle/HRSG plants. Also, when any FAC-damaged surfaces from plant are viewed at higher magnification with an SEM, then the appearance for both single- and two-phase is scalloped. Figure 33 shows four examples.

Figure 20 previously showed an example from single-phase FAC in a nuclear plant. Although there isn't a full understanding of the scalloping mechanism, the authors always look for this scalloped appearance to confirm that the damage mechanism is FAC as compared to an erosion or cavitation mechanism, where these scallops are not present. This also applies to laboratory simulations of FAC to ensure the conditions and results are realistic in terms of simulating plant FAC.

Figure 26 shows some general views of different FAC damage at the tube entries of ACC. Figure 34 shows two more detailed examples of this damage from two ACCs. The FAC damage shows up as white areas in the two photographs at the ACC tube entries and on the support structure. It is now understood that the white areas on the support structures are possibly due to liquid droplet impingement from larger droplets of moisture. Only two ACC tubes from two units have been removed and analysed in detail to characterize the general and detailed surface appearances of FAC in ACCs [20]; Figure 35 shows details from one of these tubes. The left photograph shows the typical surface appearance with adjacent white (damaged) and black (deposit) areas. The white

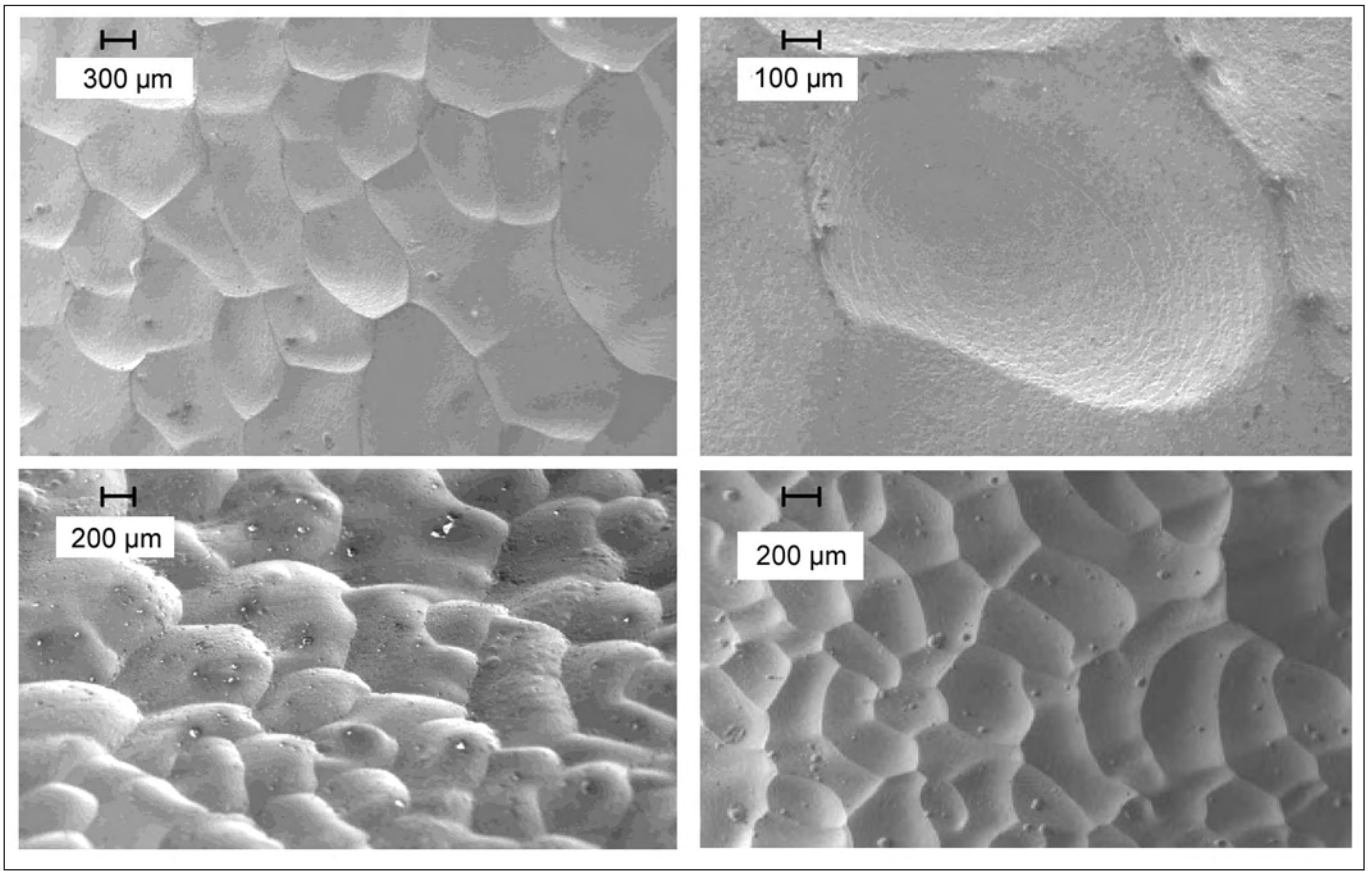

Figure 33:
Typical scalloped surface appearance of FAC in fossil and combined-cycle/HRSG plants. The upper two photographs are from two-phase FAC damage in HRSG economizer tubing. The lower two photographs are from single-phase FAC in fossil plants (note similarities with the scalloping in the CANDU reactor primary coolant piping in Figure 20 and the experimental FAC probe in Figure 22).

Figure 34:
Surface appearance of FAC at the entries of ACC tubes and on support structure. The left photograph shows a view along the upper ducting of a supercritical unit operating on OT at a $pH_{25°C}$ of about 9.0. The right photograph shows a closer view of the ACC tube entries on a sub-critical once-through unit operating on OT with a $pH_{25°C}$ of about 9.4.

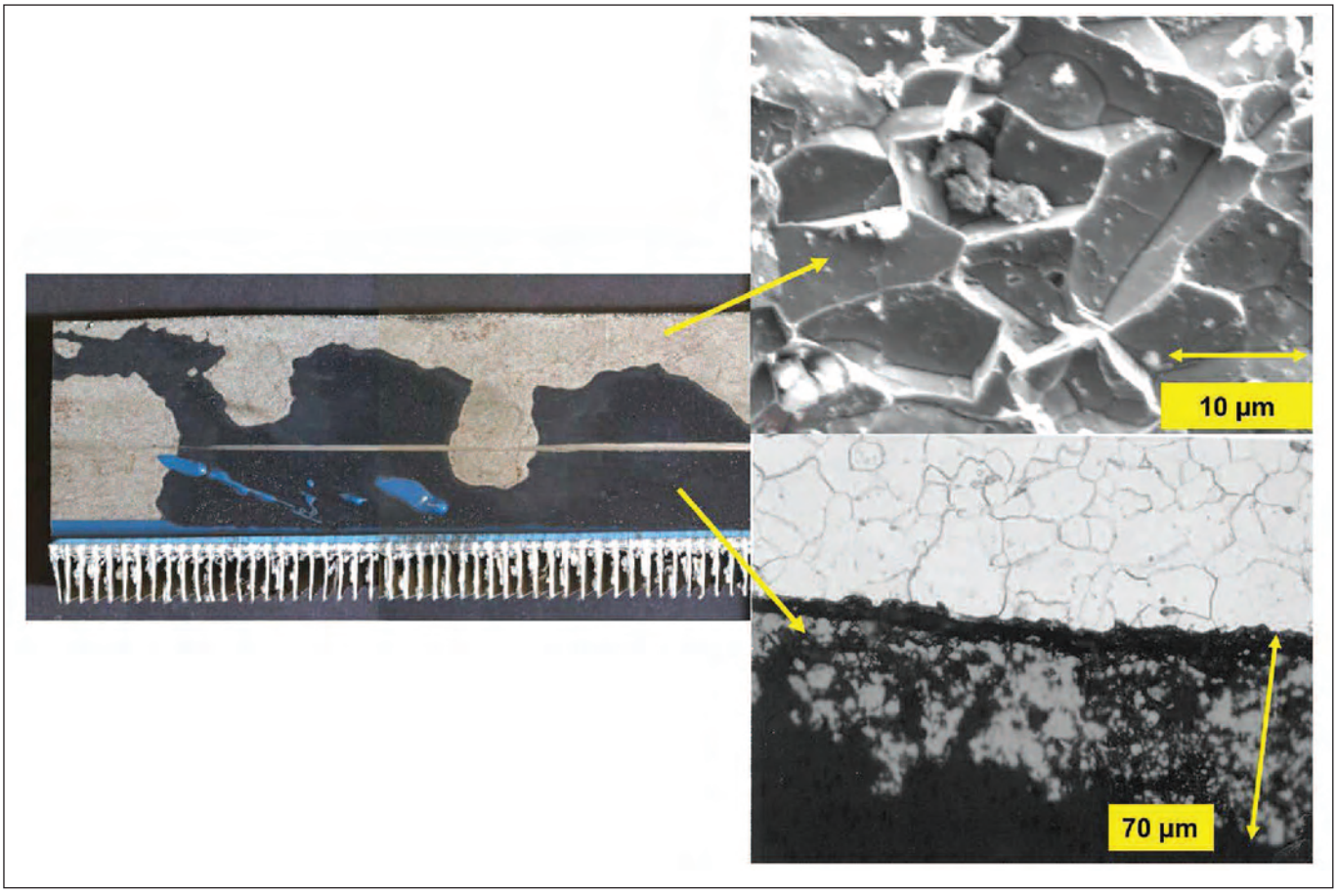

Figure 35:
Surface appearance of FAC on an ACC tube just below the tube entry. The left photograph shows the visual appearance of white damaged locations such as seen in Figure 34 from a unit operating at a $pH_{25°C}$ of about 9.4. The top right photograph shows an SEM higher magnification view of the white surface. The bottom right photograph shows a metallurgical cross-section through a black surface region where magnetite particles are clearly seen in the deposit.

Figure 36:
Arresting two-phase FAC damage in ACCs can take a long time. The FAC damage at the tube entries after operating for about 4 000 hours with a condensate $pH_{25°C}$ of about 9.0 has arrested after a period of operating of about two years with a condensate $pH_{25°C}$ of about 9.8 using ammonia (source: I. Richardson and G. Joy, presented at Air-Cooled Condenser User Group (ACCUG 2011) [127]).

damaged areas are seen as intergranular corrosion under this higher SEM magnification (top right photograph); these do not have the same scalloped morphology as seen in Figure 33, but also do not show any mechanical or erosive damage. The black areas are regions of deposited particulate magnetite as clearly seen in the cross-section shown in the lower right photograph of Figure 35, which is similar to the black deposits often seen adjacent to two-phase FAC in fossil and combined-cycle/HRSG plants.

FAC damage in ACCs is most often arrested by an increase in condensate $pH_{25°C}$ up to 9.8 [20], but it takes some time for the white damaged areas to become protected with grey magnetite. Figure 36 shows the change from a DHACI of 4 when operating with a $pH_{25°C}$ of about 9.0 to a DHACI of 2 after operating for nearly two years with a $pH_{25°C}$ of 9.8. The tube entries then show very little white FAC areas, but the support structures have not fully been repaired. Numerous examples have been shown of arrested damage at ACC tube entries using a film-forming substance (FFS); Figure 37 shows an example.

5 Overall Management Approach for FAC in Generating Plants

Section 2 has described in detail the mechanisms of FAC and Section 4 has provided examples of FAC in generating plants. The complex interactions of the cycle chemistry and flow hydrodynamics control and locate FAC, respectively. An overall comprehensive management approach to identify and control FAC is required to mitigate or eliminate any damage in steam generating plants. Examples of these programs were described in detail in a previous review [18] along with two road maps for conventional fossil and combined-cycle/HRSG plants to illustrate the process. These are still as applicable today and the descriptions are not repeated, but the two road maps, Figure 38, are included in this current paper as examples and act as reference for the remaining sections. For nuclear plants, the Nuclear Energy Agency (NEA), an agency of the Organisation for Economic Co-operation and Development (OECD), has recently published a review of programmes on managing FAC in member countries [130]. The review is part of CODAP (Component Operational Experience, Degradation and Ageing Programme).

Figure 37:
The FAC at the tube entries has been arrested after a period of operating using a film-forming product (source: B. Stroman, presented at Air-Cooled Condenser User Group (ACCUG 2011) [127]).

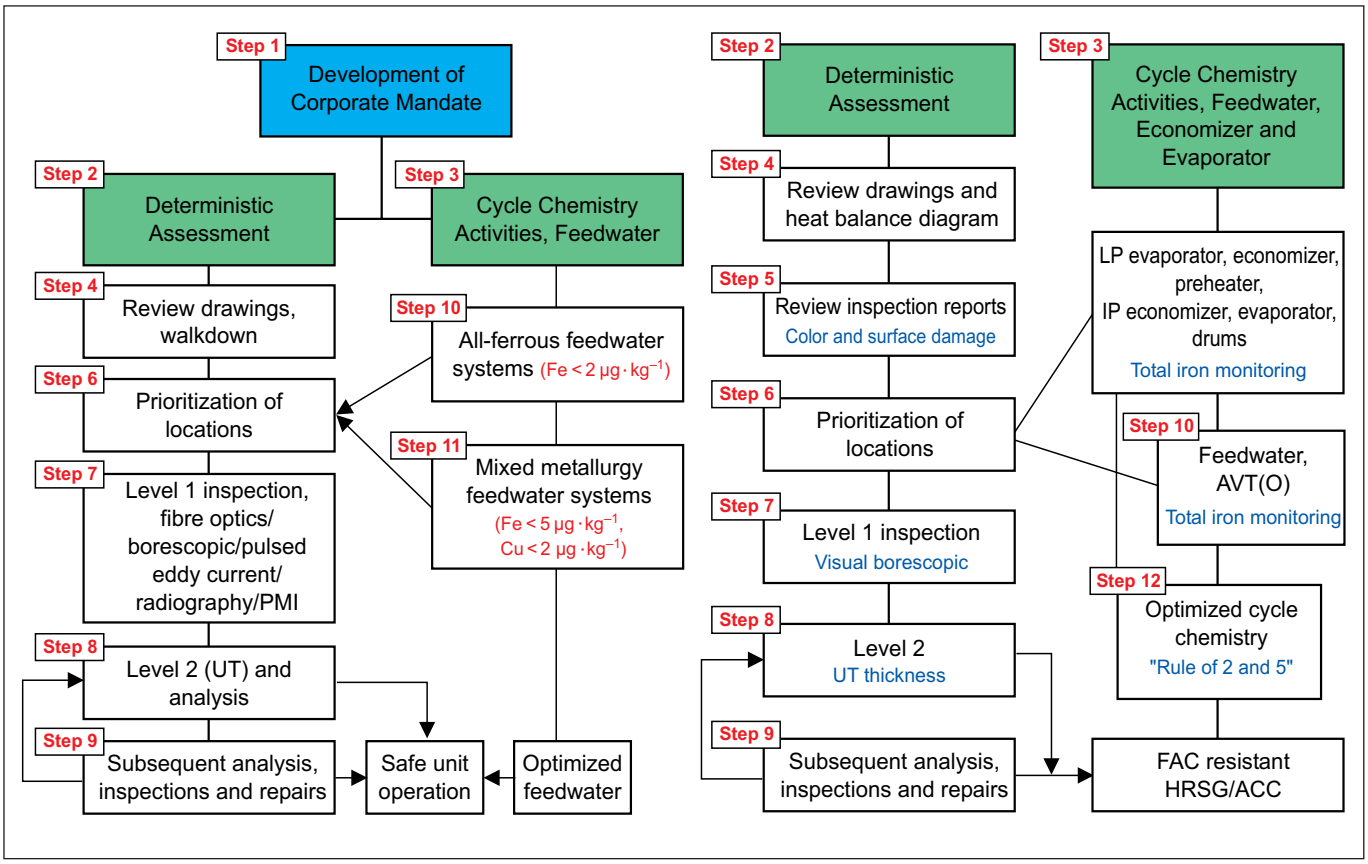

Figure 38:
Examples of the overall approach to mitigating and eliminating FAC in conventional fossil plants (left) and combined-cycle/HRSG plants (right). Adapted from [18].
PMI positive metal indication
UT ultrasonic thickness

These documents, the road maps in particular, should make it crystal clear that optimizing and monitoring the cycle chemistry and conducting NDE/inspections should never be separated in a comprehensive FAC programme. Only identifying the locations of FAC and addressing them superficially (disposition and reassessment, repair, welding, weld overlay) does not address the root cause of the problem, which in most cases relates to the cycle chemistry, especially for fossil and combined-cycle/HRSG plants. Only optimizing the cycle chemistry minimizes the wall loss and the possible FAC sites.

6 Inspection and Monitoring of FAC

As mentioned in the last section, an overall comprehensive programme for FAC is required to ensure a generating plant remains safe. As shown in Figure 38, this should include inspection processes, and on-line total iron monitoring. These are briefly introduced in this section.

6.1 Inspection Processes for FAC in Generating Plants

Section 5 and Figure 38 have introduced the overall approach for mitigating FAC in generating plants. After conducting a deterministic analysis (Step 2) (or using model prediction) to identify possible locations of FAC in fossil and combined-cycle plants (typical locations provided in Tables 3–5), two inspection steps are advocated. Level 1 (Step 7) includes techniques such as fibre optics, pulsed eddy current (PEC), and digital radiography to confirm that FAC is present at that location. Level 2 (Step 8) provides detailed thickness and wear measurements using gridded ultrasonic thickness (UT) measurements. An overview of the techniques available along with an indication of the strengths and weaknesses is shown in Table 6.

As explained earlier, frequent and systematic pipe and component monitoring is essential in nuclear plants. The techniques are the same as in fossil plants, as outlined in Table 6. In the case of monitoring the outlet feeders of the primary coolant in PHWRs, which are intricate inter-twined piping systems in high radiation-field areas, remote multi-head ultrasonic devices that travel around the tight-radius bends close to the reactor face are employed.

6.2 Monitoring of Total Iron as an Indicator of FAC

As is clear in Sections 2 and 4, one of the most important aspects in understanding and controlling FAC in fossil and

	Main Strength	Main Weakness	Proposed Primary Use
Ultrasonic Testing	Accurate wall thickness reading needed for predicting FAC rate	Low coverage per measurement; needs insulation removal and gridding of pipe or pressure vessel	Level 2. Measurement of wall thickness; Successive measurements at long intervals can provide FAC rate.
(Digital) Radiographic	Volumetric detection, understandable image	Radiation hazard	Level 1. Screening of complex components like valves, pumps, reducers and small bore piping
Positive Metal Indication (PMI)	Identifies material composition	Only detects the material not the corrosion or rate	Level 1. Pre-selection and verification of susceptible components; material composition
Pulsed Eddy Current (PEC)	Inspection through insulation without radiation; non-intrusive	Average wall thickness (AWT); no accurate wall thickness	Level 1. Screening of insulated components like bends, pipes and heater shells
Visual and Borescopic (Fibre Optics)	Easily identifies single- and two-phase FAC surface appearances (see sub-section 4.7)	Access can be difficult	Level 1. Screening for level control valves, feedwater heater shells and HRSG tubing

Table 6:
Summary of non-destructive techniques for inspection of FAC in generating plants (adapted from Walker, S. [131]).

Feedwater (economizer inlet in fossil plants and feedpump discharge in HRSGs)		
OT	Total Fe	$< 1\ \mu g \cdot kg^{-1}$ (ppb)
AVT	Total Fe	$< 2\ \mu g \cdot kg^{-1}$ (ppb)
AVT (mixed)	Total Fe & Cu	$< 2\ \mu g \cdot kg^{-1}$ (ppb)
HP/LP heater drains	Total Fe & Cu	$< 10\ \mu g \cdot kg^{-1}$ (ppb)
HRSG Evaporators/Drums		
AVT/PT/CT	Total Fe	$< 5\ \mu g \cdot kg^{-1}$ (ppb)
Air-Cooled Condenser (ACC)		
ACC outlet	Total Fe	$< 10\ \mu g \cdot kg^{-1}$ (ppb)
Post condensate filter	Total Fe	$< 5\ \mu g \cdot kg^{-1}$ (ppb)

Table 7:
Total iron levels indicating that FAC is under control in conventional fossil and combined cycle plants [23].

combined-cycle/HRSG plants is the level of total iron monitored for the different plants and chemistries, which provides an indication that FAC is under control. Steps 10 and 11 in the overall FAC programmes (Figure 38) illustrate the criticality of knowing that the total iron measured in fossil and combined-cycle/HRSG plants is at a level which indicates that both single- and two-phase FAC are under control. Table 7 adapted from IAPWS [23] provides these guidance levels.

Boiling water reactors (BWRs) inject depleted zinc oxide (ZnO with reduced Zn^{64}) into reactor feedwater to control shutdown radiation fields (the zinc forms a spinel oxide with iron that reduces contamination from radioactive cobalt on out-core surfaces). From efficient filtration and condensate polishing, iron levels are typically maintained below 0.5 $\mu g \cdot kg^{-1}$ (ppb) [132] with several achieving levels below 0.1 $\mu g \cdot kg^{-1}$ (ppb) [108], so fuel performance in the core is not compromised.

Pressurized water reactors (PWRs) typically have iron concentrations in feedwater at about 1 $\mu g \cdot kg^{-1}$ (ppb) or less and PHWRs have similar levels. Control by pH adjustment has been demonstrated in Japanese units, where systems without copper-bearing alloys in the cycle have seen a fall in iron levels from several $\mu g \cdot kg^{-1}$ (ppb) to 1 $\mu g \cdot kg^{-1}$ (ppb) on imposing high pH regimes, with ammonia giving $pH_{25°C}$ values up to 10.0 (condensate polishers may have to be by-passed at the high pH levels) [133]. High pH regimes have been imposed in VVERs and French PWRs, where $pH_{25°C}$ values of 9.2 or less with just ammonia have caused excessive FAC in some units; values between 9.5 and 10.0, depending on the amine and its volatility and dissociation, are commonly achieved. Condensate polishers have been by-passed and even eliminated in all-ferrous systems with elevated ammonia [134]. A similar strategy has been followed at German PWRs [135]. It is interesting to note that one of the first indications of excessive FAC in the outlet feeders of CANDU reactors was a rise in the temperature of the primary coolant to the reactor, caused largely by a loss of heat transfer efficiency from fouling of the tube side of the steam generators by deposited iron corrosion products.

7 The Role of Cycle Chemistry Control and Management in the Mitigation of FAC

It is clear from recent conferences, publications and assessments that there remain some uncertainties about the various indicators of FAC, the differences between single- and two-phase FAC, whether FAC is active or whether it can be slowed down or stopped by a change of chemistry, and what the various surface morphologies and colours indicate. Section 2 has tried to clarify the mechanisms through careful descriptions of the theories behind oxide growth and accelerated dissolution by hydrodynamic characteristics of the flow. In this section the large experience base from plant assessments, a small part of which has been included in Section 4, and the intimate knowledge of the IAPWS Cycle Chemistry Guidance [23–26,45,110] have been integrated with the latest understanding of the theory and mechanism of FAC, and assembled into the following sub-sections to provide outlines for optimizing the cycle chemistry for mitigation of FAC in generating plant. These are the key features and controlling aspects of the FAC mechanisms. The recommendations for controlling FAC in nuclear plants are made by the various industry/utility organizations around the world, so this section concentrates on providing a source document for fossil and combined-cycle plants. The basic principles, however, are universally applicable.

7.1 Key Cycle Chemistry Aspects of FAC Mitigation for Conventional Fossil Plants

Based on the current understanding of the FAC mechanism (Section 2), the various plant experiences of FAC (Section 4) and reviews of hundreds of organizations' fossil plant FAC programmes around the world by the authors, the following represent the key aspects of controlling FAC in fossil plants (Figure 38):

- Single-phase FAC can be controlled by the potential (ORP) of feedwater chemistry. FAC occurs under reducing conditions (low feedwater oxygen levels typical less than 5 $\mu g \cdot kg^{-1}$ (ppb) and a reducing agent) at locations where increased turbulence is generated by the system geometry.
- In all-ferrous feedwater systems (copper alloys may be in the condenser), an oxidizing feedwater treatment (AVT(O) or OT) will minimize corrosion, FAC and thus the transport of corrosion products (total iron) to the boiler. The optimum $pH_{25°C}$ range is 9.4 to 9.8 [24]; the actual choice of optimum pH for FAC mitigation should be determined by monitoring total iron corrosion products at levels provided in Table 7. Levels below 1 $\mu g \cdot kg^{-1}$ (ppb) for units on oxygenated treatment and below 2 $\mu g \cdot kg^{-1}$ (ppb) for units on AVT are typically easily achievable with optimized cycle chemistry.
- In mixed-metallurgy feedwater systems (copper alloys in the feedwater heaters and maybe also in the condenser) a reducing feedwater treatment (AVT(R)) will provide protection to the copper alloys [136]. The interconnecting carbon steel components and pipework will also be operating under reducing conditions and therefore may be subjected to FAC depending on the hydrodynamics (Section 2). Operating in the $pH_{25°C}$ range of 9.1 to 9.3 will provide optimum protection for the copper alloys and will help to prevent dissolution of magnetite from the carbon steel components and FAC better than operating at a $pH_{25°C}$ below 9.0. The actual choice of optimum pH should be determined by monitoring total iron and copper corrosion products at levels provided in Table 7. In some cases, the optimum $pH_{25°C}$ has been determined through monitoring to be higher than 9.3. Levels of total iron and copper each below 2 $\mu g \cdot kg^{-1}$(ppb) for units on AVT are typically easily achievable with optimized cycle chemistry.
- It is important to change the feedwater chemistry (challenge the status quo) when a change of feedwater heater tube material has been made. Probably the most common example is the change from copper alloy tubed feedwater heaters to stainless steel. If this change (eventually) encompasses all the LP and HP heaters, then this markedly increases the risk of FAC and mandates an immediate change/optimization of the chemistry to oxidizing and an increase of the $pH_{25°C}$ above that used in the mixed-metallurgy situation.
- For all types of feedwater systems, monitoring the total iron (and copper) levels will indicate whether the feedwater chemistry is optimized and FAC is under control. Levels of corrosion products indicating minimum FAC rates have been assembled by IAPWS [23] and are provided in Table 7.
- Two-phase FAC regions (deaerators, LP heater shells) (Section 4) in the feedwater system generally require a materials solution using a 1.25 % Cr or higher alloy (Section 2). This is applicable to rebuilding thickness with weld material or equipment replacement. Weld overlaying with carbon steel material will introduce surface roughness which has no better FAC resistance than the original pressure vessel material. Also, it is always preferable to replace a component or part of a component in kind than to try to introduce a "better" flow hydrodynamic situation: the experience is also that these can have higher FAC rates than the original.
- Two-phase FAC is most frequent in feedwater heater cascading drain lines downstream of control valves (Section 4). Thinned or failed sections should always be replaced with at least a 1.25 % Cr alloy. The iron levels in the cascading HP and LP drain lines often provide a good indicator of the extent and activity of FAC (Table 7). Levels of total iron below 10 $\mu g \cdot kg^{-1}$ (ppb) are typically easily achievable with optimized cycle chemistry. Replacement of the control valves and downstream piping should always be in a chromium containing material (P11, P22 or P5). All new plants should have these materials designed into these locations. Two-phase FAC is also predominant on HP and LP feedwater heater shells in areas close to the entry of higher pressure heater drains (Section 4).
- All the activities of a comprehensive FAC programme involving prediction, inspection and a combination of Level 1 and 2 NDE techniques will also be required (Section 5 and Figure 38).

7.2 Key Cycle Chemistry Aspects of FAC Mitigation for Combined-Cycle/HRSG Plants

Based on the current understanding of the FAC mechanism (Section 2), the various plant experiences of FAC (Section 4) and reviews of hundreds of organizations' HRSG plant FAC programmes around the world by the authors, this section represents the key aspects of controlling FAC in combined-cycle/HRSG plants (Figure 38).

- First there are three basic guiding principles for controlling FAC in combined-cycle/HRSG plants:

  a) An oxidizing treatment AVT(O) or OT must be used to prevent single-phase FAC [24]. No reducing agent should be used at any time during operation or shutdown.

b) An elevated pH with a volatile amine is needed to control two-phase FAC (up to $pH_{25°C}$ 9.8) [24,25].

c) The total iron corrosion products should be monitored [23] to compare with the values in Table 7 and to verify that the chemistry is optimum.

- The locations of single-phase FAC (Section 4) can be controlled by feedwater and evaporator chemistry [24,25]. Multi-pressure HRSGs should operate only on an oxidizing cycle (AVT(O)) without any reducing agents. This decision should preferably be made during the specification/design stages of an HRSG, but if this stage has been missed then the change should be made as early in the life of an HRSG as possible.
- Two-phase FAC of IP and LP evaporator tubing and other locations (Section 4) can be addressed by evaporator chemistry by operating at high $pH_{25°C}$ levels with ammonia or an amine [24,45] or by adding either tri-sodium phosphate or NaOH to the LP drum [25] provided that the LP drum doesn't provide feed for upper pressure HRSG circuits or superheater/reheater attemperation.
- Some two-phase FAC will need to be addressed by a materials solution (Section 2). If obvious susceptible tube locations can be identified, then these should be replaced by a 1.25 % Cr or higher alloy if the cycle chemistry cannot be optimized to mitigate FAC. Ideally the susceptible locations should be designed with the chromium containing materials. Steam separating equipment in the LP/IP drums and the LP/IP risers should also be designed or replaced with at least a 1.25 % Cr steel.
- Monitoring of iron in the feedwater and LP drum will identify whether FAC is active or is in agreement with Table 7. Satisfying the "rule of 2 and 5", where the total iron level is consistently less than 2 $\mu g \cdot kg^{-1}$ (ppb) in the feedwater and less than 5 $\mu g \cdot kg^{-1}$ (ppb) in each drum, will provide an indication that FAC is not active [23].
- For multi-pressure HRSGs the level of deposits in the HP evaporator provides an indirect confirmation that the total iron levels in the lower pressure HRSG circuits are within the "rule of 2 and 5". Removal of HP evaporator tubing and analysis of the deposit levels also provides an indication of the risk for under-deposit corrosion, and thus the need for chemically cleaning the HRSG [137].
- All the activities of a comprehensive FAC programme involving prediction, inspection and a combination of Level 1 and 2 NDE techniques will also be required (Section 5 and Figure 38).

7.3 Key Cycle Chemistry Aspects of FAC Mitigation for Plants with ACC

ACCs in fossil and combined-cycle plants control the cycle chemistry that is required on a plant. Operating with non-optimum chemistry can result in very high levels of corrosion products being transported into the condensate and feedwater of the plant. It has not been unusual with low condensate pH (below $pH_{25°C}$ 9.4) for levels of iron to be in the hundreds of ppb. An example is shown in Figure 39 for the ACC shown in Figure 36.

- Air-cooled condensers are a special case within the fossil and combined-cycle/HRSG plant FAC envelope. Monitoring of the iron levels at the condensate pump discharge provides the important indicator of the extent and activity of FAC at the tube entries in the upper ducting. Worldwide experience indicates that initially the $pH_{25°C}$ level around the cycle should be higher than the 9.2 to 9.6 historically adequate for all-ferrous systems. Usually a condensate $pH_{25°C}$ of close to 9.8 will be required. Total iron corrosion product levels should be in line with Table 7.
- Figure 39 shows an example reproduced many times worldwide of the beneficial effect of increasing pH on mitigating FAC in ACCs. During initial operation on OT at a condensate $pH_{25°C}$ of about 9.0, the total iron levels in the condensate were very high (80–100 $\mu g \cdot kg^{-1}$ (ppb)). Over a period of about two years the $pH_{25°C}$ was gradually increased with a concomitant decrease in the total iron levels to less than 10 $\mu g \cdot kg^{-1}$ (ppb). Application of a condensate filter (5 microns absolute) will allow the iron levels to be consistently less than 5 $\mu g \cdot kg^{-1}$ (ppb).
- As shown in Figure 37, there is also an increasing experience base that application of an FFS into the ACC ducting provides similar protection to a high pH level with low total iron values (10 $\mu g \cdot kg^{-1}$ (ppb)).

7.4 Appearance of Generating Plant Surfaces in Relation to FAC and Flow Regimes

The authors have noted some uncertainties with regards to surface features and colouration associated with FAC, and when FAC has been mitigated. The figures in Section 4 show numerous examples to assist in identification of both single- and two-phase FAC damage, and have illustrated that FAC is a local phenomenon. These areas of FAC are located by the local flow phenomena and/or geometry which produce increased turbulence in the flow, which is referred to as "accentuated turbulent flow" (downstream of bends, restrictions, etc.). Once the flow downstream of these returns to "fully developed turbulent flow" the FAC rate generally decreases to zero. The surface appearances upstream and downstream of the FAC as well as the FAC itself provide very important visual

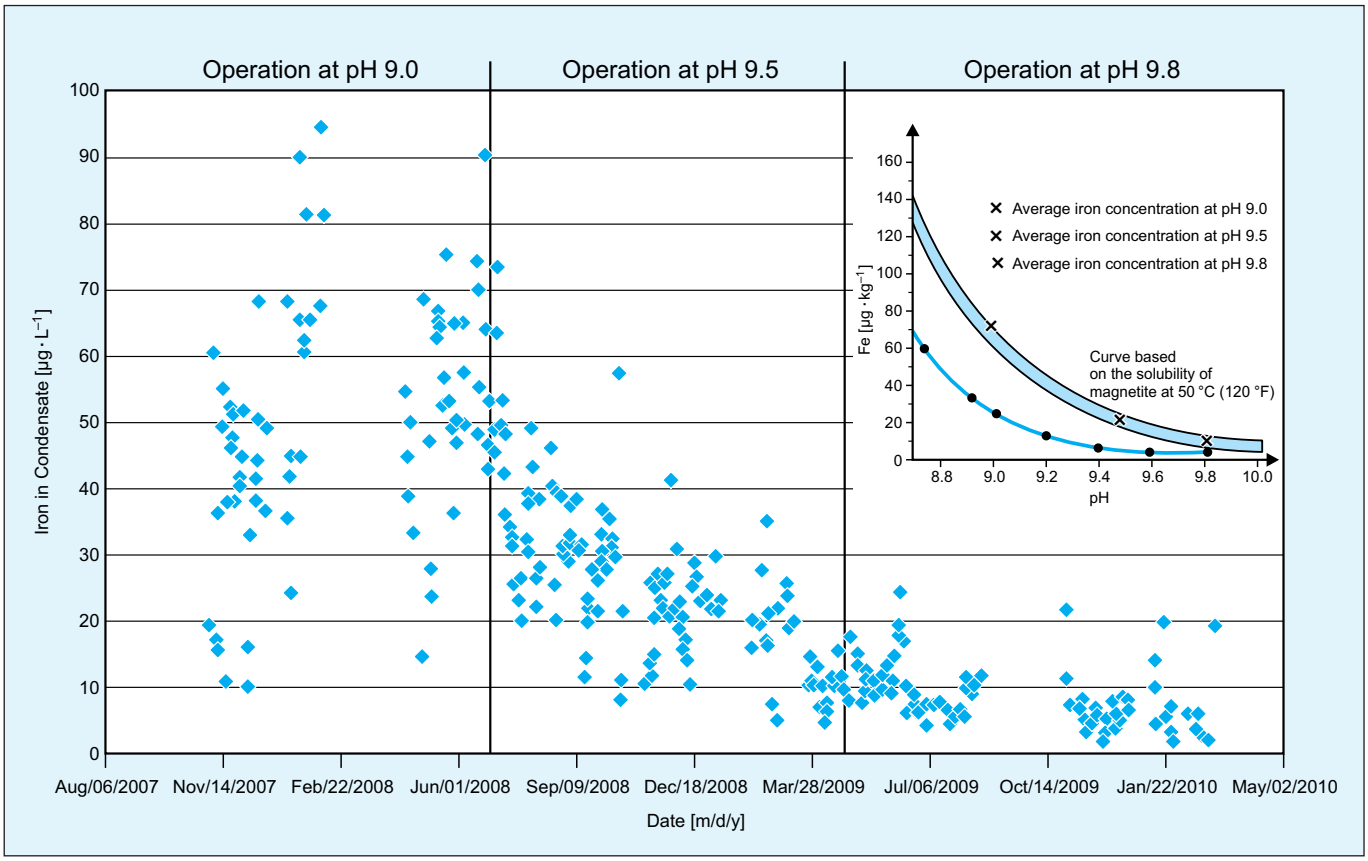

Figure 39:
Total iron corrosion product levels monitored in the condensate of the plant/ACC shown in Figure 36. Figure shows the reduction of iron as the $pH_{25°C}$ is increased from 9.0 to 9.8 in agreement with the "Dooley-Aspden Relationship" [20] superimposed on the right of the figure (source: I. Richardson and G. Joy, presented at Air-Cooled Condenser User Group (ACCUG 2011) [127]).

clues as to whether the FAC is single- or two-phase, and most importantly whether the damage is active. The information can then be used to initiate a focused cycle chemistry review. Table 8 provides an overview of these various flow regimes and the possible chemistries as a function of oxidizing power or potential (ORP or ECP) and pH. The previous sections have summarized the key approaches for conventional fossil and combined-cycle plants. The "intensity of fluid dynamics" on the table represents first an area where FAC is not active (first column), to an area where there is accentuated turbulent flow and FAC occurs (second column), and finally to an area where flow returns to fully developed turbulent flow (third column).

7.5 Assessment of Cycle Chemistry in Controlling FAC in Fossil and Combined-Cycle Plants – Use of Repeat Cycle Chemistry Situation (RCCS) Analysis

The understanding of cycle chemistry influenced FAC mechanisms in conventional fossil and combined-cycle/HRSGs is very advanced, and has been known and documented for more than 30 years. The latest theory has been discussed in Section 2. In spite of this, chemistry influenced damage and the associated availability losses due to deficient chemistry practices are often enormous and can be fatal. FAC damage and component failure incidents persist as illustrated in Section 4 in both conventional fossil and combined-cycle units, as well as in nuclear plants. It is thus very clear that the approaches taken by organizations operating these plants to prevent such damage are frequently unsuccessful.

In 2008 a concept was developed to identify the reasons behind cycle chemistry influenced failure and damage, including FAC, and which could be used to prevent damage/failure proactively [138]. This involves identifying repeat cycle chemistry situations (RCCS) which can be regarded as the basics of cycle chemistry, and which are allowed to continue by the chemistry or operating staff or are imposed on the plant/organization as a consequence of inadequate management support for cycle chemistry. For FAC damage and failure, assessment and analysis make it clear that every incident can be related backwards

	Intensity of Fluid Dynamics		
Flow Regime / **Locations and Conditions**	**A. Fully Developed Turbulent Flow** Stable fluid boundary layer in contact with oxide on component surface	**B. Accentuated Turbulent Flow** Turbulent eddies from geometry (bend, restriction, etc.) reduce thickness of boundary layer locally; possible flow separation and reattachment	**C. Fully Developed Turbulent Flow** Downstream of flow disturbance, returns to A
1. Areas with single-phase flow in units with reducing chemistries	Normal magnetite growth on surface (Section 2). Semi-protective dull black or grey oxide dependent on the temperature. Moderate dissolution of Fe^{++} into flow. Low or no FAC.	Increased fluid forces and dissolution of Fe^{++} – thinner and less protective magnetite. Chevron markings from FAC. With severe turbulence, the surface looks like "orange peel" (Figures 20 and 28).	Flow reestablishes conditions under 1A. Surface oxide also as in 1A.
2. Areas with two-phase flow in units with reducing chemistries	As 1A.	Areas become shiny black with some dimples from FAC (Figures 29–32).	Reestablishes conditions under 2A. HRSG tubing and air-cooled condensers have black deposits very close to active FAC regions in 2B (e.g., Figure 35).
3. Areas with single-phase flow in units with oxidizing chemistries	No FAC. Surfaces become red – ferric oxides form on top of magnetite formed by corrosion/FAC under previous AVT(R). The "ruggedness of the redness" depends on the oxidizing power (level of oxygen).	As 3A. Red "orange peel" appearance from previous severe FAC under AVT(R).	Reestablishes conditions under 3A.
4. Areas with two-phase flow in units with oxidizing chemistries	Surfaces are generally as in 1A and 2A. Surfaces in upper ACC ducts can be red due to ferric oxide formation during shutdown (Figures 34 and 36).	FAC occurs in severely turbulent areas with grey or shiny black oxide (Figures 30– 32). The surfaces remain black even when the pH has been increased.	Reestablishes conditions under 4A. There is usually a sharp visible boundary between the red (protected) and shiny black areas.
5. Air-cooled condenser with two-phase steam-water flow under oxidizing or reducing chemistries	Lower steam transport surfaces are generally grey. Upper ducting can be red (formed on shutdown) (Figure 27).	Transport ducting has white (metallic) areas (Figure 27). Tube entries and supports in upper ducts have white areas (Figure 26).	As 5A.

Table 8:

Summary of the expected surface appearances of FAC in conventional fossil and combined-cycle/HRSG plants as a function of chemistry and flow (updated from [18] with information from previous sections).

in time to multiples of RCCSs which were not recognized or properly addressed and allowed to repeat or continue. In some cases, the chemistry staff had not recognized the importance of the situation and allowed it to continue. In other cases, the chemistry staff recognized the importance, but was not successful in convincing the management (either plant or executive) that action was required. Also, it became obvious that plants/organizations can get away with having one or two RCCSs, but once this number increases then failure/damage is a certainty.

In total there are ten RCCSs [138] but not all are associated with FAC in fossil and combined-cycle plants. Continuing analysis of RCCSs associated with FAC assessments at close to 200 plants worldwide indicates that there are multiple sub-categories, and identification of more than three RCCSs at a plant indicates that failure/damage will occur and that FAC could be active. To assist the readers in understanding how RCCSs influence FAC and whether they exist in their plants, the following provide a few notes on some of the most important RCCS categories contributing to FAC.

Corrosion Products Monitoring of total iron is the key indicator of FAC. The levels presented in Table 7 provide an indicator of achievable levels in fossil and combined-cycle plants and in units with ACC. Categories of RCCS to look for as indicators that FAC is occurring in a plant include: the corrosion product levels are not known or monitored; the levels are too high and much above international guideline values (Table 7); there are inadequate and/or not sufficient locations being monitored; sampling has been conducted at the same time/shift each time; techniques are used with incorrect detection limits; and a most common feature is only the soluble part of the total iron is monitored due to not digesting the sample. A key easy-to-observe verification aspect of this RCCS for FAC is black deposits in the steam and water sampling (wet rack) troughs for units on AVT(O). All of these categories are discussed in detail in the IAPWS Technical Guidance Document [23].

Conventional Boiler Waterwall/HRSG Evaporator Deposits The corrosion products from FAC deposit on boiler waterwalls or HRSG HP evaporator tubing, and are an indirect indicator of FAC in the lower temperature/pressure parts of the cycle. Categories to look for as indicators that FAC is occurring in a plant include: HRSG HP evaporator samples have not been taken for analysis; there is no knowledge of deposit levels and deposition rate in HP evaporators; samples are taken but not analysed comprehensively; deposits are excessive and exceed criteria to chemical clean [137]; the HRSG HP evaporator deposits are not linked with chemistry in the lower pressure circuits or to the levels of transported total iron [23]; the HP evaporator has been sampled and needs cleaning but management delayed or cancelled. For combined-cycle/HRSGs all of these categories are discussed in detail in the IAPWS Technical Guidance Document [137].

Continuous On-line Cycle Chemistry Instrumentation [26] Section 2 has indicated the importance of the chemistry parameters pH and potential in controlling FAC, and Sections 7.1–7.3 have provided the key parameter values to mitigate FAC. Categories to look for as indicators that FAC is occurring in a plant include: installed and operating instrumentation is at a low percentage compared to IAPWS [26] (a normal assessed level is between 58 and 65 %); too many instruments are out of service, not maintained or calibrated; instruments are not alarmed for operators and many are shared by multiple locations and not/never switched; plant relies on grab samples to control plant (1 to 3 times per day/shift).

Challenging the Status Quo This RCCS is most important in addressing or preventing FAC in plant cycles and the categories to look for as indicators include: no change in chemistry since commissioning; using incorrect or outdated guidelines; continuing to use reducing agents in combined-cycle/HRSGs and thus risking or experiencing single-phase FAC; continuing to use the wrong pH; not having a chemistry manual for the unit, plant or organization; incorrect addition point for chemicals (most often reducing agent with AVT(R)); not questioning the use of proprietary chemical additions (phosphate blends, amines, FFPs) and therefore not knowing the composition of chemicals added to the unit/plant; not determining through monitoring the optimum feedwater pH to prevent/control FAC.

The RCCS analysis has been applied during 197 plant assessments. 118 of these were at conventional fossil plants and 79 were combined-cycle/HRSG plants involving HRSGs from 17 manufacturers. Table 9 shows the most recent ranking order of RCCSs for these conventional fossil and combined-cycle/HRSG plants, and illustrates that the same RCCSs occur in both types of plant with approximately the same ranking order. The table illustrates that the four RCCSs that relate most closely to FAC, as described previously, are the most frequent indicators of cycle chemistry problems in fossil and combined-cycle/HRSG plants. This illustrates why FAC continues to occur despite the excellent understanding of the mechanism (Section 2) and the well-documented locations (Section 4).

RCCS Categories	In 118 Conventional Fossil Plants	In 79 Combined-Cycle/HRSG Plants
Corrosion products	90	92
Conventional fossil waterwall/ HRSG evaporator deposition	45	62
Chemical cleaning	15	< 10
Contaminant ingress	16	< 10
Drum carryover	80	88
Air in-leakage	40	< 10
Shutdown protection	77 (& 92*)	65 (& 92*)
On-line alarmed instrumentation	80	92
Not challenging the status quo	81	77
No action plans	N/A	N/A

Table 9:
Analysis of repeat cycle chemistry situations (RCCS) in conventional fossil and combined-cycle/HRSG plants. The numbers in the table represent the percentage of plants where the particular RCCS was identified.
* Percentage of plants not using dehumidified air (DHA) on steam turbine during shutdown.

8 Concluding Remarks

FAC is still occurring at a high rate in fossil, combined-cycle and nuclear plants worldwide. In HRSGs it remains the leading cause of failure/damage. FAC has been researched for over 50 years, and scientifically all the major influences are well recognized. However, the application of this science and understanding to generating plants has not been entirely satisfactory. Fatalities have occurred in generating plants, and major failures are still occurring at locations which are basically the same as they were in the 1980s and 1990s (Section 4). The latest theory of the major aspects of the mechanism has been developed in Section 2. The subsequent sections provide details on the major locations of FAC in plants, the key identifying surface features of the types of FAC, the cycle chemistries used in the plants and the key monitoring tools to identify the presence of FAC. The management aspects should consolidate the inspection, predictive, and chemistry approaches into a company-wide coordinated FAC programme to link all these tools into an overall programmatic approach. It is clear that the cycle chemistry used on the generating plants has the major influence on both single- and two-phase FAC: the IAPWS Technical Guidance Documents cover all the major aspects for optimizing the cycle chemistry, and these have been customized for plant practice (Section 7). The principles espoused in Section 7 apply broadly to nuclear plants, which have their own industry/utility guidelines.

REFERENCES

[1] Koch, G. H., Brongers, M. P. H., Thompson, N., Virmani, Y. P., Payer, J. H., *Corrosion Costs and Preventive Strategies in the United States*, **2002**. Federal Highway Administration, Washington, DC, USA, FHWA-RD-01-156.

[2] Gorman, J., Arey, M., Koch, G., *Cost of Corrosion in the Electric Power Industry*, **2001**. Electric Power Research Institute, Palo Alto, CA, USA, EPRI 1004662.

[3] Chexal, V. K., Horowitz, J., Dooley, R. B., Millett, P., Wood, C., Jones, R., Bouchacourt, M., Remy, F., Nordmann, F., Saint Paul, P., Kastner, W., *Flow-Accelerated Corrosion in Power Plants*, **1998**. Electric Power Research Institute, Palo Alto, CA, USA, TR-106611-R1.

[4] Dooley, R. B., Chexal, V. K., "Flow-Accelerated Corrosion of Pressure Vessels in Fossil Plants", *International Journal of Pressure Vessels and Piping* **2000**, 77, 85.

[5] *Nondestructive Evaluation of Ferritic Piping for Erosion-Corrosion*, **1987**. Electric Power Research Institute, Palo Alto, CA, USA, EPRI Report NP-5410.

[6] Dooley, B., Anderson, R., *SPECIAL REPORT: HRSG Assessments Identify Trends in Cycle Chemistry, Thermal Transient Performance*, **2014**. Available from http://www.ccj-online.com.

[7] Hömig, H. E., *Physicochemical Basis of Feedwater Chemistry*, **1963**. Vulkan-Verlag Dr. W. Clasen, Essen, Germany, 232 [in German].

[8] Hömig, H. E., *Metal and Water*, **1964**. Vulkan-Verlag Dr. W. Clasen, Essen, Germany, 2nd Edition [in German].

[9] Hömig, H. E., *Metal and Water*, **1971**. Vulkan-Verlag Dr. W. Clasen, Essen, Germany, 3rd Edition, 138 [in German].

[10] Moller, G. E., *Metallurgical and Corrosion Engineening Analysis of a Ruptured Carbon Steel Elbow*, **1983**. Failure Analysis Associates, FaAA 3108.

[11] Wu, P. C., *Erosion/Corrosion-Induced Pipe Wall Thinning in US Nuclear Plants*, **1989**. United States Nuclear Regulatory Commission, Washington, DC, USA, NUREG-1344.

[12] Sweeney, T. J., Hooper, C. M., Breedlove, I. L., "A Review of the Virginia Power Erosion/Corrosion Program", *Proc., ASME Joint Power Generation Conference*, **1991** (San Diego, CA, USA). American Society of Mechanical Engineers, New York City, NY, USA.

[13] *Summary of Responses to NRC Bulletin 87-01, Thinning of Pipe Walls in Nuclear Power Plants*, **1988**. United States Nuclear Regulatory Commission, Rockville, MD, USA, Information Notice No. 88-17.

[14] Patulski, S. A., *Pleasant Prairie Unit 1 Feedwater Line Failure*. A Report to Fomis. June **1995**.

[15] McAllister, D. A., *Pleasant Prairie Unit 1 Feedwater Line Failure*, **1996**. Chemistry Committee Experience Report, Corpus Christi, TX, USA.

[16] *Secondary Piping Rupture at the Mihama Power Station in Japan*, **2006**. United States Nuclear Regulatory Commission, Rockville, MD, USA, NRC Information Notice 2006-08.

[17] Chiu, C., Gockel, L. B., "Iatan Desuperheater Pipe Failure Caused by FAC: September 28, 2007", *Proc., ASME Pressure Vessels and Piping Conference*, **2010** (Bellevue, WA, USA) American Society of Mechanical Engineers, New York City, NY, USA, Vol. 6, Parts A and B, 601.

[18] Dooley, R. B., "Flow-Accelerated Corrosion in Fossil and Combined Cycle/HRSG Plants" *PowerPlant Chemistry* **2008**, 10(2), 68.

[19] Dooley, R. B., Anderson, R., "Assessments of HSRGs – Trends in Cycle Chemistry and Thermal Transient Performance", *PowerPlant Chemistry* **2009**, 11(3), 132.
Also published in: *Combined Cycle Journal* **2009**, 115.

[20] Dooley, R. B., Aspden, A. G., Howell, A. G., du Preez, F., "Assessing and Controlling Corrosion in Air-cooled Condensers", *PowerPlant Chemistry* **2009**, 11(5), 264.

[21] *Review and Benchmark of Calculation Methods of Piping Wall Thinning due to Erosion-Corrosion in Nuclear Power Plants*, **2012**. International Atomic Energy Agency, Vienna, Austria, Coordinated Research Project, CRP-121022.

[22] Lister, D. H., Uchida, S., "Reflections on FAC Mechanisms", *PowerPlant Chemistry* **2010**, 12(9), 550.

[23] *Technical Guidance Document: Corrosion Product Sampling and Analysis for Fossil and Combined Cycle Plants*, **2014**. International Association for the Properties of Water and Steam, IAPWS TGD6-13(2014). Available from http://www.iapws.org.

[24] *Technical Guidance Document: Volatile Treatments for the Steam-Water Circuits of Fossil and Combined-Cycle/HRSG Power Plants*, **2015**. International Association for the Properties of Water and Steam, IAPWS TGD3-10(2015). Available from http://www.iapws.org.

[25] *Technical Guidance Document: Phosphate and NaOH Treatments for the Steam-Water Circuits of Drum Boilers of Fossil and Combined-Cycle/HRSG Power Plants*, **2015**. International Association for the Properties of Water and Steam, IAPWS TGD4-11(2015). Available from http://www.iapws.org.

[26] *Technical Guidance Document: Instrumentation for Monitoring and Control of Cycle Chemistry for the Steam-Water Circuits of Fossil-Fired and Combined-Cycle Power Plants*, **2015**. International Association for the Properties of Water and Steam, IAPWS TGD2-09(2015). Available from http://www.iapws.org.

[27] Poulson, B., "Predicting and Preventing Flow Accelerated Corrosion in Nuclear Power Plants", *International Journal of Nuclear Energy* **2014**, Article ID 423295. Available from https://www.hindawi.com/journals/ijne.

[28] Betova, I., Bojinov, M., Saario, T., *Predictive Modelling of Flow-Accelerated Corrosion – Unresolved Problems and Issues*, **2010**. VTT Technical Research Centre of Finland, Espoo, Finland, VTT-R-08125-10.

[29] Berl, E., van Taack, F., *Forschungsarbeiten auf dem Gebiete des Ingenieurwesens*, **1930**. Berlin, Germany, Issue 330.

[30] Uhlig, H. H., *The Corrosion Handbook*, **1948**. John Wiley & Sons, Inc., New York and London.

[31] Moore, J. B., Jr., Jones, R. L., "Growth Characteristics of Iron Oxide Films Generated in Dilute Lithium Hydroxide Solution at 300 °C", *Journal of the Electrochemical Society* **1968**, 115(6), 576.

[32] Potter, E. C., Mann, G. M. W., "Oxidation of Mild Steel in High Temperature Aqueous Systems", *Proc., First International Congress on Metallic Corrosion*, **1961** (London, United Kingdom). Butterworths, London, United Kingdom, 417.

[33] Castle, J. E., Masterson, H. G., "The Role of Diffusion in the Oxidation of Mild Steel in High Temperature Aqueous Solutions", *Corrosion Science* **1966**, 6(3–4), 93.

[34] Robertson, J., "The Mechanism of High Temperature Aqueous Corrosion of Steel", *Corrosion Science* **1989**, 29(11–12), 1275.

[35] McKeen, K., Lalonde, M., Scott, A., Ross, J., "Hydrogen Effusion Probe Development and Installation at the Point Lepreau Generating Station", *presented at the 28th Annual Conference of the Canadian Nuclear Society*, **2007** (St. John, NB, Canada). Canadian Nuclear Society, Toronto, ON, Canada.

[36] Friggens, H. A., Holmes, D. R., "Nucleation and Growth of Magnetite Films on Fe in High Temperature Water", *Corrosion Science* **1968**, 8(12), 871.

[37] Smith, S. H., Bloom, M. C., *A Study of Hydrogen Evolution during Aqueous Oxidation of Mild Steel*, **1969**. Naval Research Laboratory, Washington, DC, USA, NRL Report 6887.

[38] Bohnsack, G., *The Solubility of Magnetite in Water and in Aqueous Solutions of Acid and Alkali*, **1987**. Hemisphere Publishing Corp., Washington, New York, London.

[39] Poulson, B., Greenwell, B. S., Chexal, B., Horowitz, G., "Modelling Hydrodynamic Parameters to Predict Flow Assisted Corrosion", *Proc., 5th International Conference on Environmental Degradation of Materials in Nuclear Power Systems*, **1992** (Monterey, CA, USA). American Nuclear Society, La Grange Park, IL, USA. (Original diagram published as: Bignold, G. J., de Whalley, C. H., Garbett, K., Woolsey, I. S., "Mechanistic Aspects of Erosion-Corrosion under Boiler Feedwater Conditions", *Water Chemistry of Nuclear Reactor Systems 3*, **1983**. British Nuclear Energy Society, London, United Kingdom, 219.)

[40] Mancey, D., *Proc., Workshop on FAC*, **2016** (Ajax, ON, Canada). CANDU Owners Group (COG).

[41] Bignold, G. J., Garbett, K., Woolsey, I. S., "Mechanistic Aspects of the Temperature Dependence of Erosion-Corrosion", *Proc., Specialists Meeting on Erosion-Corrosion in High Temperature Water and Wet Steam*, **1982** (Les Renardières, France). Électricité de France, Paris, France.

[42] Sturla, P., "Oxidation and Deposition Phenomena in Forced Circulating Boilers and Feedwater Treatment", *presented at the Fifth National Feedwater Conference*, **1973** (Prague, Czechoslovak Socialist Republic).

[43] Tremaine, P. R., LeBlanc, J. C., "The Solubility of Magnetite and the Hydrolysis and Oxidation of Fe^{2+} in Water at 300°C", *Journal of Solution Chemistry* **1980**, 9(6), 415.

[44] Slade, J. P., Gendron, T. S., "Flow Accelerated Corrosion and Cracking of Carbon Steel Piping in Primary Water – Operating Experience at the Point Lepreau Generating Station", *Proc., 12th Int. Conf. on Environmental Degradation of Materials in Nuclear Power Systems*, **2005** (Salt Lake City, UT, USA). The Minerals, Metals and Materials Society.

[45] *Technical Guidance Document: Application of Film Forming Amines in Fossil, Combined Cycle and Biomass Plants*, **2016**. International Association for the Properties of Water and Steam, IAPWS TGD8-16. Available from http://www.iapws.org.

[46] Fruzzetti, K., "A Pathway to Application of Filming Amines in PWRs", *presented at the International Conference on Film Forming Amines and Products*, **2017** (Lucerne, Switzerland). International Association for the Properties of Water and Steam.

[47] Betova, I., Bojinov, M., Saario, T., *Film-Forming Amines in Steam/Water Cycles – Structure, Properties, and Influence on Corrosion and Deposition Processes*, **2014**. Technical Research Center of Finland (VTT), Espoo, Finland, Research Report VTT-R-03234-14.

[48] Lister, D., Weerakul, S., Caravaggio, M., "The Effects of a Film-Forming Amine on Flow-Accelerated Corrosion in Single- and Two-Phase Flows", *Proc., International Conference on Flow-Accelerated Corrosion*, **2016** (Lille, France). Électricité de France, Paris, France.

[49] Jack, M., Weerakul, S., Lister, D. H., "The Interaction of a Film-Forming Amine with Surfaces of a Recirculating Experimental Water Loop", *Proc., Heat Exchanger Fouling and Cleaning XI*, **2015** (Enfield, Dublin, Ireland). Heat Transfer Research, Inc., Navasota, TX, USA.

[50] Hater, W., de Bache, A., Petrick, T., "Dry Lay-up of Steam Generators with Film Forming Amines: Studies and Field Experience", *PowerPlant Chemistry* **2014**, 16(5), 284.

[51] Weerakul, S., Lister, D., Hater, W., "The Sorption Behaviour of a Film-Forming Amine (FFA) and Its Effect on Flow-Accelerated Corrosion (FAC)", *presented at the International Conference on Film Forming Amines and Products*, **2017** (Lucerne, Switzerland). International Association for the Properties of Water and Steam.

[52] Charintara, S., Kongvarhodom, C., Lister, D. H., Mori, S., "The Effect of Film-Forming Amines (FFAs) on Flow-Accelerated Corrosion (FAC) of Carbon Steels in Single-Phase Water", *Proc., Pure and Applied Chemistry International Conference*, **2018** (Hat Yai, Songkhla, Thailand). Prince of Songkla University, Hat Yai, Songkhla, Thailand.

[53] Weerakul, S., *The Effects of Film-Forming Amines on Flow-Accelerated Corrosion*, **2018**. Ph.D. Thesis, University of New Brunswick, Fredericton, NB, Canada.

[54] Lertsurasakda, C., Srisukvatananan, P., Liu, L., Lister, D., Mathews, J., "The Effects of Amines on Flow-Accelerated Corrosion in Steam-Water Systems", *PowerPlant Chemistry* **2013**, 15(3), 181.

[55] McCann, P., Smith, B., Hater, W., de Bache, A., "Experiences with the Application of Film Forming Amines at Connah's Quay CCGT", *presented at the International Conference on Film Forming Amines and Products*, **2017** (Lucerne, Switzerland). International Association for the Properties of Water and Steam.

[56] Huijbregts, W. M. M., "Erosion-Corrosion of Carbon Steel in Wet Steam", *Materials Performance* **1984**, 23(10), 39.

[57] Bouchacourt, M., *Paper presented at the EPRI Workshop on Erosion-Corrosion of Carbon Steel Piping*, **1987** (Washington, DC, USA). Electric Power Research Institute, Palo Alto, CA, USA.

[58] Phromwong, P., Lister, D. H., Uchida, S., "Modelling Material Effects in Flow-Accelerated Corrosion", *Proc., International Conference on Environmental Degradation of Materials in Nuclear Power Systems*, **2011** (Colorado Springs, CO, USA). The Minerals, Metals and Materials Society, Pittsburgh, PA, USA.

[59] Lister, D. H., Feicht, A. D., Fujiwara, K., Khatibi, M., Liu, L., Ohira, T., Uchida, S., "The Mitigation of Flow-Accelerated Corrosion in the Feedwater Systems of Nuclear Reactors – the Influence of Dissolved Oxygen under Different Operating Conditions", *PowerPlant Chemistry* **2011**, 13(4), 188.

[60] Woolsey, I. S., Bignold, G. J., De Whalley, C. H., Garbett, K., "The Influence of Oxygen and Hydrazine on the Erosion-Corrosion Behaviour and Electrochemical Potentials of Carbon Steel under Boiler Feedwater Conditions", *Water Chemistry of Nuclear Reactor Systems 4*, **1986**. British Nuclear Energy Society, London, United Kingdom, 337.

[61] Ferrell, R. T., Himmelblau, D. M., "Diffusion Coefficients of Nitrogen and Oxygen in Water", *Journal of Chemical and Engineering Data* **1967**, 12(1), 111.

[62] Berger, F. P., Hau, K.-F., "Mass Transfer in Turbulent Pipe Flow Measured by the Electrochemical Method" *International Journal of Heat and Mass Transfer* **1977**, 20(11), 1185.

[63] Sanchez-Caldera, L. E., Griffith, P., Rabinowicz, E., "The Mechanism of Corrosion-Erosion in Steam Extraction Lines of Power Stations", *Transactions of ASME* **1988**, 110, 180.

[64] Lister, D. H., Lang, L. C., "A Mechanistic Model for Predicting Flow-Assisted Corrosion and General Corrosion of Carbon Steels in Reactor Primary Coolants", *Proc., CHIMIE* **2002** (Avignon, France). Société Française d'Energie Nucléaire, Paris, France.

[65] Khatibi, M., *Parameters Influencing Flow-Accelerated Corrosion (FAC) in the Secondary Side of Nuclear Power Plants*, **2010**. Ph.D. Thesis, University of New Brunswick, Fredericton, NB, Canada.

[66] Turner, C. W., Chi, L., "Formation of Corrosion Products of Carbon Steel under Condenser Operating Conditions", *Proc., Nuclear Plant Chemistry Conference (NPC)*, **2012** (Paris, France). Société Française d'Energie Nucléaire, Paris, France.

[67] Lister, D. H., Liu, L., Feicht, A., Khatibi, M., Cook, W., Fujiwara, K., Kadoi, E., Ohira, T., Takiguchi, H., Uchida, S., "A Fundamental Study of Flow-Accelerated Corrosion in Feedwater Systems", *Proc., 15th International Conference on the Properties of Water and Steam*, **2008** (Berlin, Germany). International Association for the Properties of Water and Steam, Electro. 04.

[68] Poulson, B., "Complexities in Predicting Erosion-Corrosion", *Wear* **1999**, 233–235, 497.

[69] Lister, D. H., Kippers, N., Raval, S., Garland, P., "Localised Pipe Wall Thinning from Disturbed Flows", *presented at 17th International Conference on the Properties of Water and Steam*, **2018** (Prague, Czech Republic), International Association for the Properties of Water and Steam.

[70] Utanohara, Y., Nagaya, Y., Nakamura, A., Murase, M., Kamahori, K., "Correlation Between Flow Accelerated Corrosion and Wall Shear Stress Downstream of an Orifice", *Journal of Power and Energy Systems* **2013**, 7(3), 138.

[71] Pietralik, J. M., Schefski, C. S., "Flow and Mass Transfer in Bends under Flow-Accelerated Corrosion Wall Thinning Conditions", *Journal of Engineering for Gas Turbines and Power* **2011**, 133(1), 012902.

[72] Berge, P., Ducreux, J., Saint-Paul, P., "Effects of Chemistry on Erosion-Corrosion of Steels in Water and Wet Steam", *Proc., 2nd International Conference on Water Chemistry in Nuclear Reactor Systems*, **1980** (Bournemouth, United Kingdom). British Nuclear Energy Society, London, United Kingdom.

[73] Gipon, E., Trevin, S., "Improvement of FAC Maintenance Program Issued from BRT-CICERO™ via CFD Calculations", *Proc., International Conference on Flow-Accelerated Corrosion*, **2016** (Lille, France). Électricité de France, Paris, France.

[74] Balakrishnan, P. V., "A Radiochemical Technique for the Study of Dissolution of Corrosion Products in High Temperature Water", *The Canadian Journal of Chemical Engineering* **1977**, 55, 357.

[75] Cleaver, J. W., Yates, B., "Mechanism of Detachment of Colloidal Particles from a Flat Substrate in a Turbulent Flow", *Journal of Colloid and Interface Science* **1973**, 44(3), 464.

[76] Nesic, S., Postlethwaite, J., "Relationship between the Structure of Disturbed Flow and Erosion-Corrosion", *Corrosion* **1990**, 46(11), 874.

[77] Schmitt, G., Bakalli, M., "Advanced Models for Erosion Corrosion and Its Mitigation", *Materials and Corrosion* **2008**, 59(2), 181.

[78] Mohajery Moghaddam, K., *The Dissolution Rate Constant of Magnetite in Water at Different Temperatures and pH Conditions*, **2014**. Ph.D. Thesis, University of New Brunswick, Fredericton, NB, Canada.

[79] Mohajery Moghaddam, K., de Pierrefeu, L. D., Lister, D., "The Dissolution Rate Constant of Magnetite in Water at Different Temperatures and pH Conditions", *Proc., Nuclear Plant Chemistry Conference (NPC)*, **2012** (Paris, France). Société Française d'Energie Nucléaire, Paris, France.

[80] Uchida, S., Naito, M., Uehara, Y., Okada, H., Lister, D. H., "Evaluation of Flow Accelerated Corrosion of PWR Secondary Components by Corrosion Analysis Coupled with Flow Dynamics Analysis", *Proc., 13th International Conference on Environmental Degradation of Materials in Nuclear Power Systems*, **2007** (Whistler, BC, Canada). Canadian Nuclear Society, Toronto, ON, Canada.

[81] Hoashi, E., Yoshihashi-Suzuki, S., Kanemura, T., et al., "Development of 3D CFD Technology for Flow-Assisted Corrosion", *Proc., Nuclear Plant Chemistry Conference (NPC)*, **2008** (Berlin, Germany). VGB PowerTech, Essen, Germany.

[82] Cook, W. G., Lister, D. H., "Some Aspects of Electrochemistry and Corrosion Mechanisms Influencing Flow Assisted Corrosion in CANDU Outlet Feeder Pipes", *Proc., International Conference on Water Chemistry of Nuclear Reactor Systems*, **2004** (San Francisco, CA, USA). Electric Power Research Institute, Palo Alto, CA, USA.

[83] Palazhchenko, O. Y., *A Comprehensive CANDU-6 Model: Primary Side Transport of Dissolved and Particulate Radioactive Species*, **2017**. Ph.D. Thesis, University of New Brunswick, Fredericton, NB, Canada.

[84] Cook, W. G., *Experiments and Models of General and Flow-Assisted Corrosion of Materials in Nuclear Reactor Environments*, **2005**. Ph.D. Thesis, University of New Brunswick, Fredericton, NB, Canada.

[85] Suzuki, H., Uchida, S., Naitoh, M., Okada, H., Koikara, S., Nagaya, Y., Nakamura, A., Koshizuka, S., Lister, D. H., *Nuclear Technology* **2013**, 183(1), 62.

[86] Mohajery, K., Liu, L., Lister, D. H., Uchida, S., "Flow-Accelerated Corrosion in Two-Phase Steam-Water Flows: Experiments and Modelling", *Proc., Nuclear Plant Chemistry Conference (NPC)*, **2016** (Brighton, United Kingdom). The Nuclear Institute, London, United Kingdom.

[87] Okada, H., Uchida, S., Naitoh, M., Xiong, J., Koshizuka, S., "Evaluation Methods for Corrosion Damage of Components in Cooling Systems of Nuclear Power Plants by Coupling Analysis of Corrosion and Flow Dynamics", *Journal of Nuclear Science and Technology* **2011**, 48(1), 65.

[88] Heymann, F. J., *Toward Quantitative Prediction of Liquid Impact Erosion. Characterization and Determination of Erosion Resistance*, **1970**. ASTM International, West Conshohocken, PA, USA, STP474, 212.

[89] Lister, D. H., Gauthier, P., Slade, J., "The Acceleration of CANDU Outlet Feeders", *Proc., International Conference on Water Chemistry in Nuclear Power Plants*, **1998** (Kashiwazaki, Japan). Japan Atomic Industrial Forum, Inc., Tokyo, Japan.

[90] Allen, J. R. L., "Bed Forms due to Mass Transfer in Turbulent Flows", *Journal of Fluid Mechanics* **1971**, 49(1), 49.

[91] Leighley, J., "Cuspate Surfaces of Melting Ice and Firn", *Geographical Review* **1948**, 38, 300.

[92] Hambrey, M., *Glaciers Online*, **2017**. Available from http://www.swisseduc.ch.

[93] Blumberg, P. N., Curl, R. L., "Experimental and Theoretical Studies of Dissolution Roughness", *Journal of Fluid Mechanics* **1974**, 65(4), 735.

[94] Villien, B., Zheng, Y., Lister, D. H., "Surface Dissolution and the Development of Scallops", *Chemical Engineering Communications* **2005**, 192(1), 125.

[95] Fijisawa, N., Uchiyama, K., Yamagata, T., "Mass Transfer Characteristics of Flow on Periodic Rough Pipe and Downstream of an Orifice", *Proc., International Conference on Flow-Accelerated Corrosion*, **2016** (Lille, France). Électricité de France, Paris, France.

[96] Le, T., Ewing, D., Schefski, C., Ching, C. Y., "Mass Transfer in Back to Back Elbows Arranged in an Out of Plane Configuration", *Proc., International Conference on Flow-Accelerated Corrosion*, **2013** (Avignon, France). Électricité de France, Paris, France.

[97] Lertsurasakda, C., *The Effect of Surface Scalloping on Flow Hydrodynamics and Pressure Drop*, **2007**. M.S. Thesis, The Petroleum and Petrochemical College, Chulalongkorn University, Bangkok, Thailand.

[98] Burrill, K. A., Cheluget, E. L., "Corrosion of CANDU Outlet Feeder Pipes", *Proc., International Conference on Water Chemistry in Nuclear Power Plants*, **1998** (Kashiwazaki, Japan). Japan Atomic Industrial Forum, Inc., Tokyo, Japan.

[99] Pope, S. B., *Turbulent Flows*, **2000**. Cambridge University Press, Cambridge and New York.

[100] Abe, H., Yano, T., Watanabe, Y., Nakashima, M., Tatsuki, T., "Characteristics of Scalloped Surface and Its Relation to FAC Rate of Carbon Steel Piping Elbow", *Transactions JSME* **2017**, 83(847) [in Japanese].

[101] Kain, V., Roychowdhury, S., Ahmedabadi, P., Barua, D. K., "Flow Accelerated Corrosion: Experience from Examination of Components from Nuclear Power Plants", *Engineering Failure Analysis* **2011**, 18(8), 2028.

[102] Barth, A., Crockett, H. M., Goyette, L. F., "Horowitz, J. S., Montgomery, R., "Flow Accelerated Corrosion – The Entrance Effect", *Proc., PVP2008, ASME Pressure Vessels and Piping Division Conference*, **2008** (Chicago, IL, USA). American Society of Mechanical Engineers, New York, NY, USA.

[103] Knook, T., Persoz, M., Trevin, S., Friol, S., Moutrille, M.-P., Dejoux, L., "Pipe Wall Thinning Management at Electricité de France (EDF)", *Journal of Advanced Maintenance 2* **2010/2011**, 1–13.

[104] Kastner, W., Erve, M., Henzel, N., Stellwag, B., "Calculation Code for Erosion Corrosion Induced Wall Thinning in Piping Systems", *Nuclear Engineering and Design* **1990**, 119(2–3), 431.

[105] Tomarov, G. V., Shipkov, A. A., "Principles of Development and Specific Features Relating to Practical Application of Software for Solving Problems Connected with Erosion-Corrosion of Metal in Power Engineering", *Thermal Engineering* **2011**, 58(2), 135.

[106] Trevin, S., "IAEA Benchmark of FAC Software", *Proc., International Conference on Flow-Accelerated Corrosion*, **2016** (Lille, France). Électricité de France, Paris, France.

[107] *Pressurized Water Reactor Secondary Water Chemistry Guidelines – Revision 7*, **2009**. Electric Power Research Institute, Palo Alto, CA, USA.

[108] Sugino, W., Fukuda, Y., Kitano, Y., Hisamune, K., Meguro, Y., "Effectiveness of Oxygen Treatment on Flow Accelerated Corrosion Mitigation in PWR Secondary System", *Proc., Nuclear Plant Chemistry Conference (NPC)*, **2012** (Paris, France). Société Française d'Energie Nucléaire, Paris, France.

[109] Wells, D. M., Fruzzetti, K., Garcia, S., McElrath, J., "Chemistry Control to Meet the Demands of Modern Nuclear Power Plant Operation", *Proc., Nuclear Plant Chemistry Conference (NPC)*, **2016** (Brighton, United Kingdom). The Nuclear Institute, London, United Kingdom.

[110] *Technical Guidance Document: Steam Purity for Turbine Operation*, **2013**. International Association for the Properties of Water and Steam, IAPWS TGD5-13. Available from http://www.iapws.org.

[111] Dooley, R. B., Macdonald, D. D., Syrett, B. C., "ORP – The Real Story for Fossil Plants", *PowerPlant Chemistry* **2003**, 5(1), 5.

[112] Dooley, R. B., Mathews, J., Pate, R., Taylor, J., *Proc., International Water Conference*, **1994** (Pittsburgh, PA, USA). Engineers' Society of Western Pennsylvania, Pittsburgh, PA, USA, IWC-94-53.

[113] Riznic, J., *Steam Generators for Nuclear Power Plants*, **2017**. Woodhead Publishing Series in Energy, Elsevier Ltd., London, United Kingdom.

[114] Moed, D. H., Weerakul, S., Lister, D. H., Leaukosol, N., Rietveld, L. C., Verliefde, A. R. D., "Effect of Ethanolamine, Ammonia, Acetic Acid and Formic Acid on Two-Phase Flow-Accelerated Corrosion in Steam-Water Cycles", *Industrial & Engineering Chemistry Research* **2015**, 54(36), 8963.

[115] Verelst, L., Dufraing, B., Wolfe, R., Denissen, P., DeBaets, G., Schildermans, K., Lecocq, R., "An Investigation into an Alternative to Hydrazine as an Oxygen Scavenger in the Secondary Systems of NPPs. Literature Review and Plant Trial", *Proc., Nuclear Plant Chemistry Conference (NPC)*, **2016** (Brighton, United Kingdom). The Nuclear Institute, London, United Kingdom.

[116] Quirk, G., Woolsey, I. S., Rudge, A., "Use of Oxygen Dosing to Prevent Flow-Accelerated Corrosion in Advanced Gas-Cooled Reactors", *PowerPlant Chemistry* **2011**, 13(4), 198.

[117] Ramminger, U., Fandrich, J., Drexler, A., "An Innovative Strategy for Secondary Side System Lay-Up Using Film-Forming Amines", *Proc., 7th International Steam Generator to Controls Conference*, **2012** (Toronto, Canada). Canadian Nuclear Society, Toronto, ON, Canada.

[118] Yurmanov, V., Rakhmanov, A., "Flow Accelerated Corrosion of Pipelines and Equipment at Russian NPPs: Problems and Solutions", *IAEA Workshop on Erosion-Corrosion Including Flow Accelerated Corrosion and Environmentally Assisted Cracking Issues in Nuclear Power Plants*, **2009** (Moscow, Russian Federation). International Atomic Energy Agency, Vienna, Austria.

[119] Rudolph, L., Fandrich, J., Ramminger, U., "CFD Calculation Method for Assessment of Film-Forming Amines on Local Deposition at Tube Sheet of Steam Generators", *Proc., Nuclear Plant Chemistry Conference (NPC)*, **2016** (Brighton, United Kingdom). The Nuclear Institute, London, United Kingdom.

[120] Choi, S., Fruzzetti, K., Caravaggio, M., Shulder, S., Marks, C., Reinders, J., Mechler, A., Kreider, M., "Filming Amines: A Pathway to Wider Use in PWRs", *Proc., Nuclear Plant Chemistry Conference (NPC)*, **2016** (Brighton, United Kingdom). The Nuclear Institute, London, United Kingdom.

[121] Bignold, G. J., Garbett, K., Garnsey, R., Woolsey, I. S., "Erosion-Corrosio in Nuclear Steam Generators", *Proc., 2nd International Conference on Water Chemistry in Nuclear Reactor Systems*, **1980** (Bournemouth, United Kingdom). British Nuclear Energy Society, London, United Kingdom.

[122] Lister, D. H., Arbeau, N., Johari, J. M. C., *Erosion and Cavitation in the CANDU Primary Heat Transport System*, **1996**. The Atomic Energy Control Board (now the Canadian Nuclear Safety Commission), Ottawa, Canada. Report RSP-0009.

[123] Dooley, R. B., Chexal, V. K., "Flow-Accelerated Corrosion", *Proc., Corrosion/1999*, **1999** (San Antonio, TX, USA). NACE International, Houston, TX, USA, Paper #99347.

[124] Daniel, P. L., Rudisaile, J. C., *Wastage of Economizer Inlet Header Tube Stubs*, **1993**. Babcock & Wilcox Enterprises, Inc., Charlotte, NC, USA, B&W 186-4016.

[125] Dooley, R. B., Shields, K. J., Shulder, S. J., "Lessons Learned from Fossil FAC Assessments", *PowerPlant Chemistry* **2010**, 12(9), 508.

[126] Gabrielli, F., "Flow Assisted Corrosion: Failures/ Water Chemistry Aspects", *Proc., International Conference on Boiler Tube and HRSG Tube Failures and Inspections (Ed.: R. B. Dooley)*, **2006**. Electric Power Research Institute, Palo Alto, CA, USA, EPRI 1013629, 243.

[127] *Guidelines for Internal Inspection of Air-Cooled Condensers*, **2015**. Air-Cooled Condensers Users Group, ACC.01. Available at http://acc-usersgroup.org.

[128] Park, Y.-H., Kang, S.-C., "Evaluation of Piping Integrity in Thinned Main Feedwater Pipes", *Nuclear Engineering and Technology* **2000**, 32(1), 67.

[129] Munson, D., "A Brief Overview of FAC Investigations, Experiences and Lessons Learned", *presented at the WANO Seminar Effective Control and Monitoring of FAC*, **2008** (Haiyan, Zhejiang, China). World Association of Nuclear Operators, London, United Kingdom, ENT000035-00-BD01.

[130] *CODAP Topical Report: Flow Accelerated Corrosion of Carbon Steel & Low Alloy Piping in Commercial Nuclear Power Plants*, **2015**. OECD Nuclear Energy Agency, Committee on the Safety of Nuclear Installations, Boulogne-Billancourt, France, NEA/CSNI/R(2014)6.

[131] Walker, S., "NDE Options for FAC", *presented at the International FAC Conference*, **2010** (Washington, DC, USA).

[132] Garcia, S. E., Giannelli, J. F., Jarvis, M. L., "Advances in BWR Water Chemistry", *Proc., Nuclear Plant Chemistry Conference (NPC)*, **2012** (Paris, France). Société Française d'Energie Nucléaire, Paris, France.

[133] Maeda, A., Shoda, Y., Ishihara, N., Murata, K., Fujiwara, H., Hayakawa, H., Matsuda, T., "Secondary Water Chemistry Control Practices and Results at the Japanese PWR Plants", *Proc., Nuclear Plant Chemistry Conference (NPC)*, **2012** (Paris, France). Société Française d'Energie Nucléaire, Paris, France.

[134] Nordmann, F., Odar, S., Rochester, D., "Issues and Remedies for Secondary System of PWR/VVER", *Proc., Nuclear Plant Chemistry Conference (NPC)*, **2012** (Paris, France). Société Française d'Energie Nucléaire, Paris, France.

[135] Roumiguière, F.-M., Fandrich, J., Ramminger, U., Hoffmann-Wankerl, S., Drexler, A., "Secondary Side Water Chemistry pH Control Strategy Improvements", *Proc., Nuclear Plant Chemistry Conference (NPC)*, **2012** (Paris, France). Société Française d'Energie Nucléaire, Paris, France.

[136] Dooley, R. B., Shields, K. J., "Alleviation of Copper Problems in Fossil Plants", *Proc., 14th ICPWS*, **2004** (Kyoto, Japan). International Association for the Properties of Water and Steam.
Also published in: *PowerPlant Chemistry* **2004**, 6(10), 581.

[137] *Technical Guidance Document: HRSG High Pressure Evaporator Sampling for Internal Deposit Identification and Determining the Need to Chemical Clean*, **2016**. International Association for the Properties of Water and Steam, IAPWS TGD7-16. Available from http://www.iapws.org.

[138] Dooley, R. B., Shields, K. J., Shulder, S. J., "How Repeat Situations Lead to Chemistry-Related Damage in Conventional Fossil and Combined Cycle Plants", *PowerPlant Chemistry* **2008**, 10(10), 564.

THE AUTHORS

Barry Dooley (B.Eng. with first class honours, Metallurgy, Ph.D., Metallurgy, both from University of Liverpool, UK, D.Sc., Moscow Power Institute, Moscow, Russia) is a Senior Associate with Structural Integrity Associates. Before joining Structural Integrity Associates he was a Technical Executive, Materials and Chemistry, at the Electric Power Research Institute (EPRI) in Charlotte, North Carolina, where he managed the Cycle Chemistry, HRSG, and Materials Programs, as well as the Boiler Tube Failure Reduction/Cycle Chemistry Improvement and FAC Programs. Before joining EPRI in 1984, Barry Dooley spent nine years with Ontario Hydro in Toronto, Canada. From 1972 to 1975, he was a research officer in the Materials Division of the Central Electricity Research Laboratories (CERL) of the former Central Electricity Generating Board (CEGB) at Leatherhead, Surrey, England.

Barry Dooley is the author or coauthor of over 290 papers and the editor of 14 international conference proceedings, primarily in the areas of metallurgy, power generation, boiler tube failures, HRSG tube failures, cycle chemistry, and life extension and assessment of fossil plants. He is the coauthor of a three-volume book on boiler tube failures, a two-volume book on steam turbine damage mechanisms, and a book on flow-accelerated corrosion in power plants. Barry Dooley is the executive secretary of the International Association for the Properties of Water and Steam (IAPWS). He was awarded an Honorary D.Sc. from the Moscow Power Institute in 2002.

Derek H. Lister (B.Sc., M.Sc., Chemical Engineering, University of Manchester, Ph.D., Physical Chemistry, University of Leicester, both in the UK) worked as a development engineer on the fuel of gas-cooled reactor systems in the UK before moving to the Chalk River facility of Atomic Energy of Canada, Ltd., where he researched the chemistry and corrosion of water-cooled reactors. In 1992, he was appointed to the Research Chair in Nuclear Engineering at the University of New Brunswick, where he continues full-time to pursue his interest in water coolant technologies, now as Professor Emeritus.

CONTACT

Barry Dooley
Senior Associate
Structural Integrity Associates, Inc.
22 Regent Close
Birkdale, Southport
PR8 2EJ
United Kingdom

E-mail: bdooley@structint.com